SAR interferometry and applications

Ramon Hanssen

2-6-2016

ESA SAR PECS course, Sofia, Bulgaria

Interferometry: mapping the millimeter

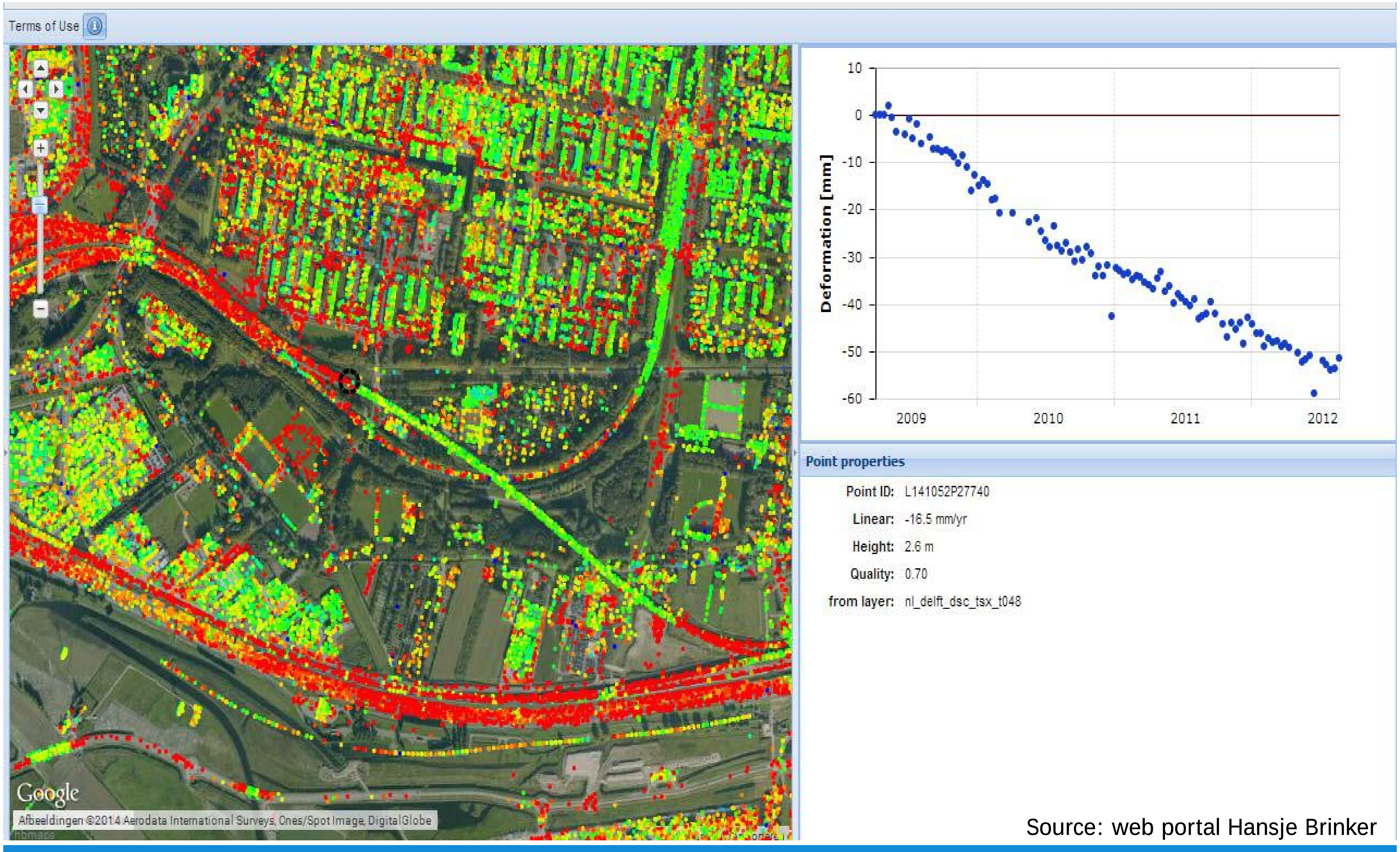

Source: web portal Hansje Brinker

Prior knowledge

- Radar principles, wavelength indications, SAR concept, resolution, satellite orbits, scattering,...
- Basic calculus: complex numbers, (rectangular form, polar form, exponential form), trigonometry,...

Learning objectives

- Interferometry: intuitive approach, physical approach
- Understanding sensitivity
- Basic observables and variables, concepts
- Practical data processing
- Quality control

14 May 2014: Oldest telescope of the Netherlands found at tunnel zone Delft (older than 1650)

Hans Lippershey’s patent, 1608

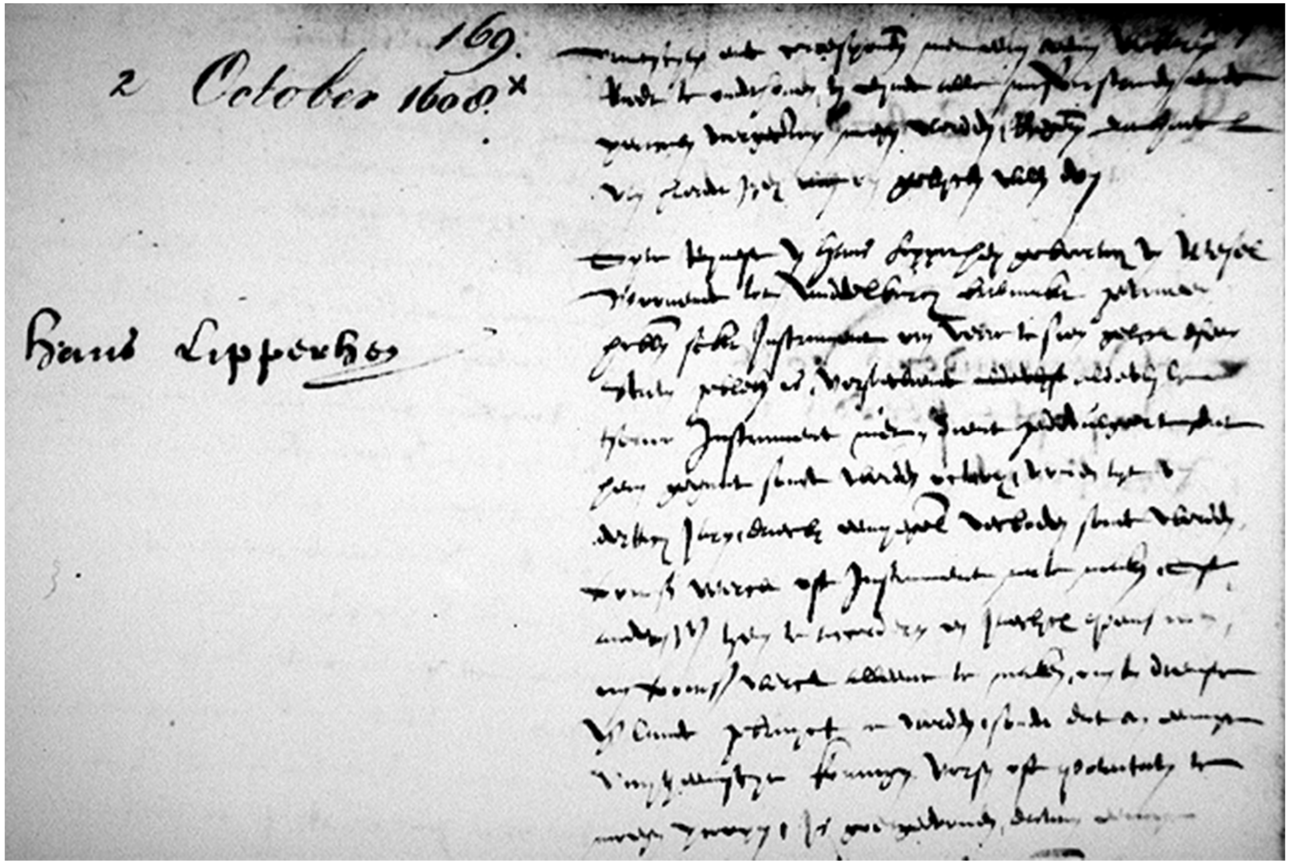

169.

2 October 1608.

Hans Lipperhey

Christiaan Huygens (1678)

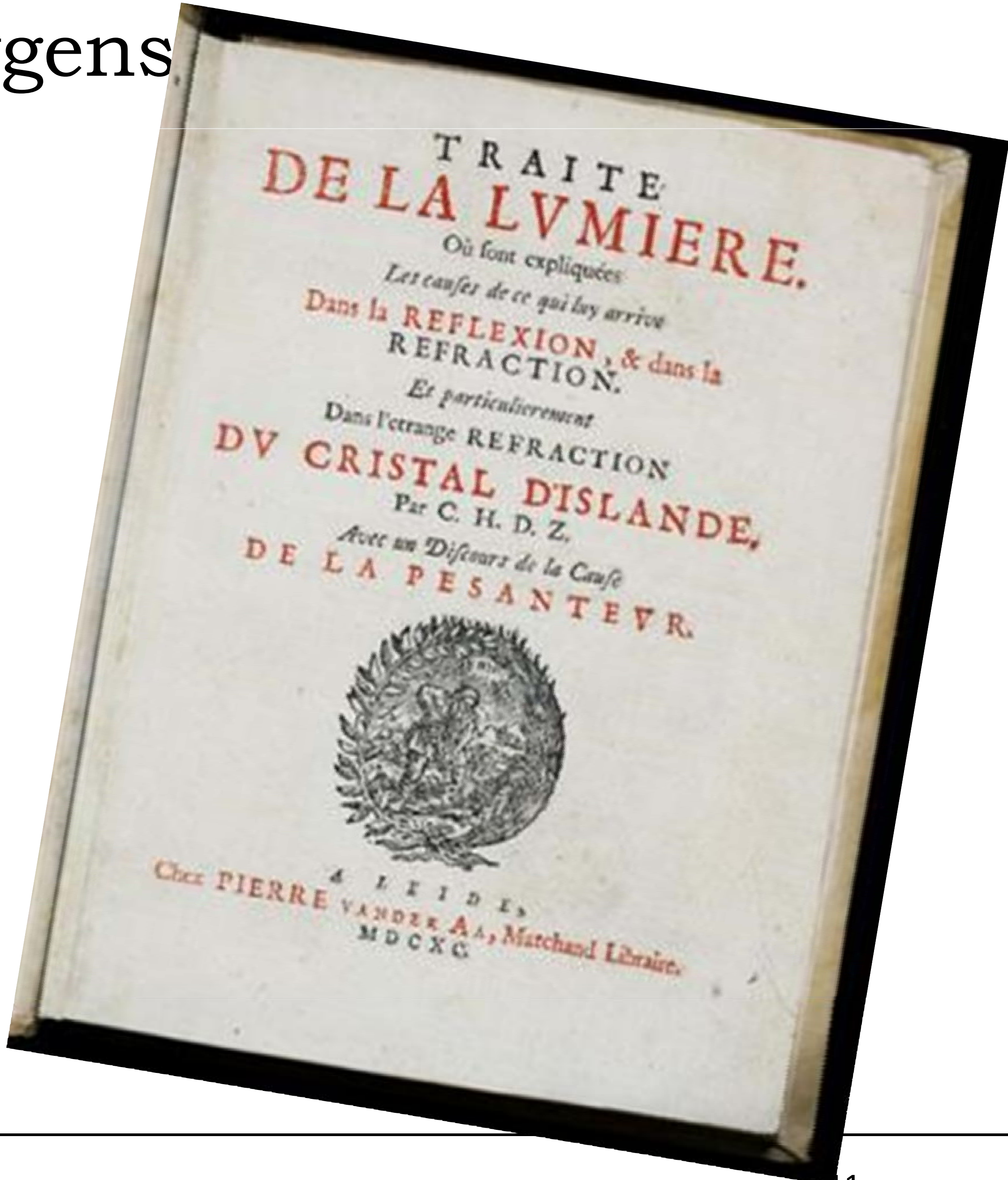

TRAITE
DE LA LVMIERE.
Où sont expliquées
Les causes de ce qui luy arrive
Dans la REFLEXION, & dans la
REFRACTION.
Et particulierement
Dans l'etrange REFRACTION
DV CRISTAL D'ISLANDE,
Par C. H. D. Z.
Avec un Discours de la Cause
DE LA PESANTEVR.

A LEIDE,
Chez PIERRE VANDER AA, Marchand Libraire.
MDCXC.

Mais il faut confiderer encore plus particulierement l'origine de ces ondes, & la maniere dont elles s'eſtendent. Et premierement il s'enſuit de ce qui à eſté dit dela production de la lumiere, que chaque petit endroit d'un corps lumineux, comme le Soleil, une chandelle, ou un charbon ardent, engendre ſes ondes, dont cet endroit eſt le centre. Ainſi dans la flame d'une chandelle, eſtans diſtinguez les points A, B, C; les cercles concentriques, decrits autour de chacun de ces points, repreſentent les ondes qui en provienent. Et il en faut concevoir de meſme autour de chaque point de la ſurface, & d'une partie du dedans de cette flame.

1993

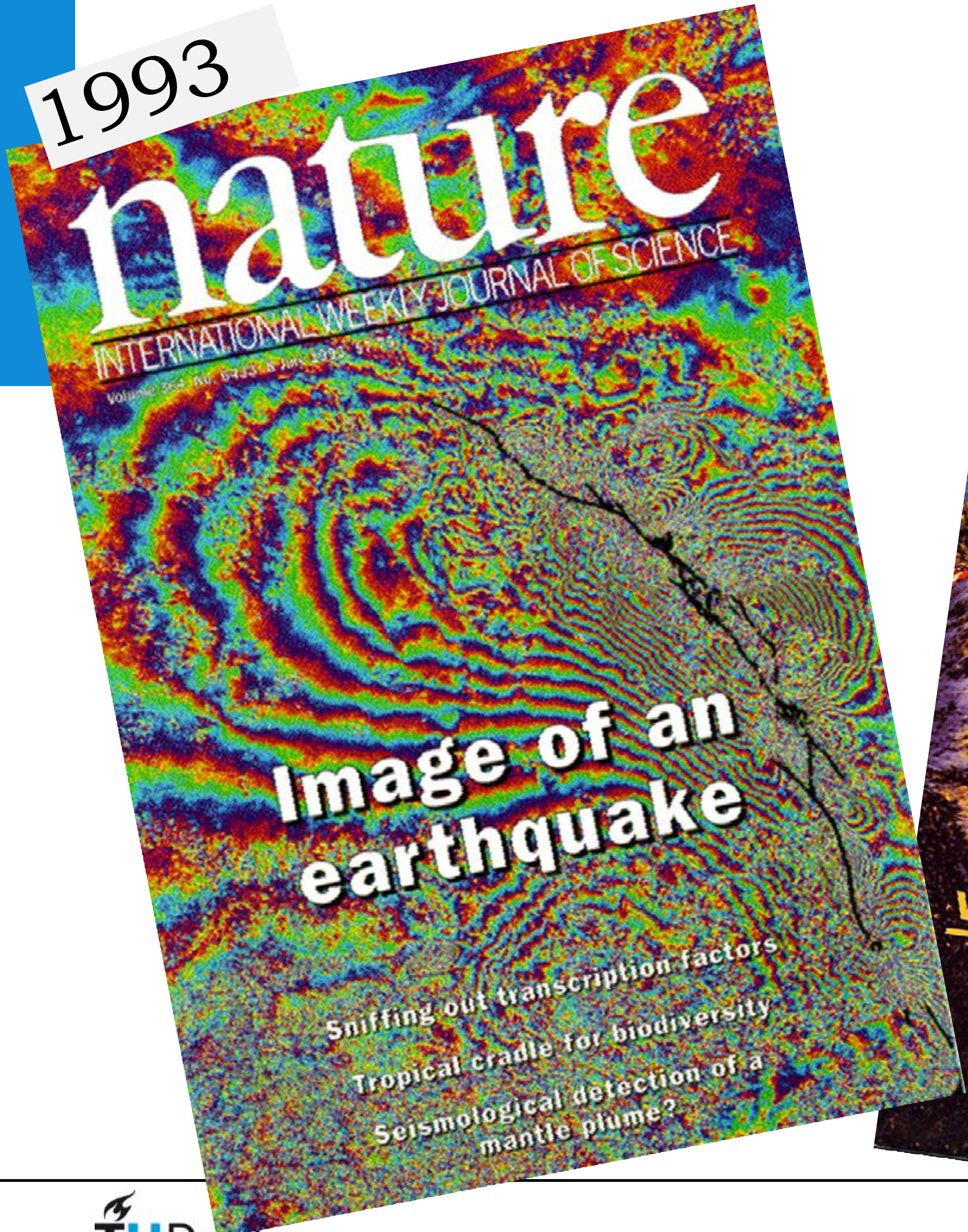
nature
INTERNATIONAL WEEKLY JOURNAL OF SCIENCE
Image of an earthquake
Sniffing out transcription factors
Tropical cradle for biodiversity
Seismological detection of a mantle plume?

1995

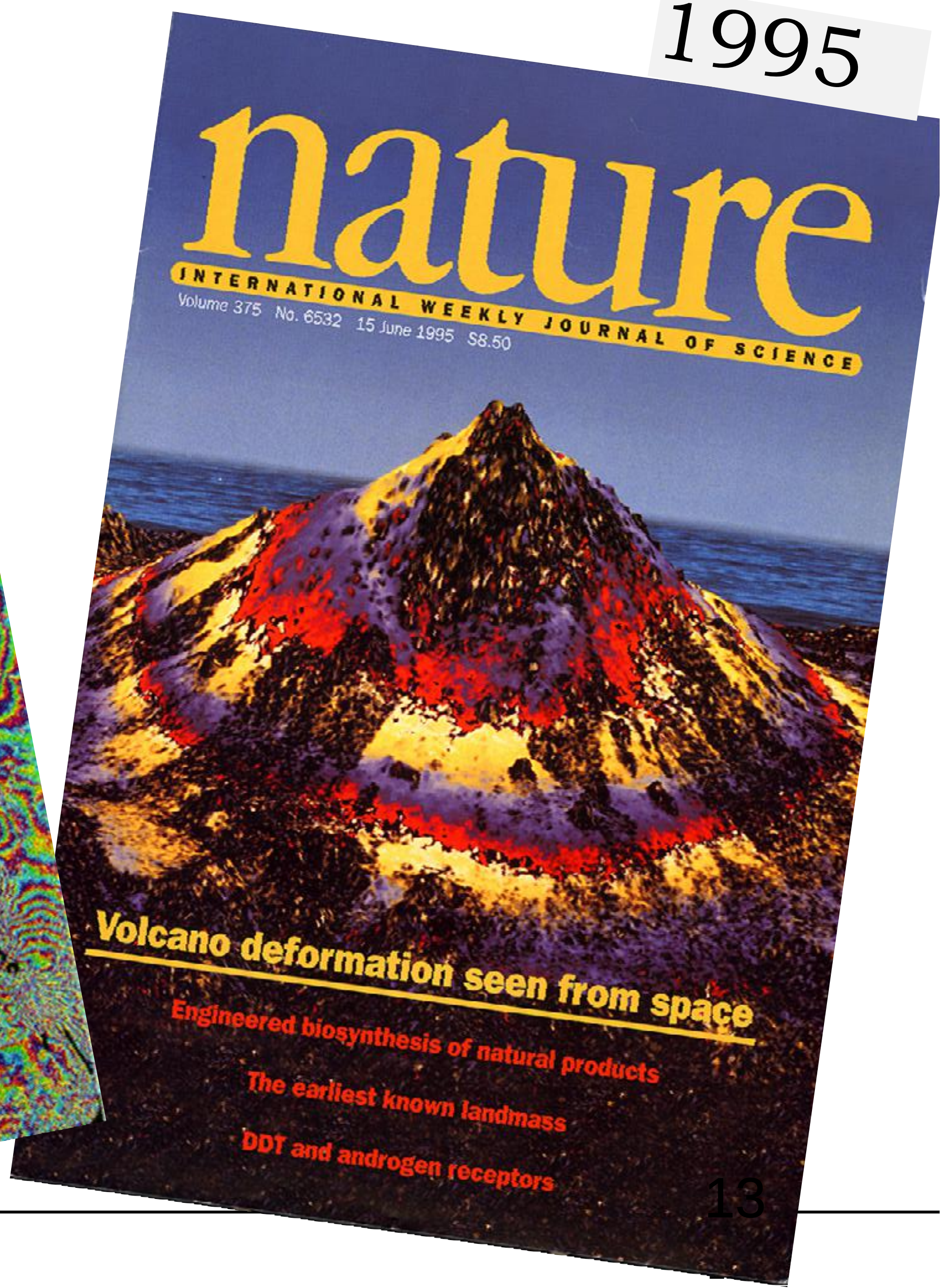
nature
INTERNATIONAL WEEKLY JOURNAL OF SCIENCE
Volume 375 No. 6532 15 June 1995 $8.50
Volcano deformation seen from space
Engineered biosynthesis of natural products
The earliest known landmass
DDT and androgen receptors

SAR SLC observations

SLC: Single-Look Complex data

•Single-look: no averaging, finest spatial resolution

•Complex: both real and imaginary (In-phase and quadrature phase) stored

Coherent imaging

$$y_1 = \boxed{|y_1|} \exp(j\boxed{\psi_1})$$

Amplitude Phase

Uninterpretable, due to scattering mechanism

Intuitive approach: geometry

Radar Interferometry

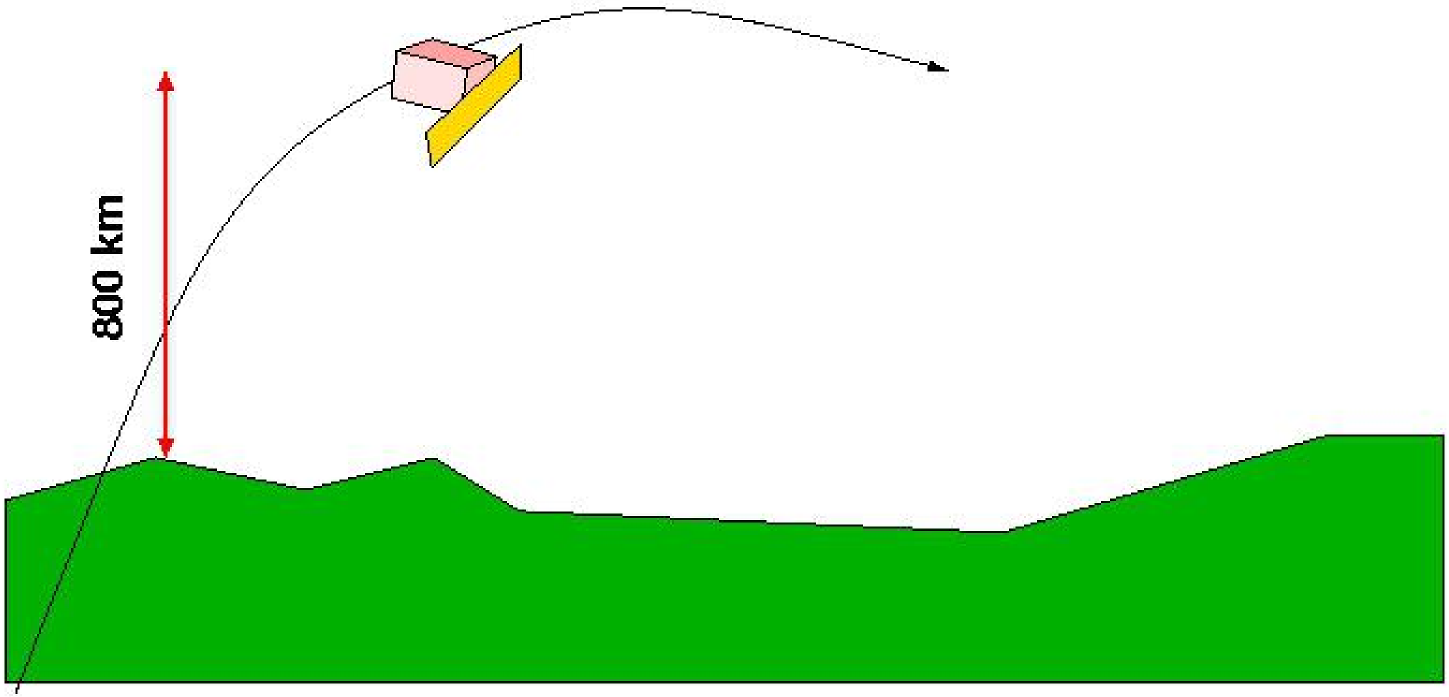

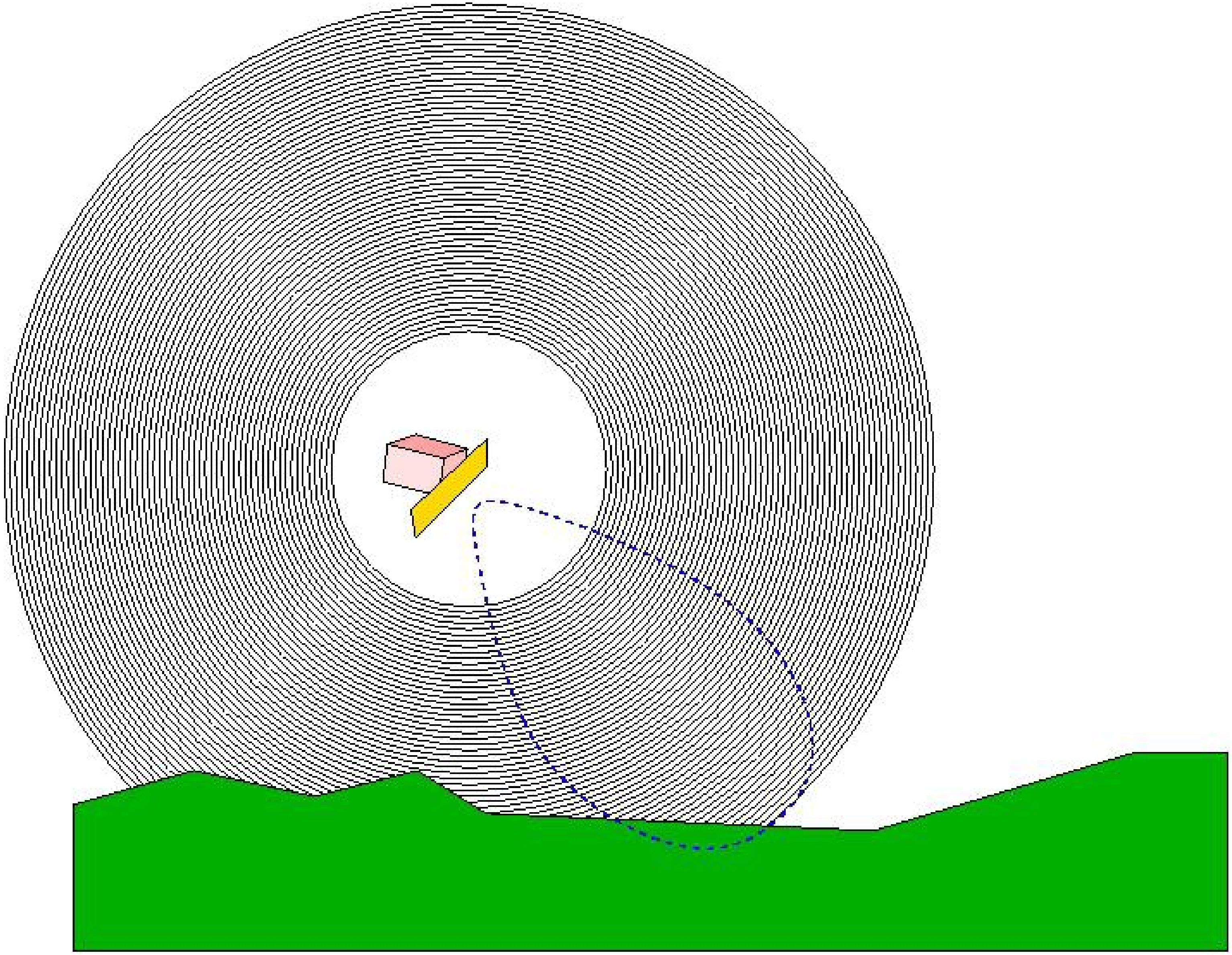

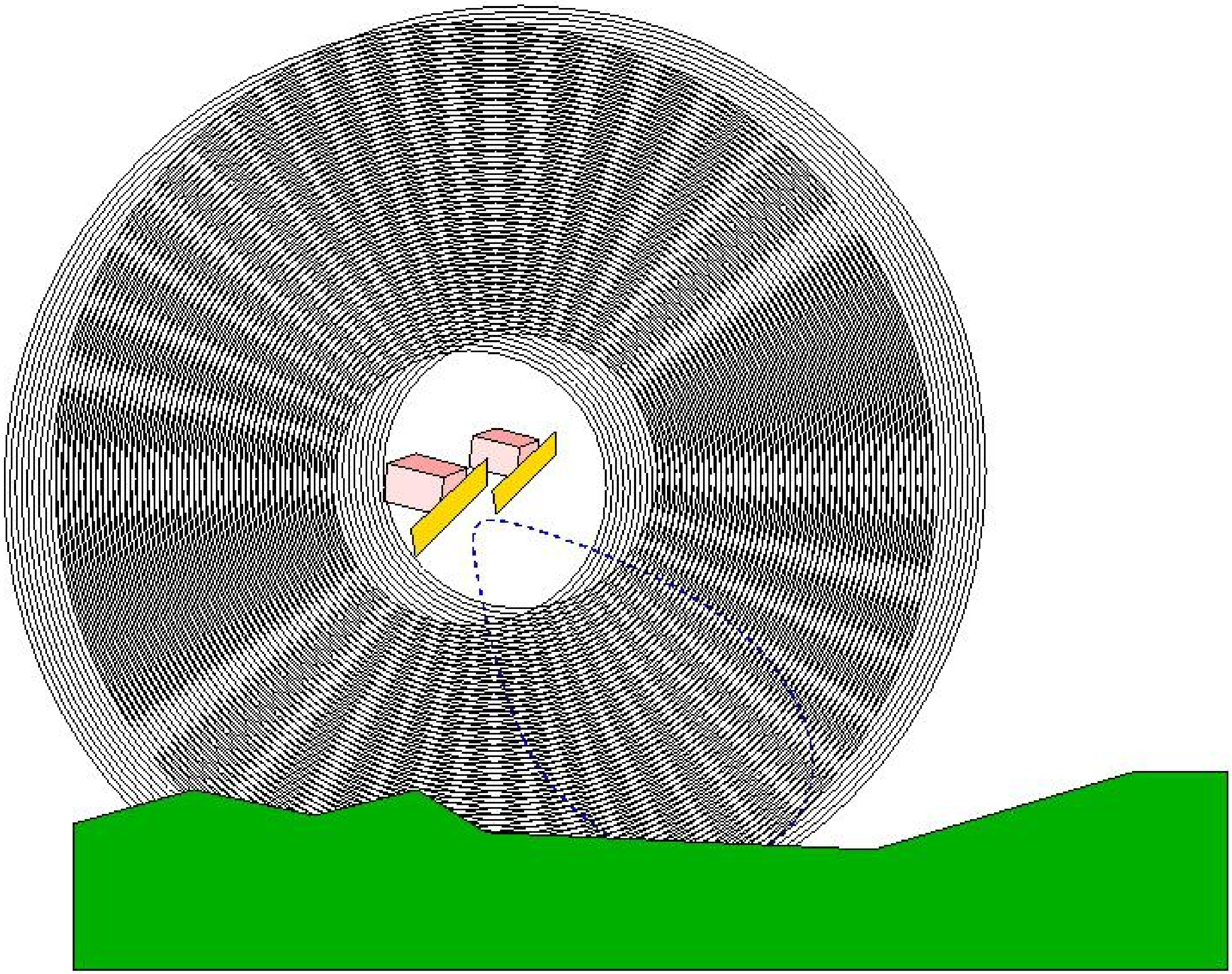

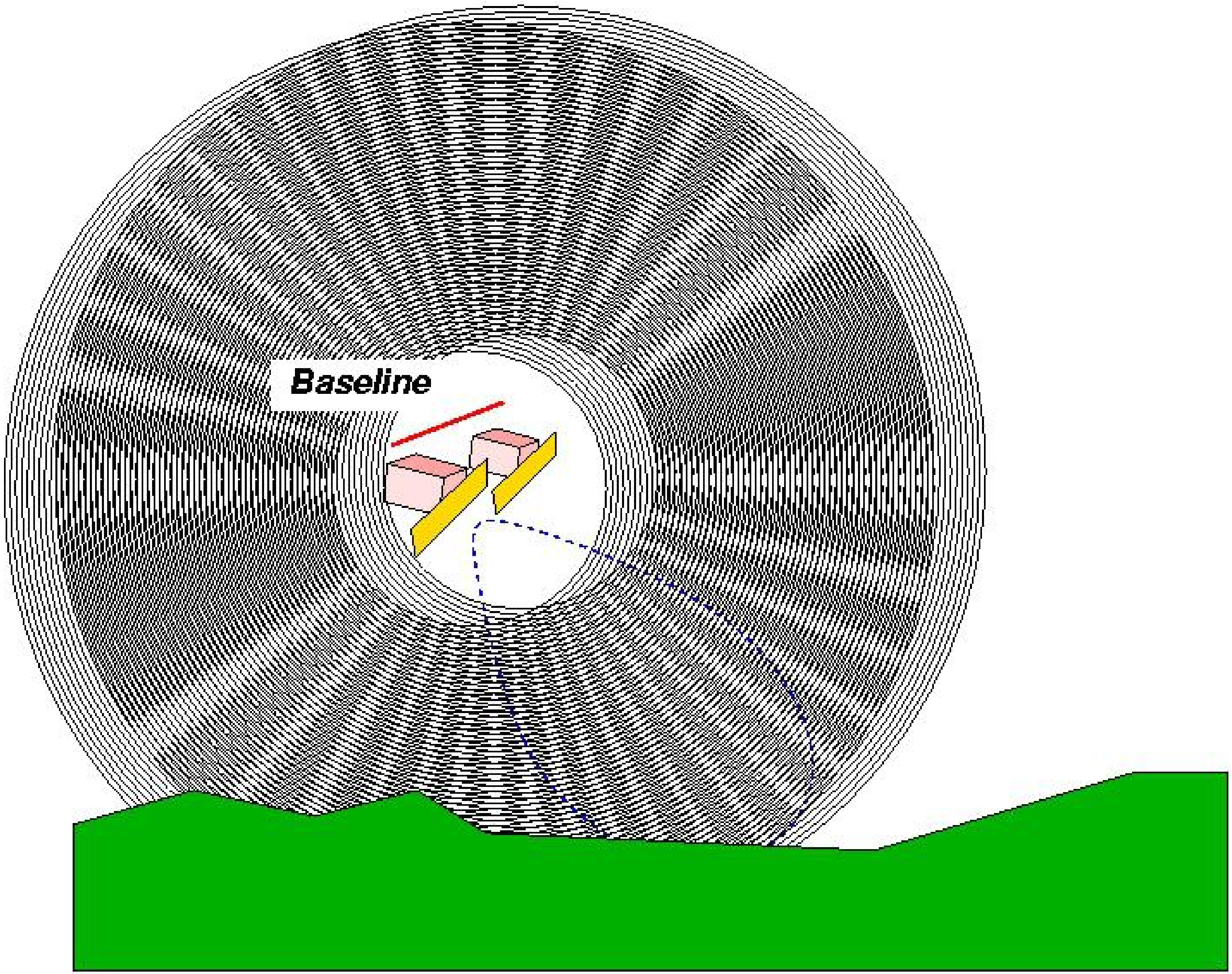
Baseline

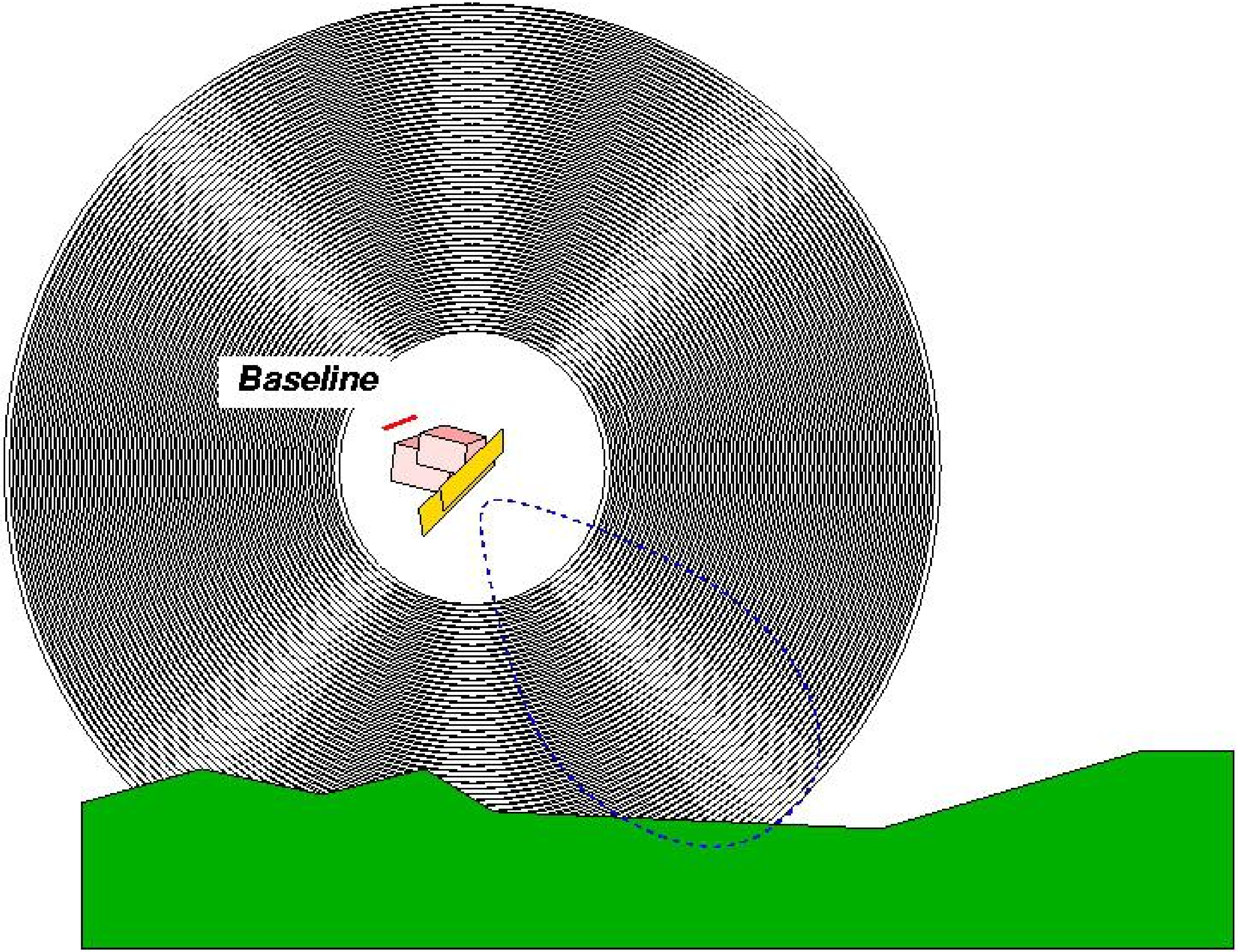
Baseline

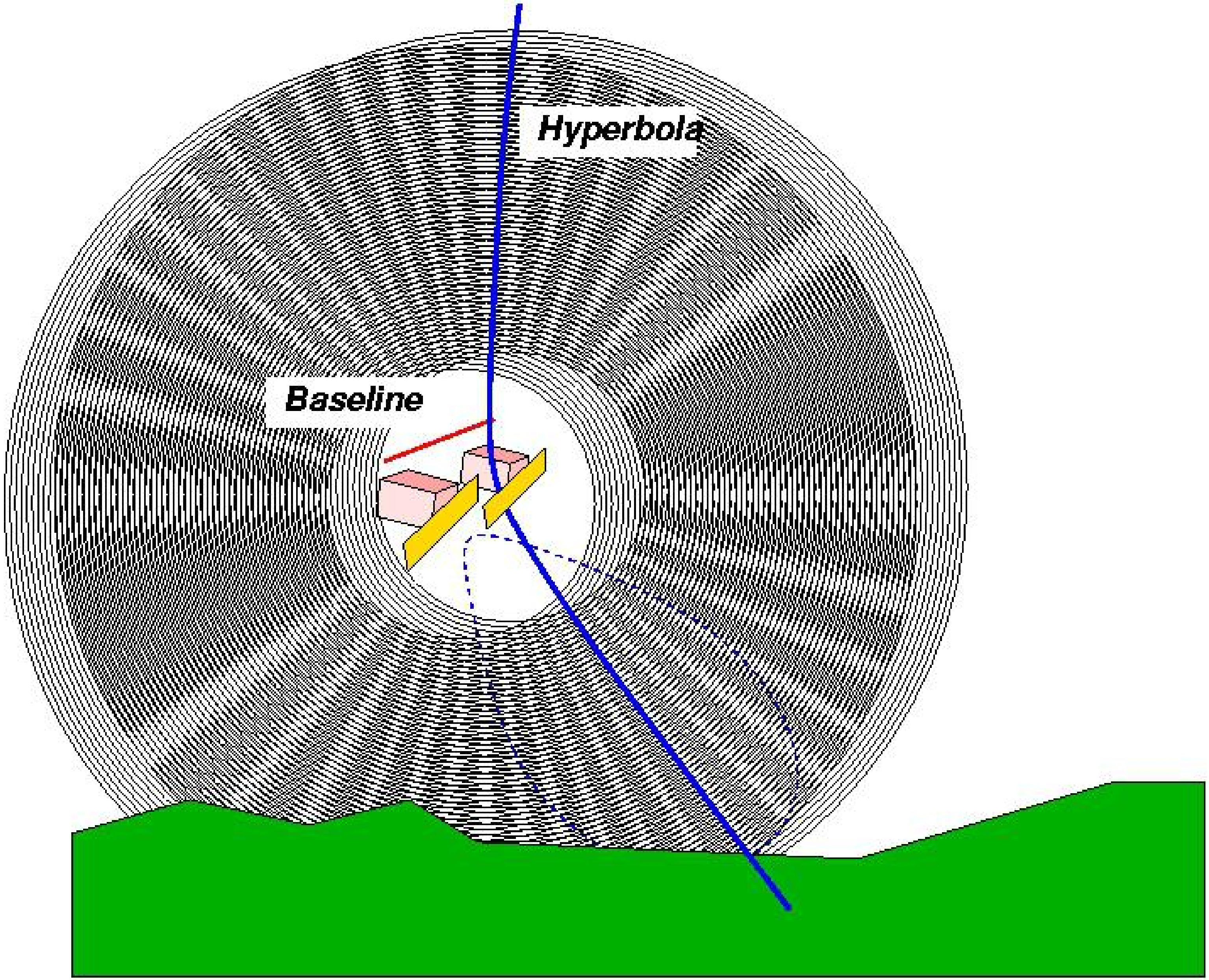
Hyperbola
Baseline

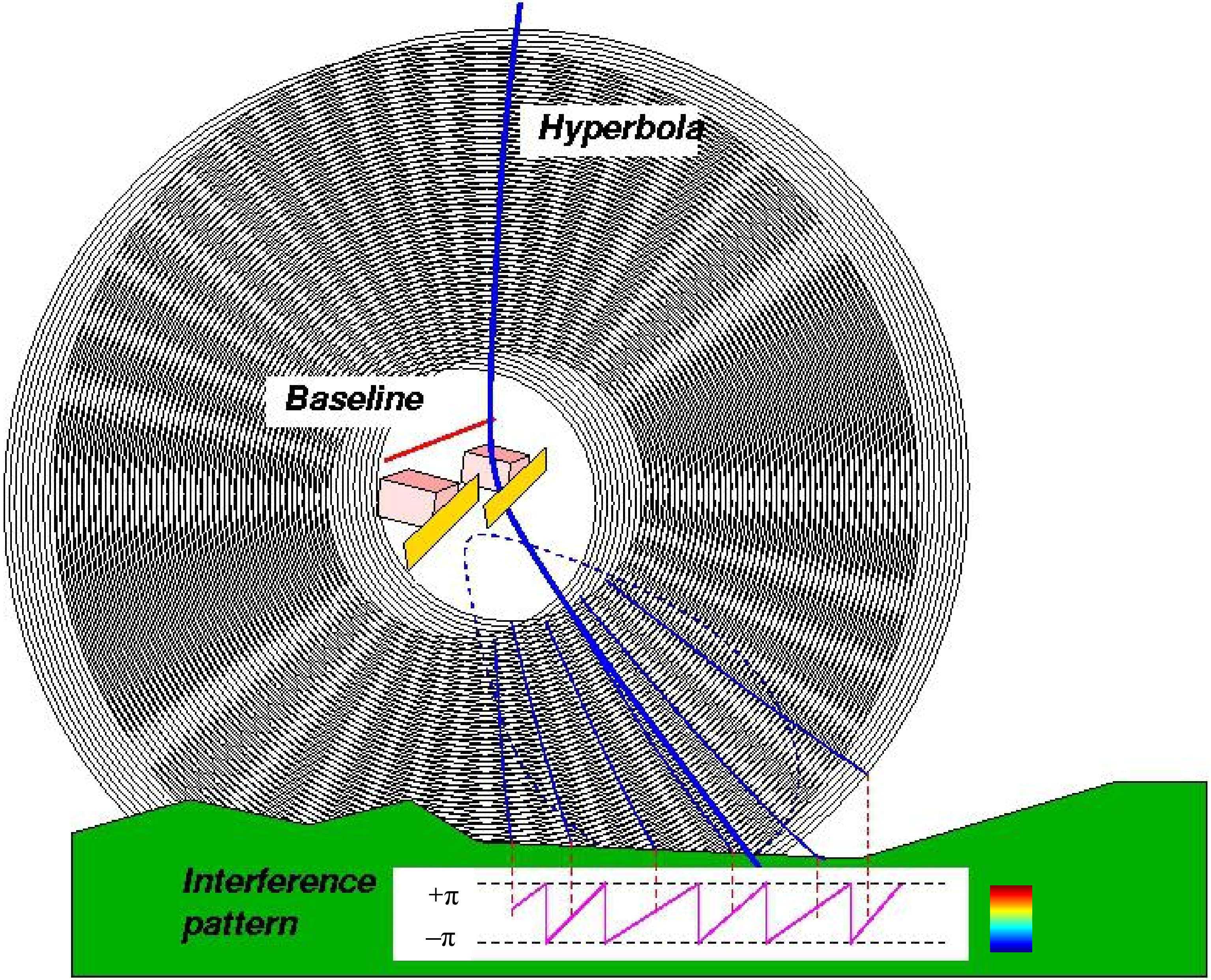
Hyperbola
Baseline
Interference pattern
+π
−π

Example in 2D: interferogram

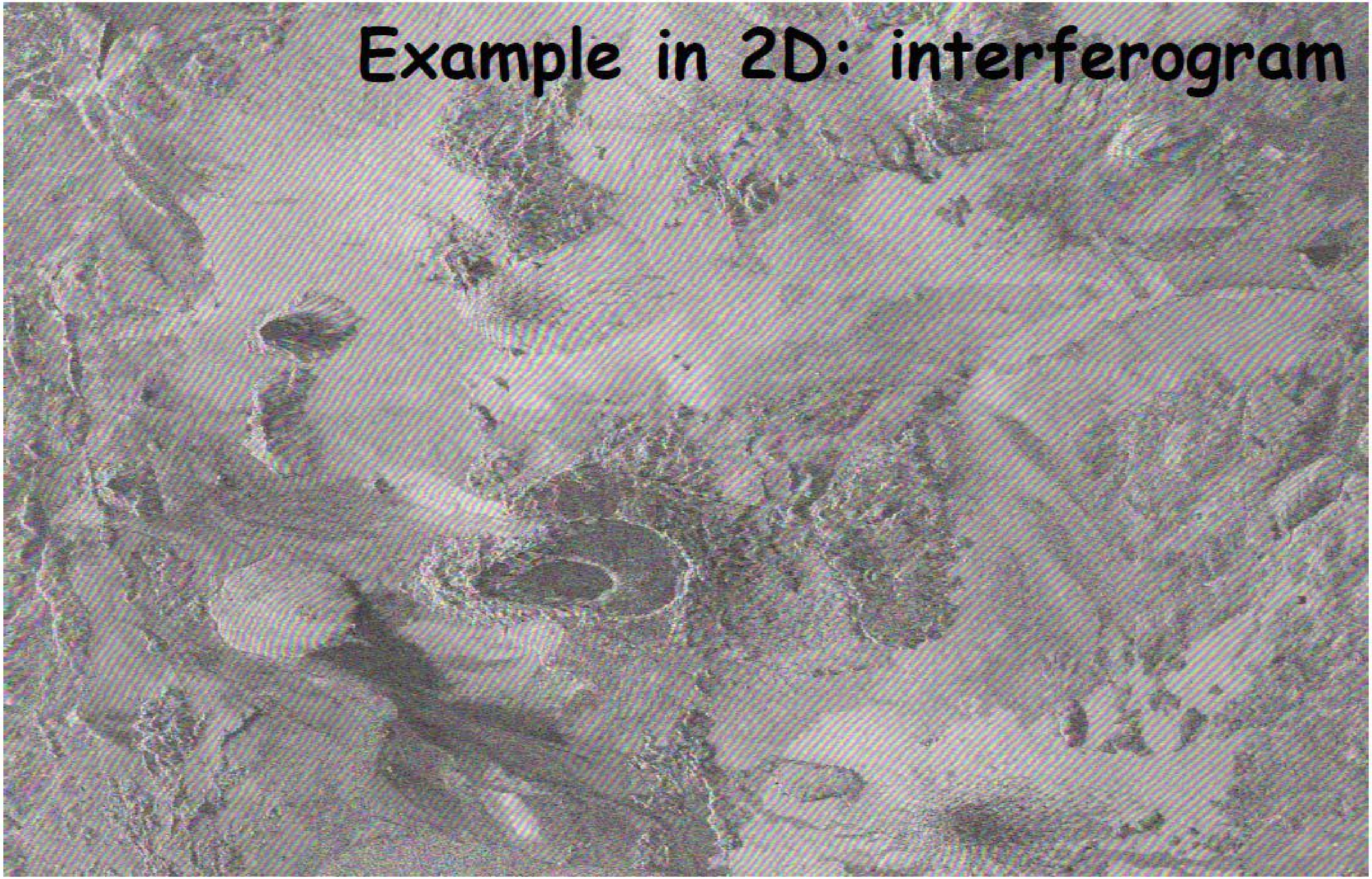

Range

Expressed as phase (radians)

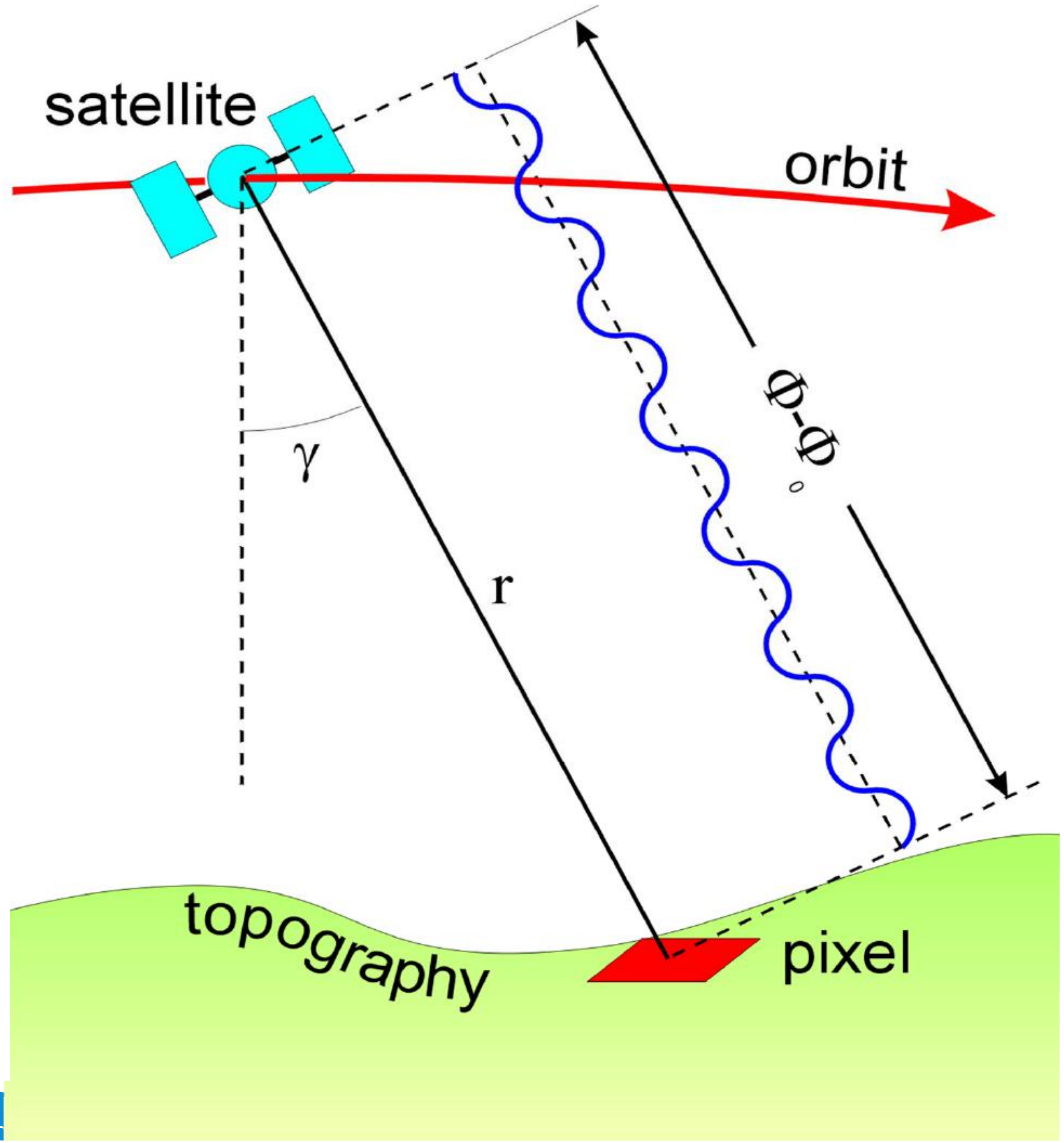

Range

Expressed as integer cycles + fractional phase

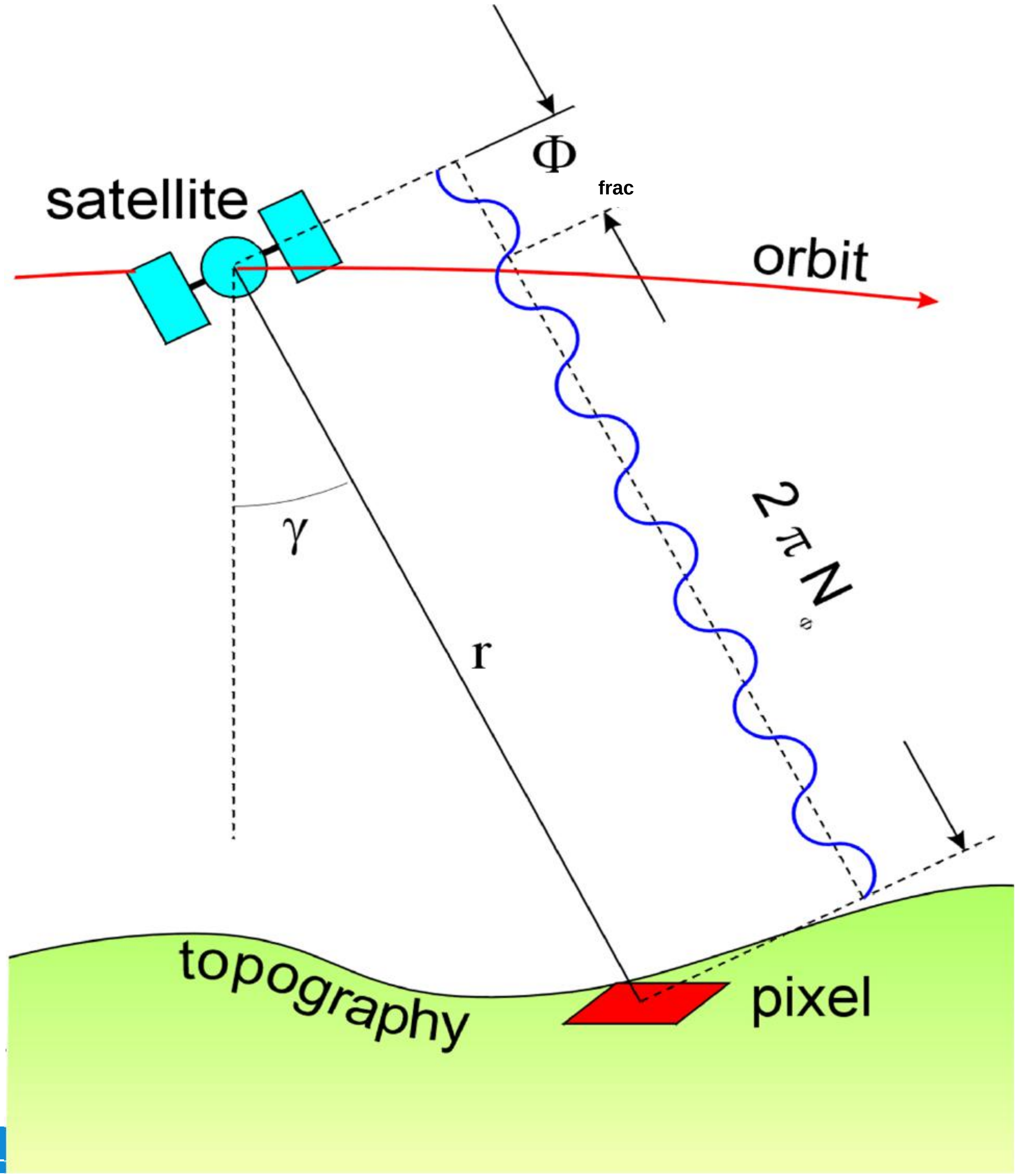

Two satellites: the 'baseline'

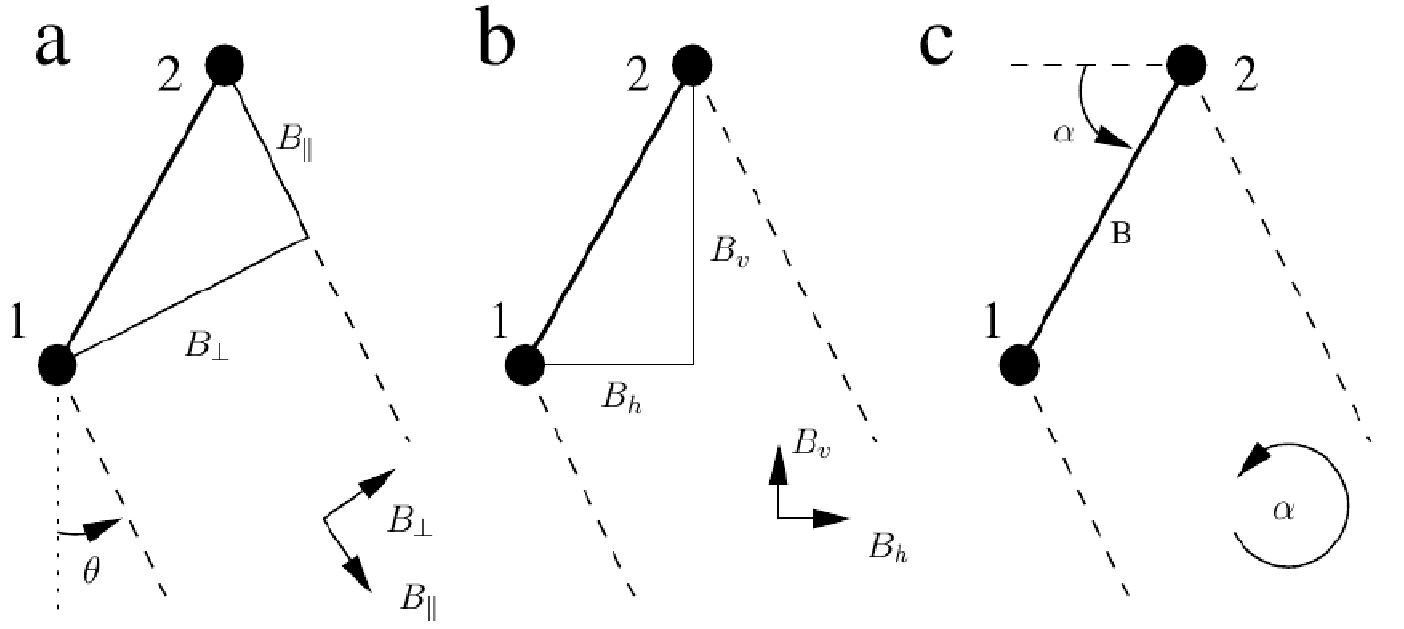

Figure B.2 Definition of the baseline parameters. (a) parallel/perpendicular; (b) horizontal/vertical; (c) length/orientation; Position 1 is the reference position. $B_{\|} > 0$ when $R_1 > R_2$, where R_i is the corresponding slant range. The angle α is defined counter-clockwise from the reference satellite (1), starting from the horizontal at the side of the look direction.

Reference phase (flat earth phase)

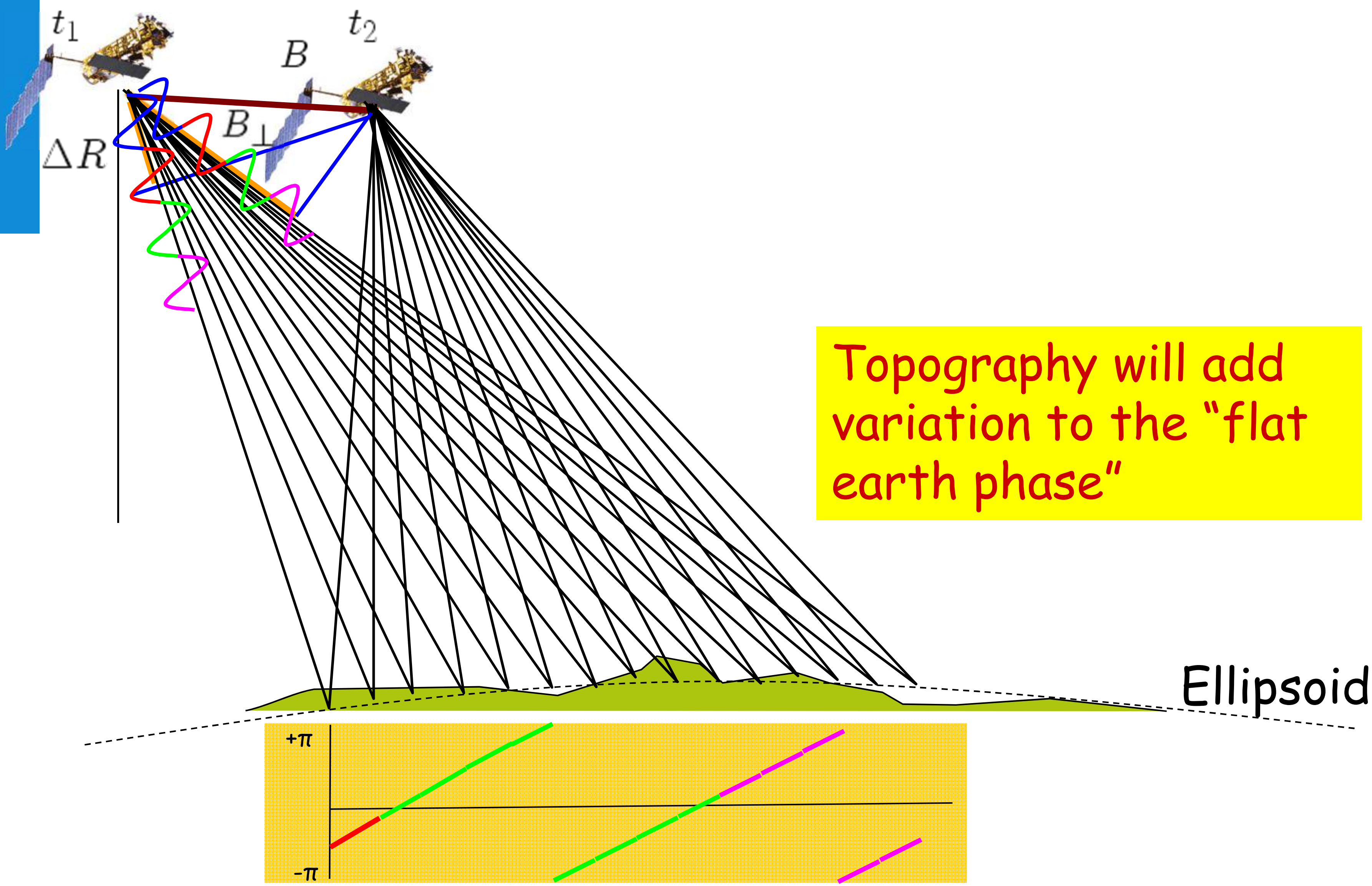

Topography will add variation to the "flat earth phase"

Example Reference Phase

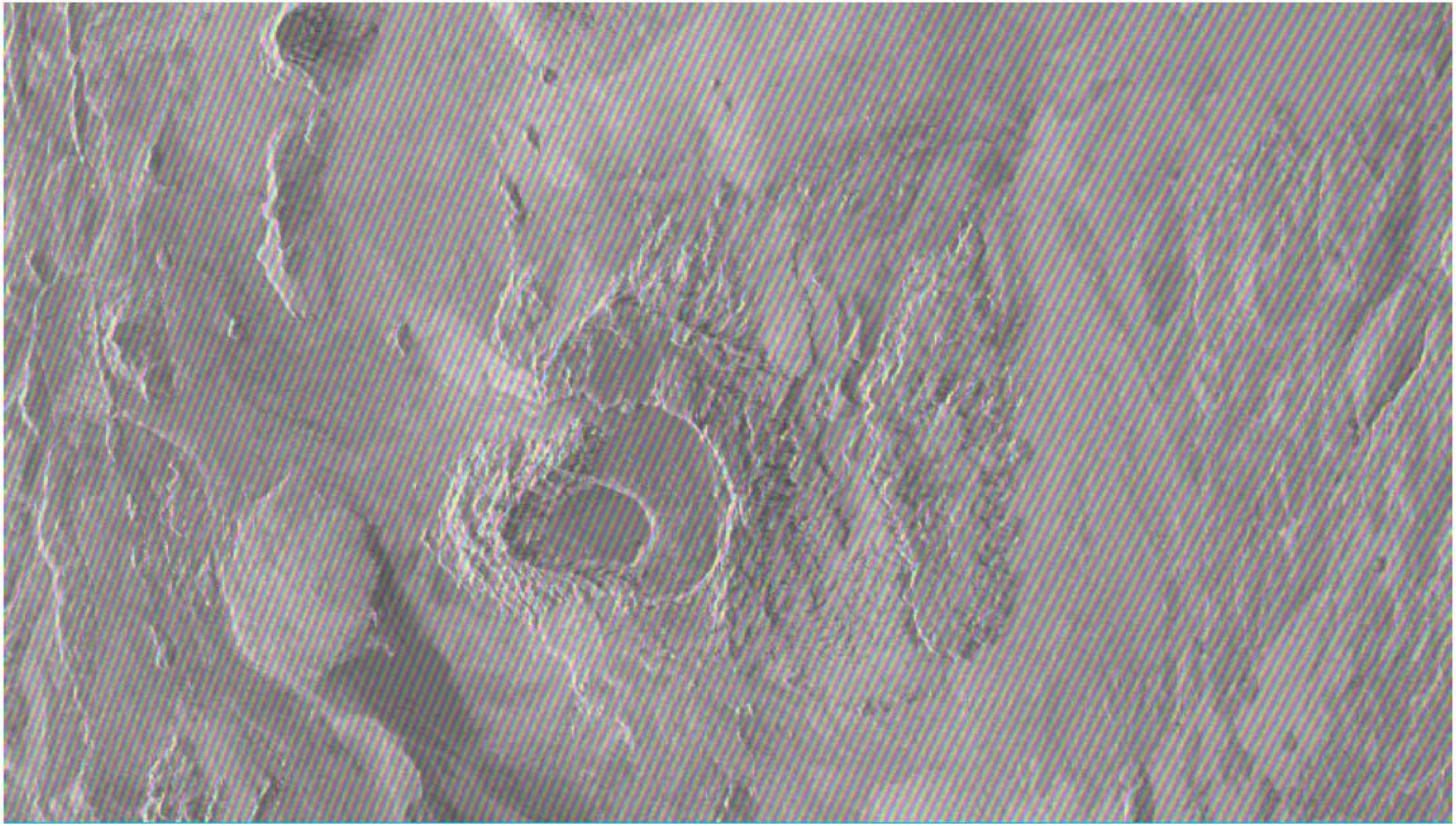

Topographic Phase

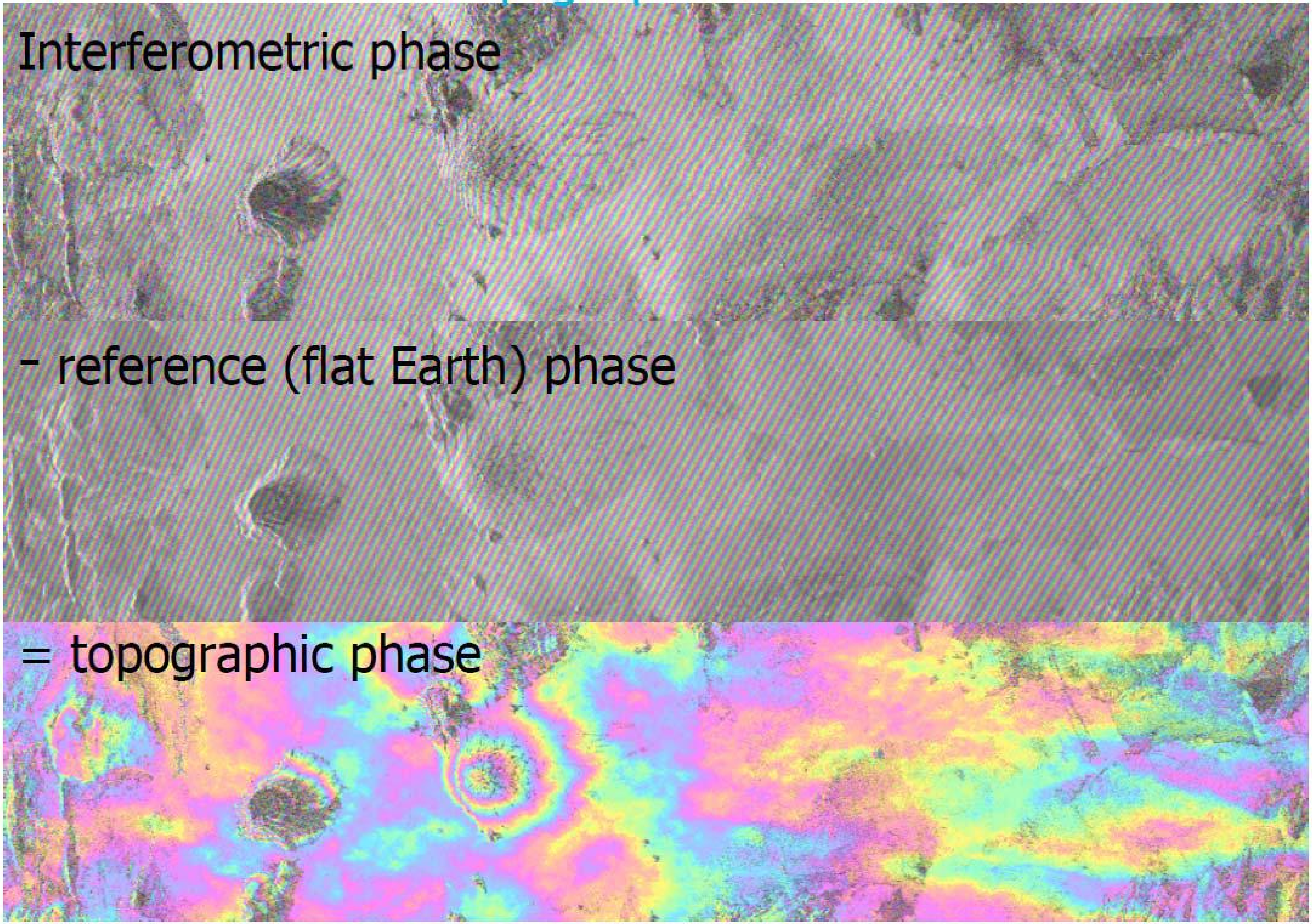

Example in 2D: interferogram

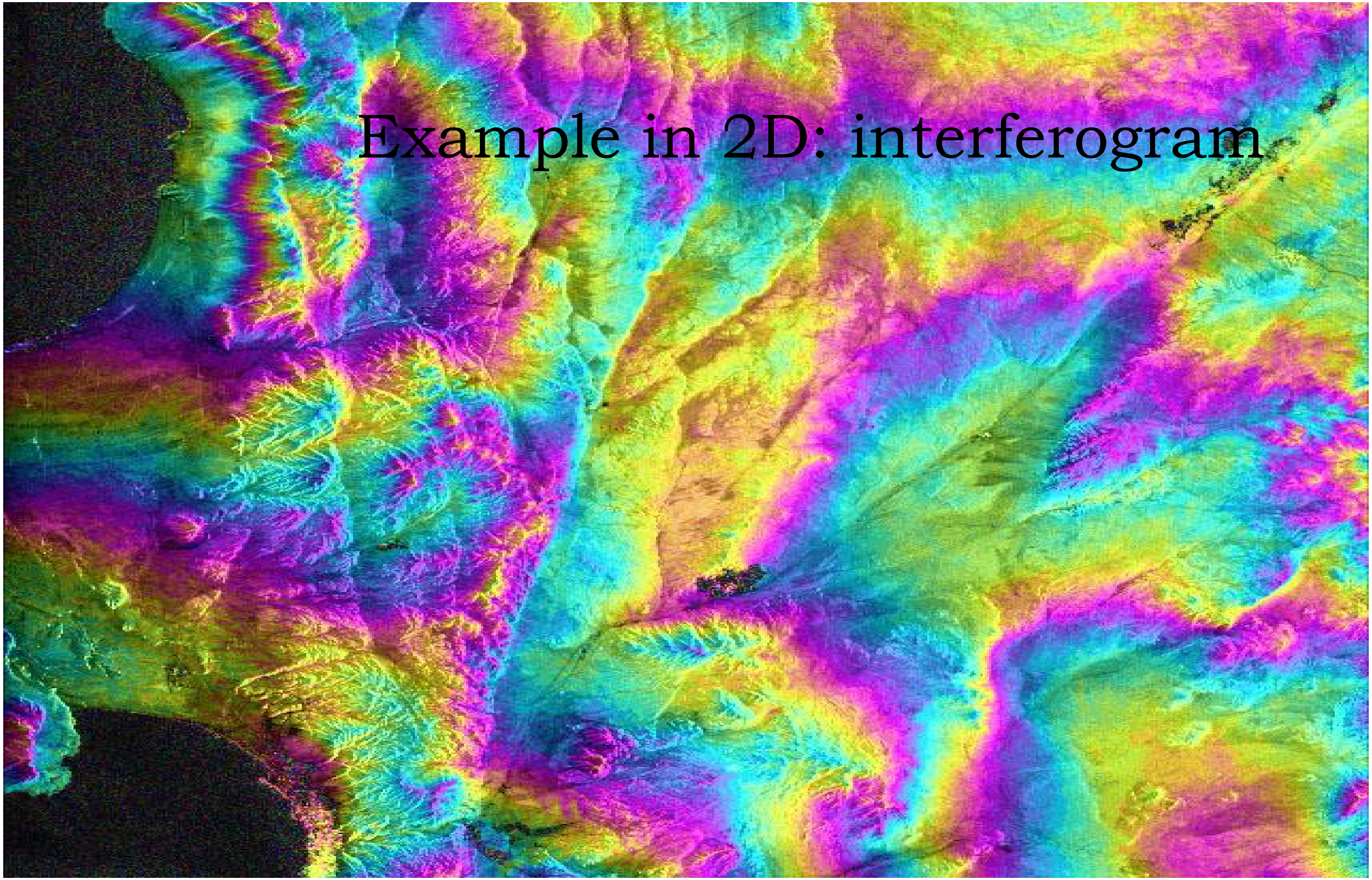

Interferometry:
deriving the equations

Phase-range relationship

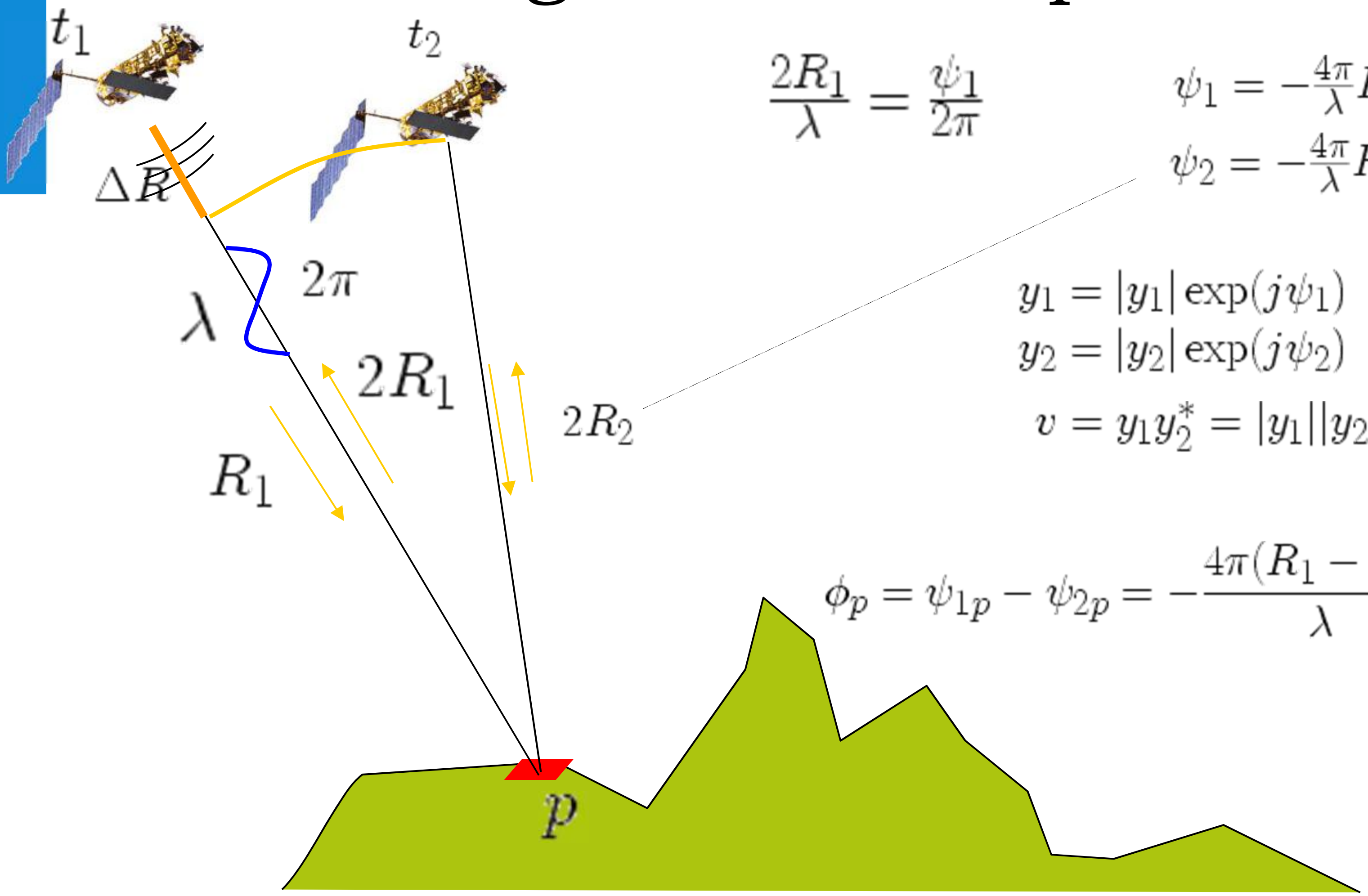

$$\frac{2R_1}{\lambda} = \frac{\psi_1}{2\pi}$$

$$\psi_1 = -\frac{4\pi}{\lambda} R_1$$
$$\psi_2 = -\frac{4\pi}{\lambda} R_2$$

$$y_1 = |y_1| \exp(j\psi_1)$$
$$y_2 = |y_2| \exp(j\psi_2)$$
$$v = y_1 y_2^* = |y_1||y_2| \exp(j(\psi_1 - \psi_2))$$

$$\phi_p = \psi_{1p} - \psi_{2p} = -\frac{4\pi(R_1 - R_2)}{\lambda} = -\frac{4\pi \Delta R}{\lambda}$$

TUDelft

This equation holds for dual-pass InSAR

Phase-height relationship

(Far-field approximation)

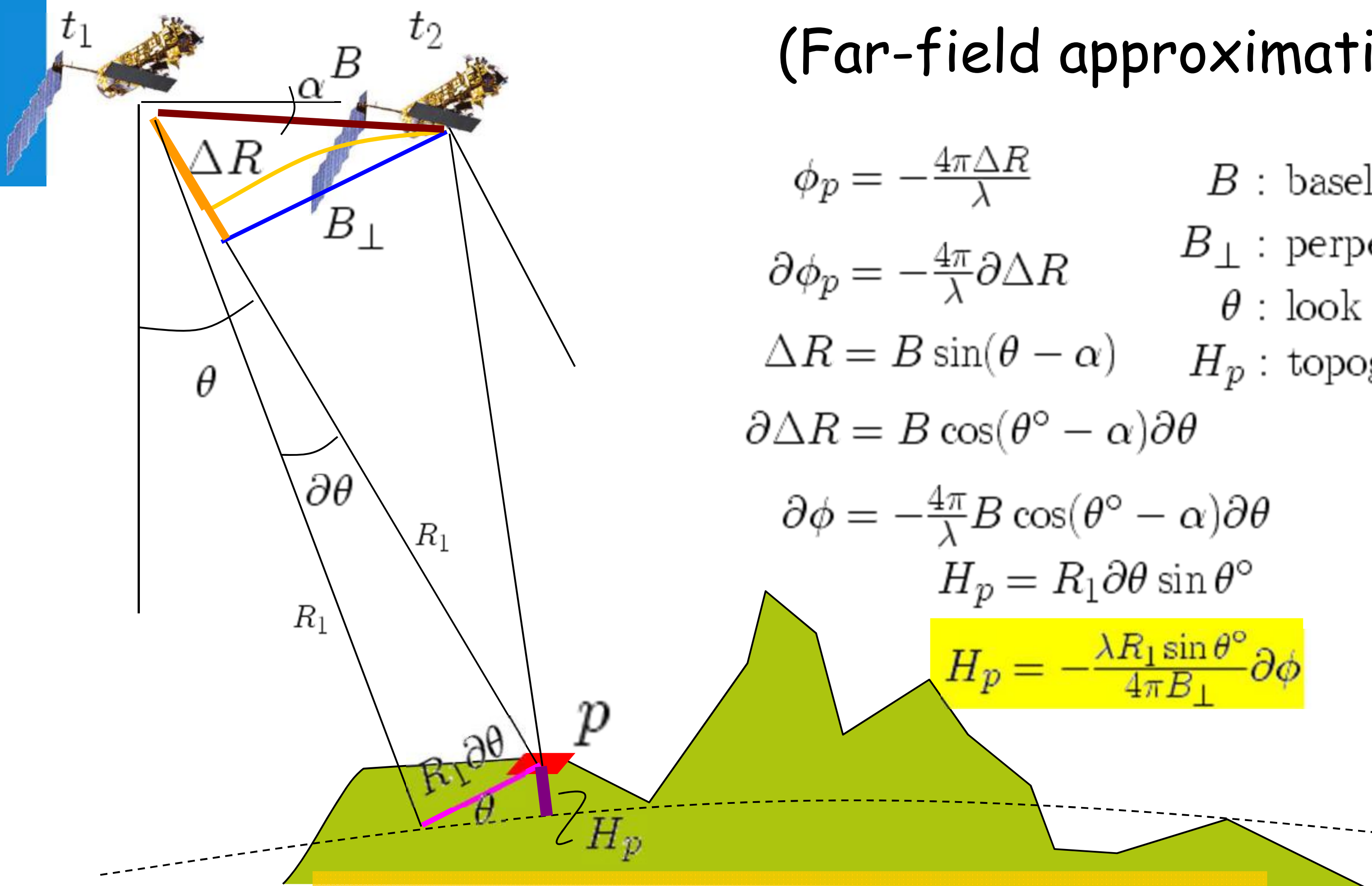

$$\phi_p = -\frac{4\pi\Delta R}{\lambda}$$

$$\partial\phi_p = -\frac{4\pi}{\lambda}\partial\Delta R$$

$$\Delta R = B\sin(\theta - \alpha)$$

$$\partial\Delta R = B\cos(\theta^\circ - \alpha)\partial\theta$$

$$\partial\phi = -\frac{4\pi}{\lambda}B\cos(\theta^\circ - \alpha)\partial\theta$$

$$H_p = R_1\partial\theta\sin\theta^\circ$$

$$H_p = -\frac{\lambda R_1\sin\theta^\circ}{4\pi B_\perp}\partial\phi$$

B : baseline
$B_\perp$: perpendicular baseline
θ : look angle
H_p : topographic height

Topographic phase is (inversely) scaled by the perpendicular baseline!

Topographic Phase

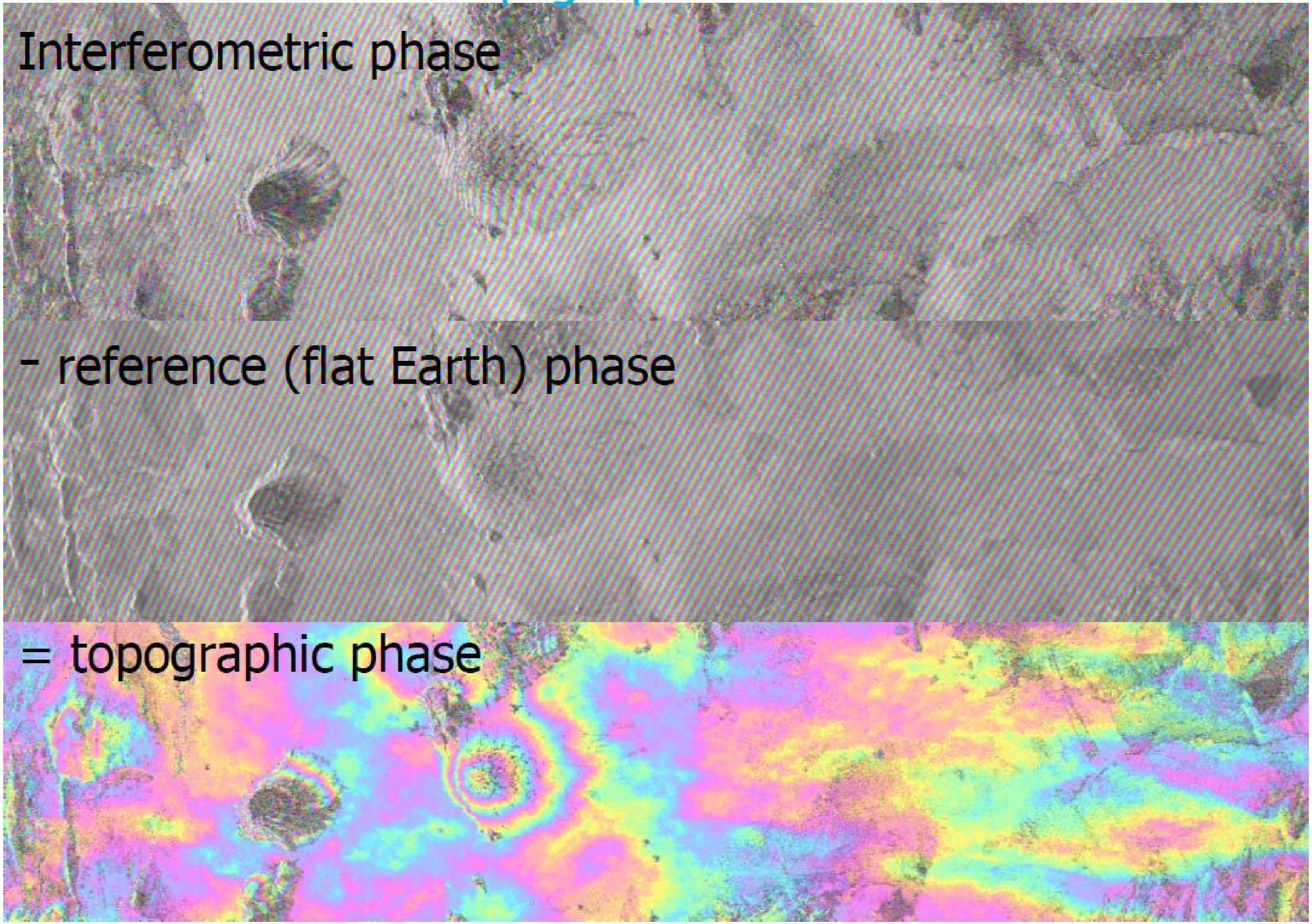

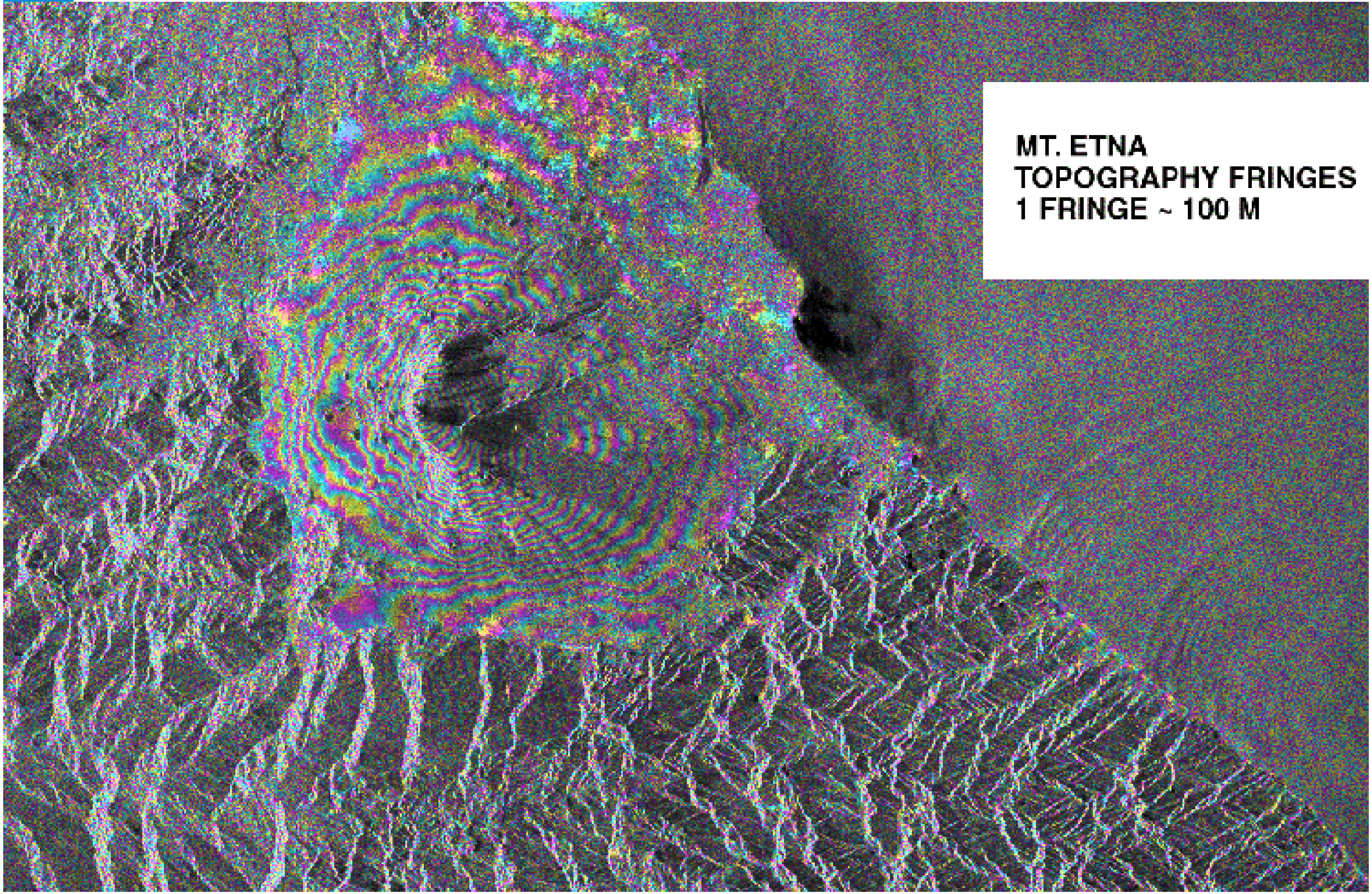
MT. ETNA
TOPOGRAPHY FRINGES
1 FRINGE ~ 100 M

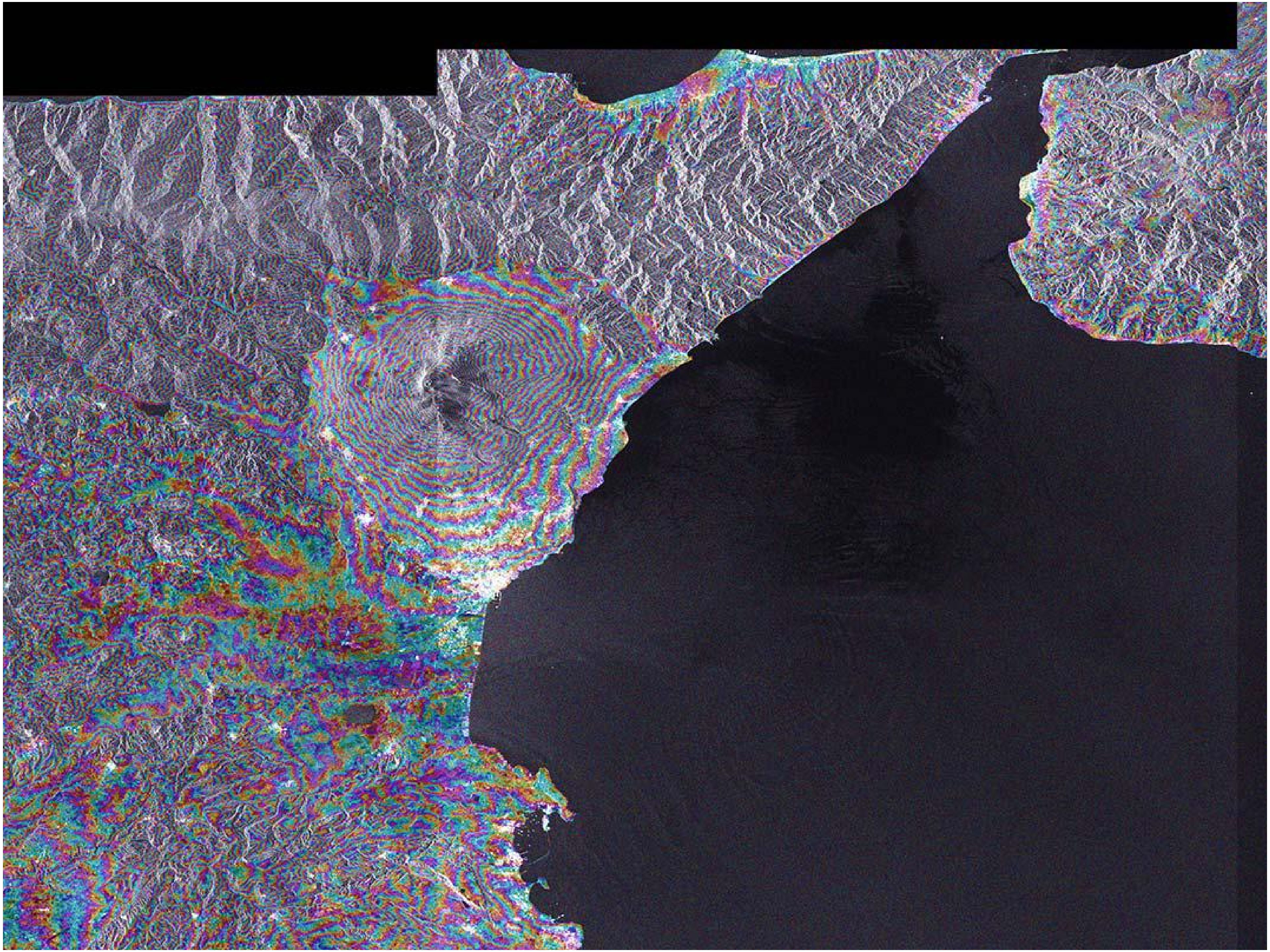

Height ambiguity

$$H_p = -\frac{\lambda R_1 \sin\theta^\circ}{4\pi B_\perp}\partial\phi$$

Height difference related to 1 phase cycle:

$$H_{2\pi} = \frac{-\lambda R_1 \sin\theta^\circ}{4\pi B_\perp}2\pi = \frac{-\lambda R_1 \sin\theta^\circ}{2B_\perp}$$

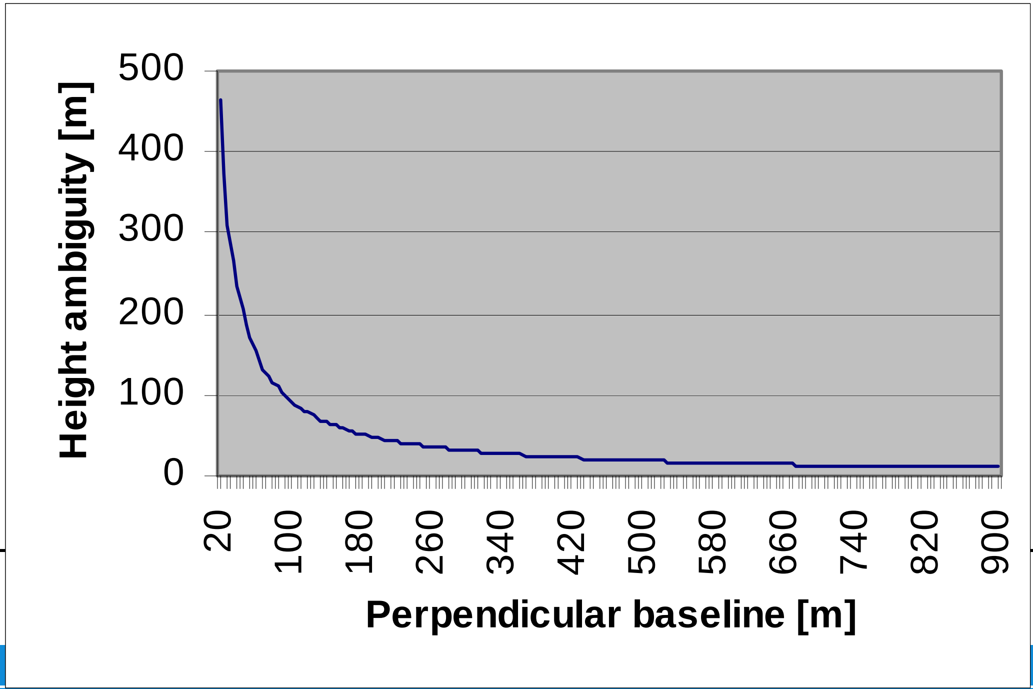

Baseline dependency, height ambiguity

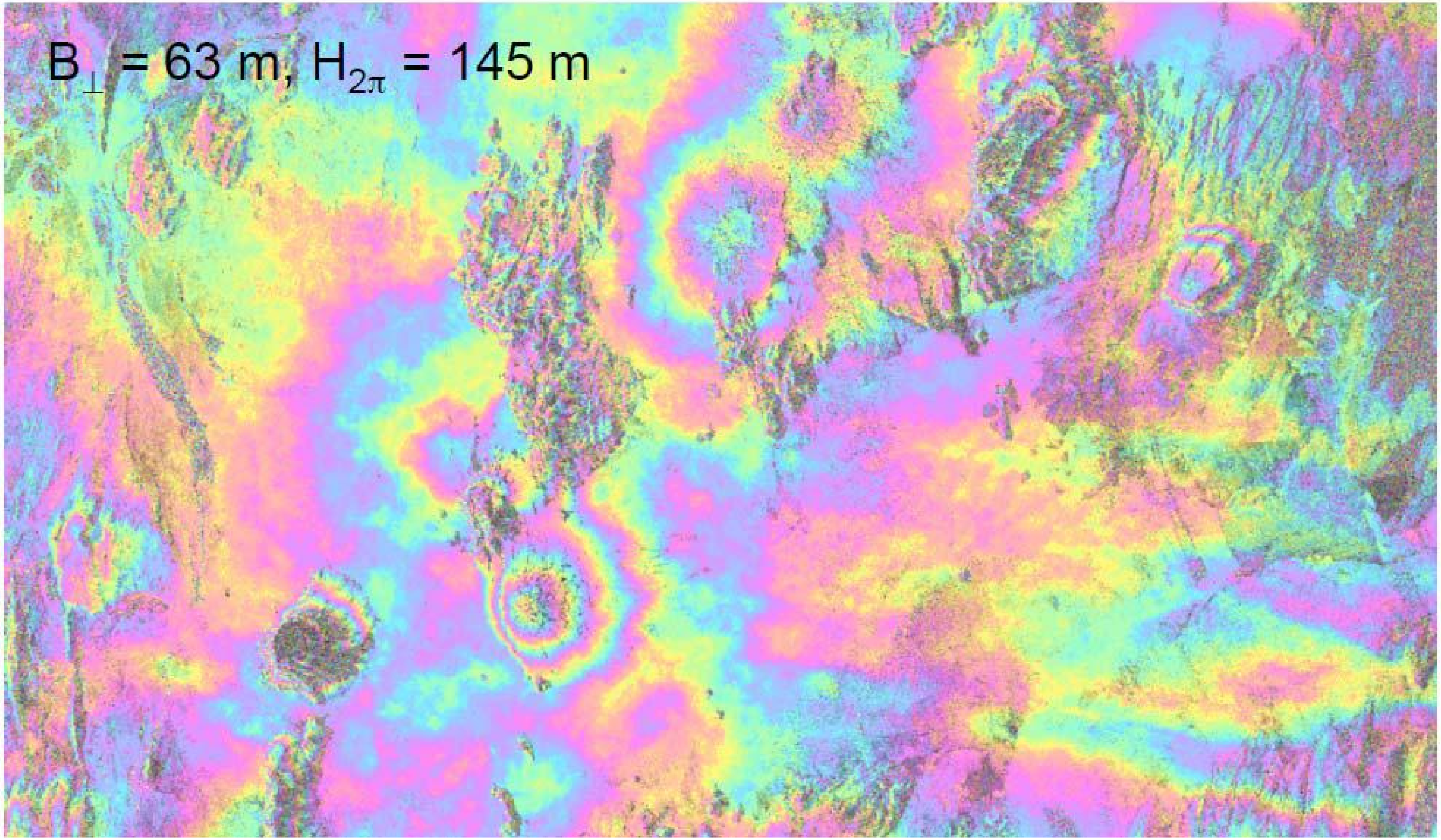

Baseline dependency, height ambiguity

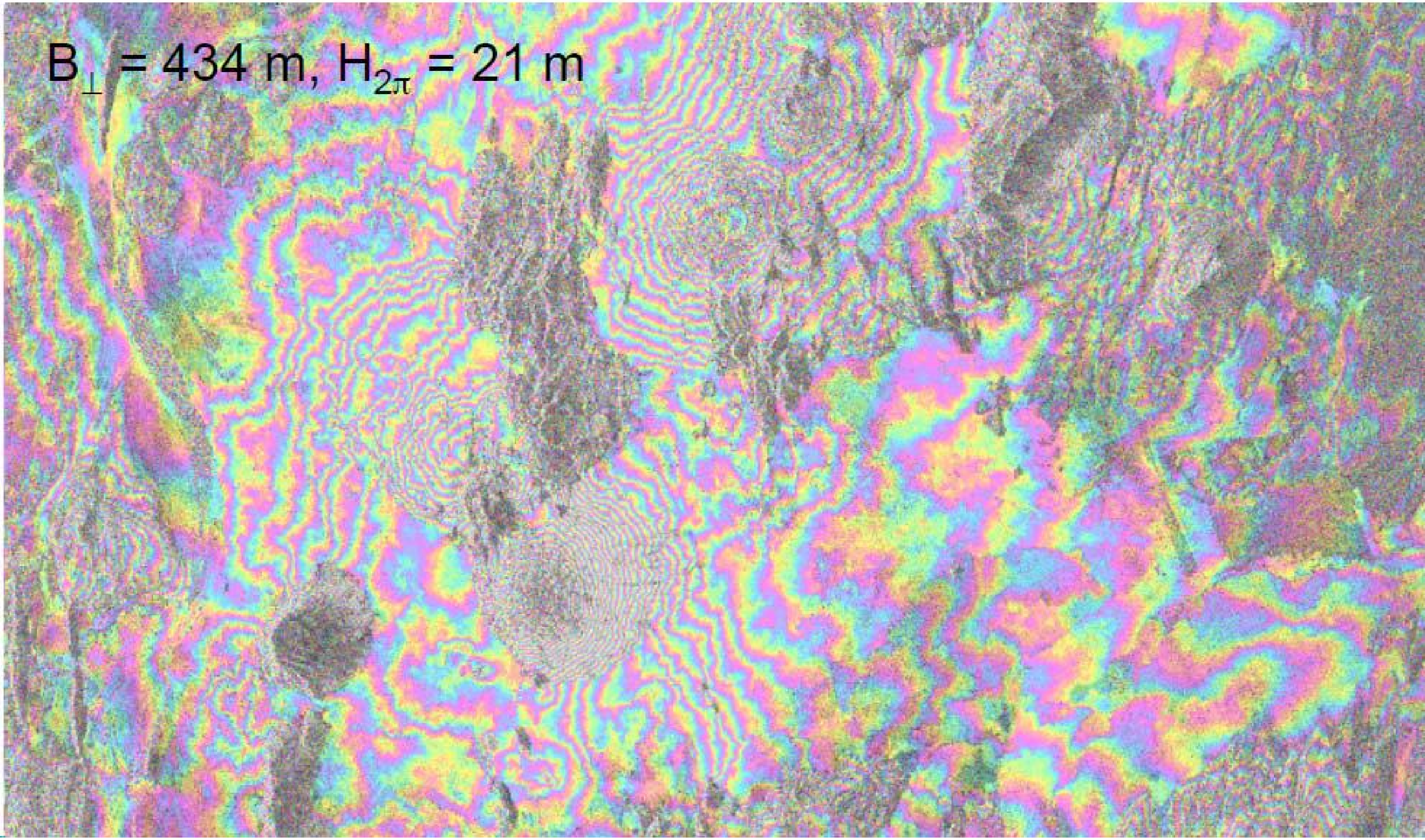

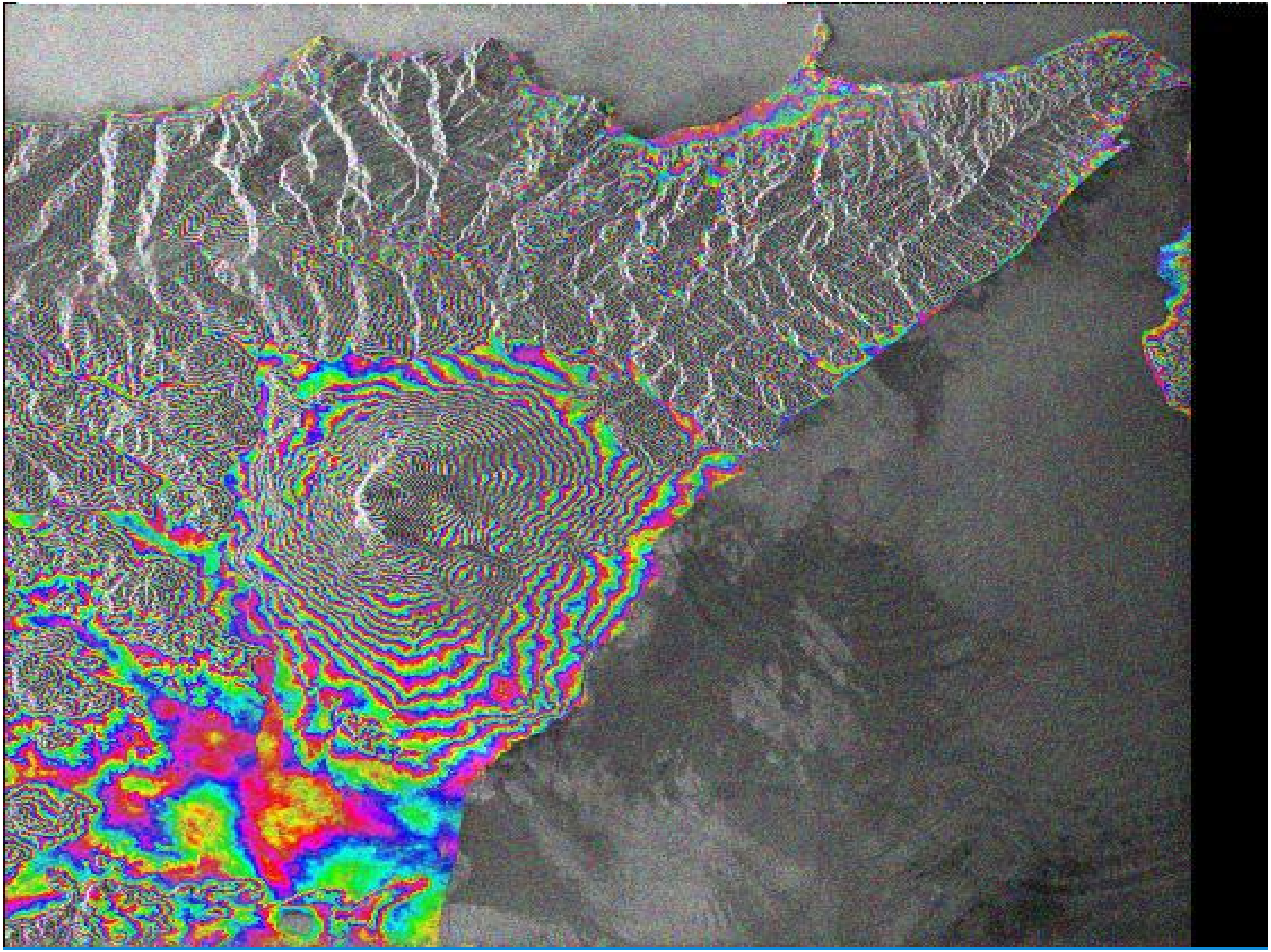

Baseline dependency, height ambiguity

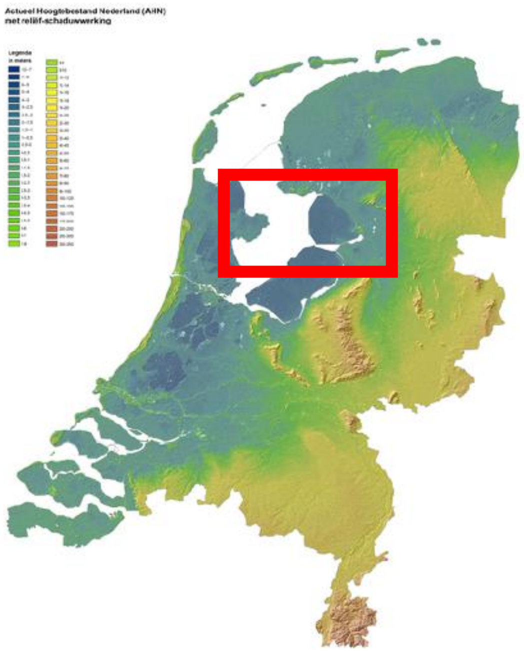

Bperp 173 m, Bt= 1day

H_{2pi}=45m

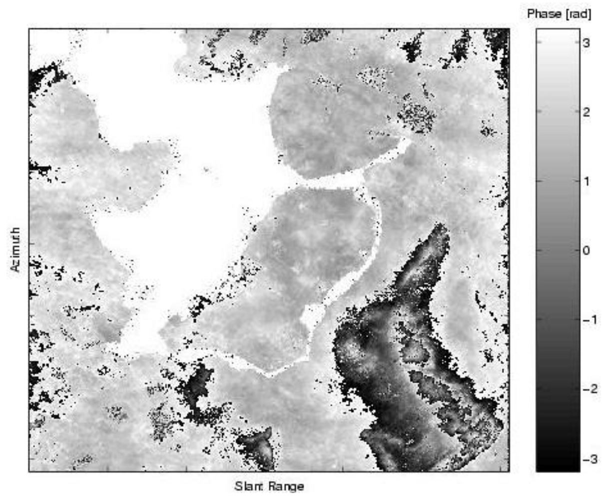

Bperp 531 m, Bt= 1 day

H_{2pi}=16m

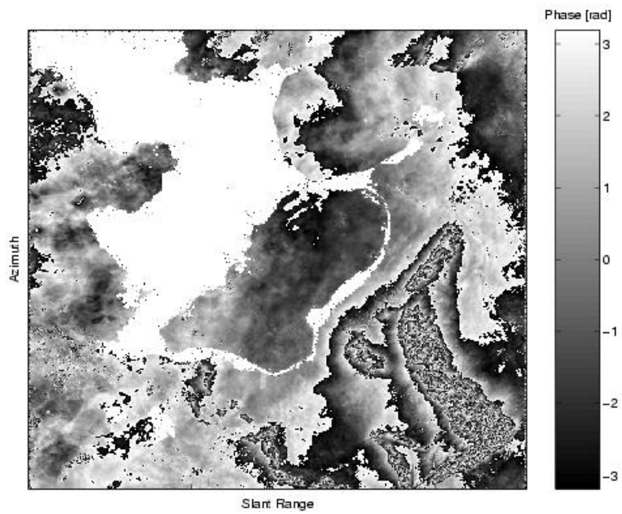

Deformation measurements

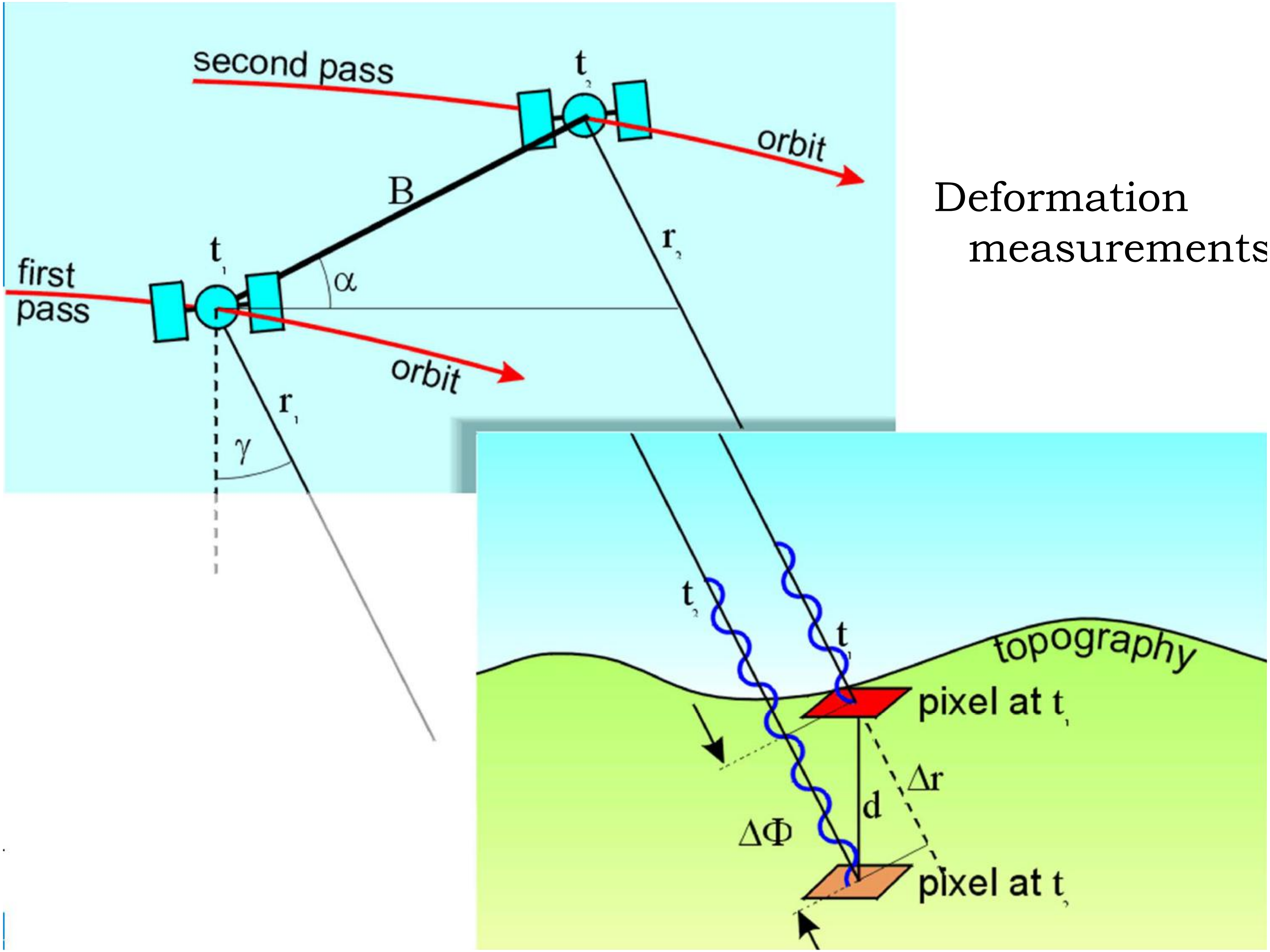

- **Coseismic interferogram, showing deformation Izmit earthquake**
- **Every color cycle 7.5 cm horizontal motion**
- **Showing which segment of fault ruptured**

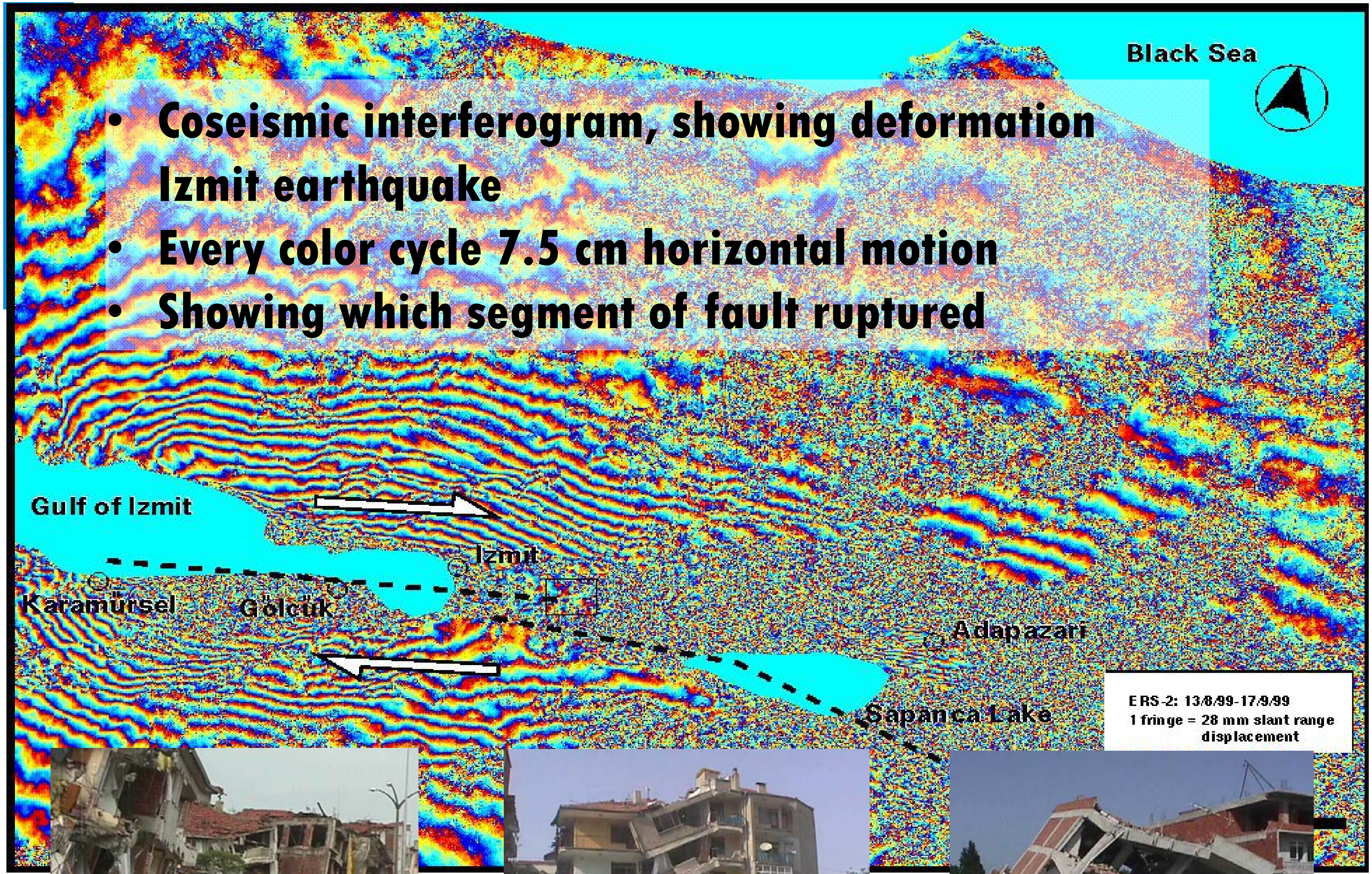

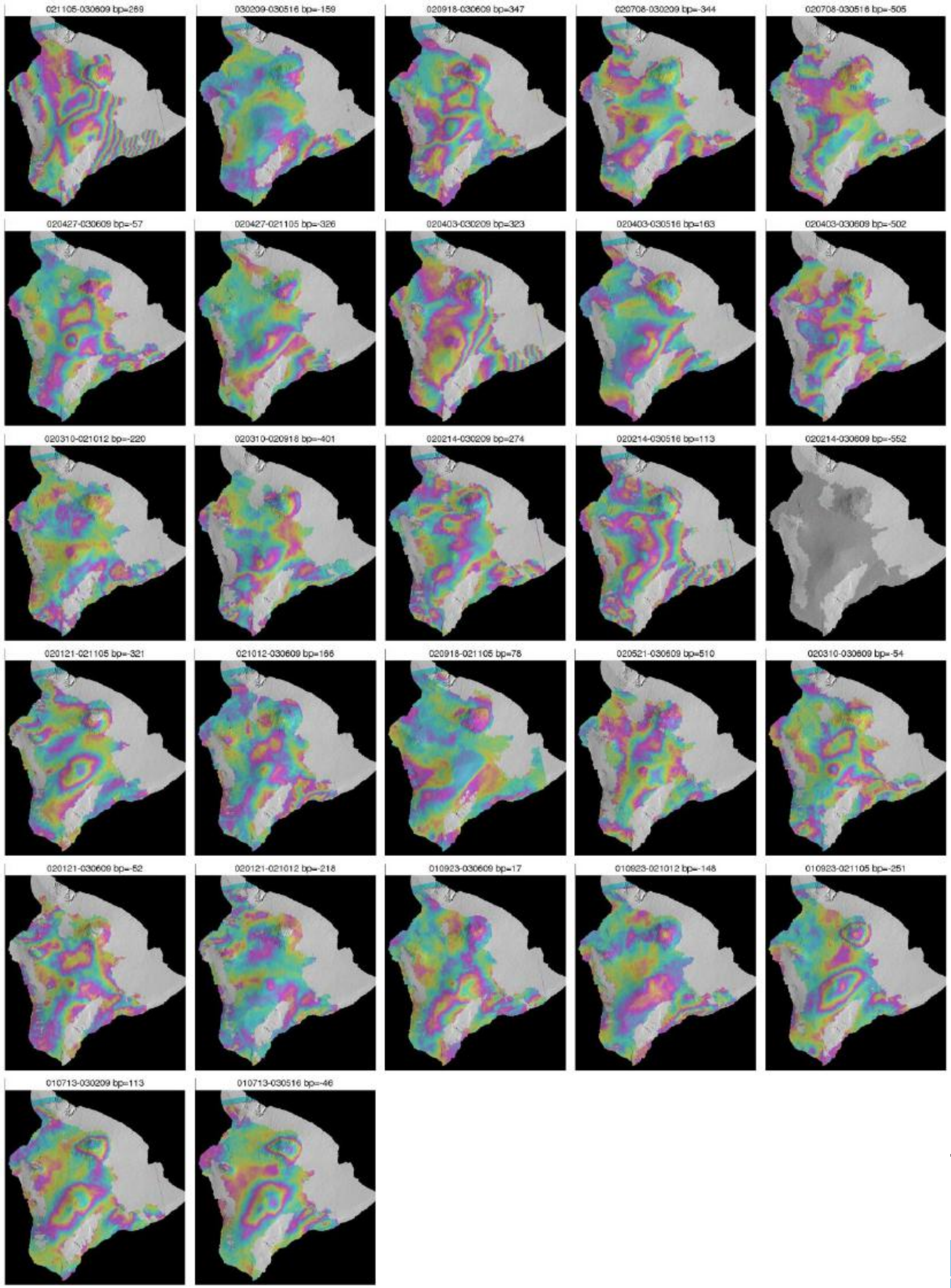

Mauna Loa, Hawaii

- Deformation (inflation) of the Mauna Loa summit
- Position of the magma chamber better determined

…Very sensitive to deformation

Subsidence Las Vegas due to ground water extraction

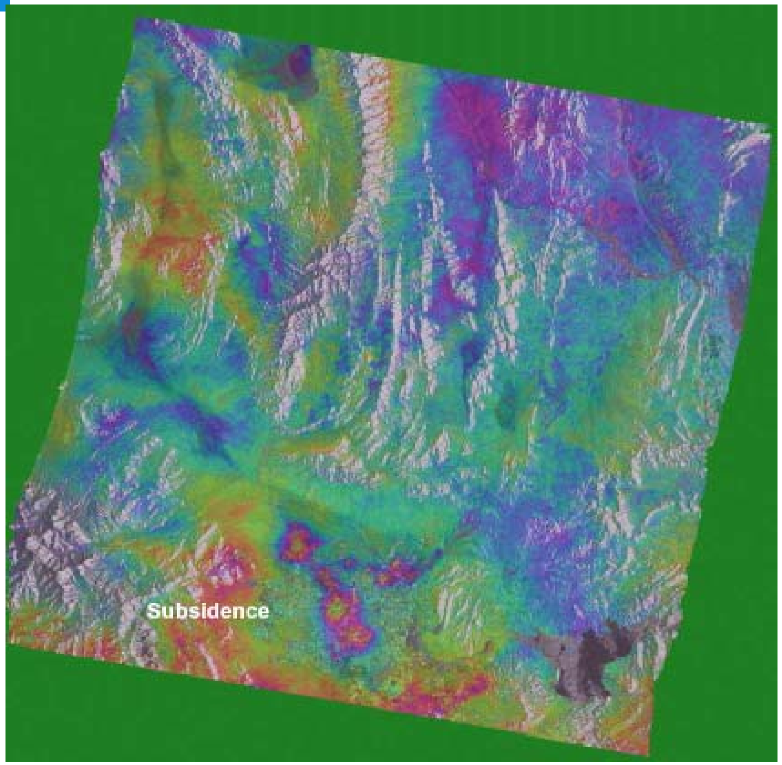

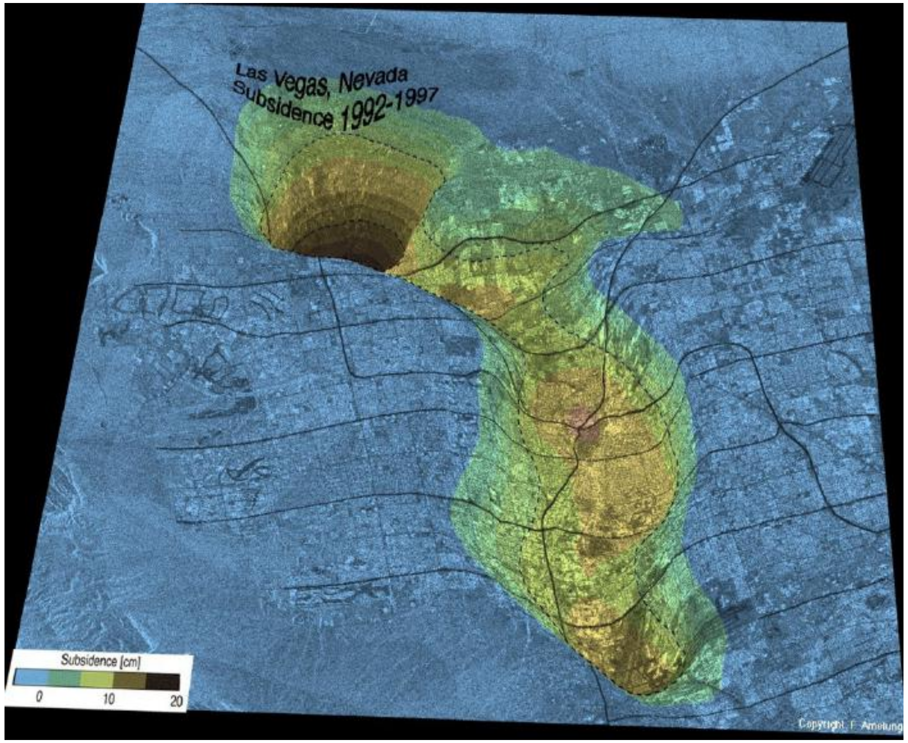

Image: Falk Amelung

Phase-deformation relationship

$$\frac{2R_1}{\lambda} = \frac{\psi_1}{2\pi}$$

$$\psi_1 = -\frac{4\pi}{\lambda}R_1$$
$$\psi_2 = -\frac{4\pi}{\lambda}R_2$$
$$R_2 = R_1 + D_p$$

$$\phi_p = \psi_{1p} - \psi_{2p} = -\frac{4\pi(R_1 - R_2)}{\lambda} =$$

$$\boxed{\phi_p = -\frac{4\pi}{\lambda}D_p}$$

D_p : line-of-sight deformation

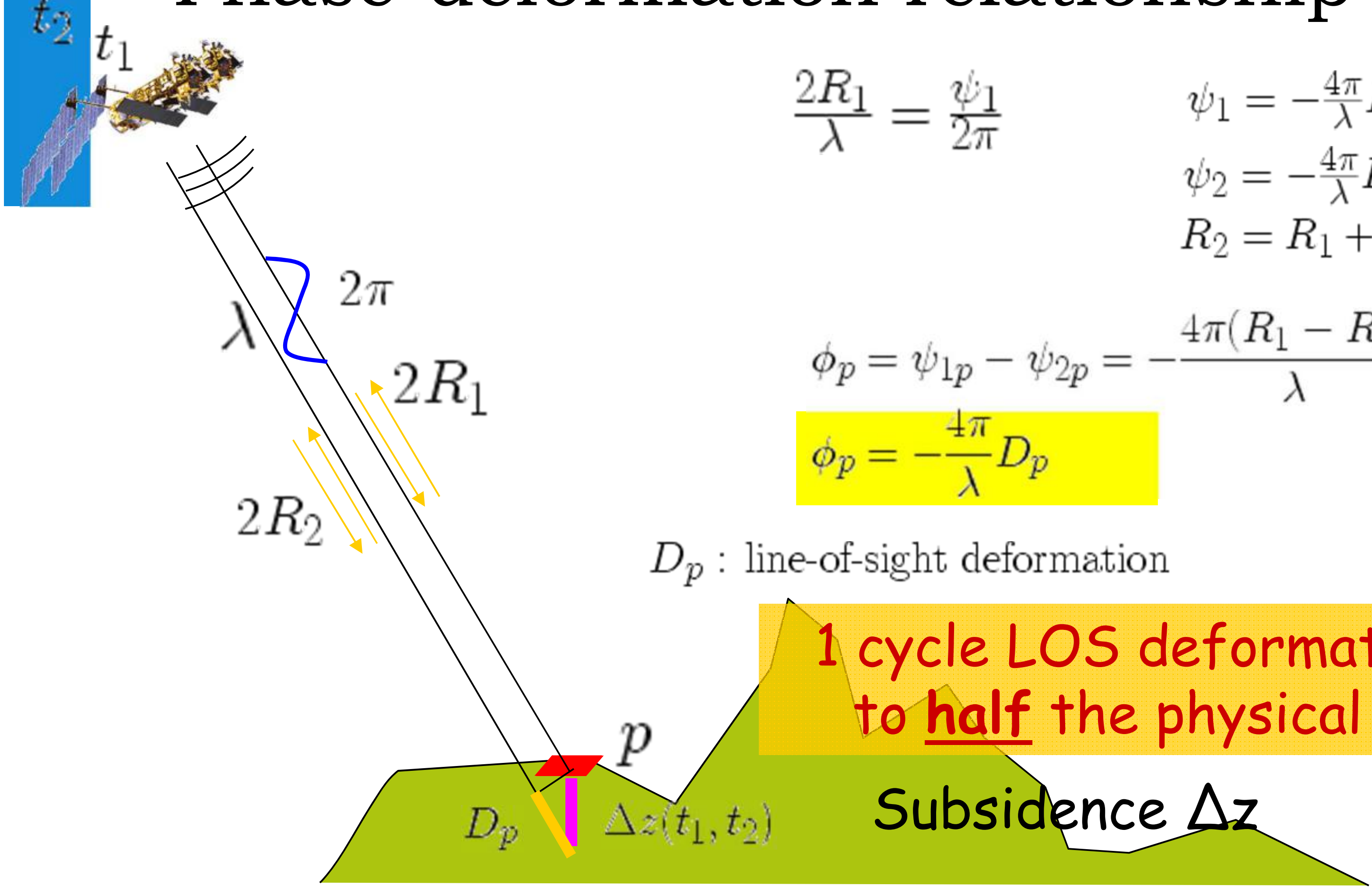

1 cycle LOS deformation is equal to **half** the physical wavelength

Topography and deformation

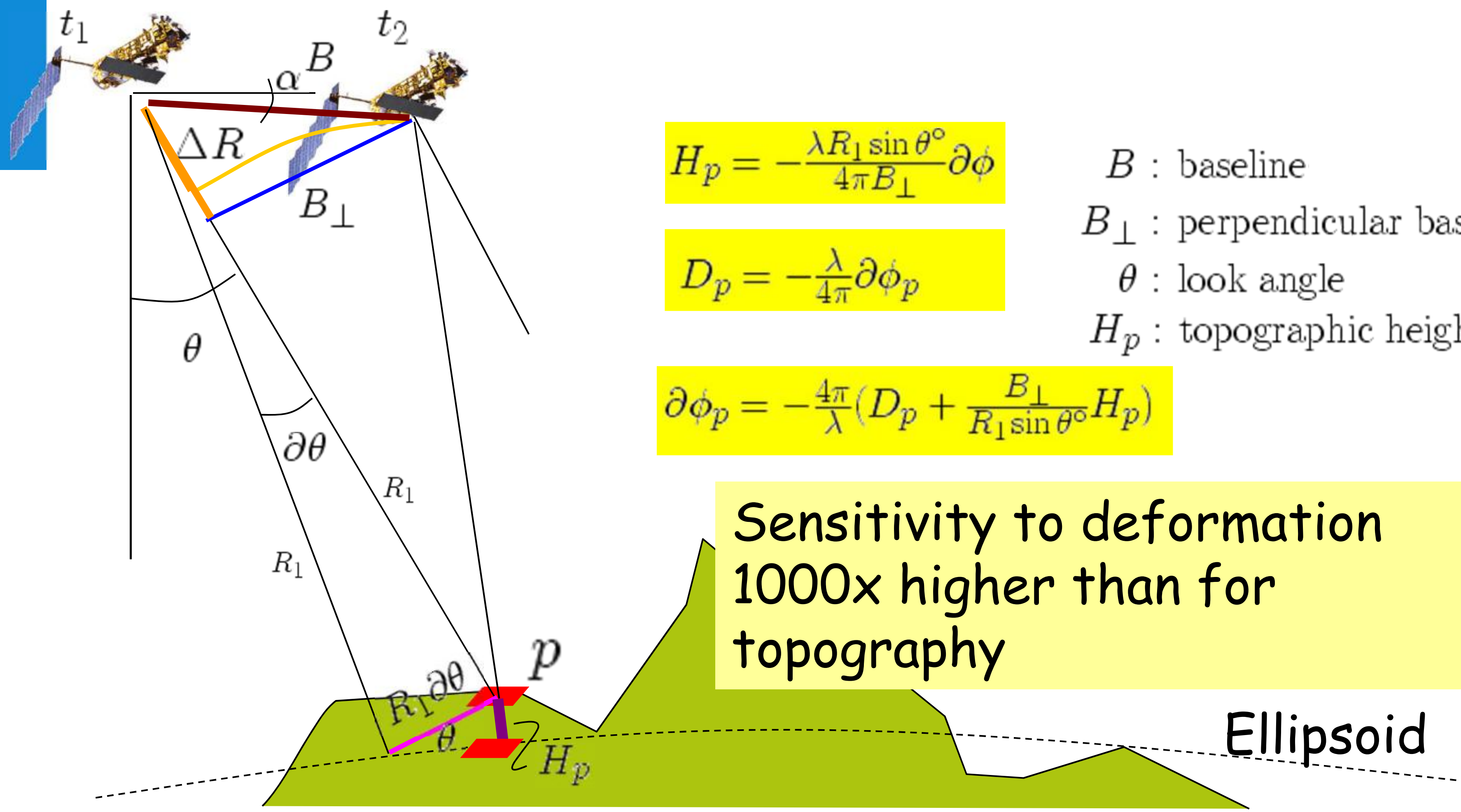

$$H_p = -\frac{\lambda R_1 \sin\theta^\circ}{4\pi B_\perp}\partial\phi$$

$$D_p = -\frac{\lambda}{4\pi}\partial\phi_p$$

$$\partial\phi_p = -\frac{4\pi}{\lambda}\left(D_p + \frac{B_\perp}{R_1 \sin\theta^\circ}H_p\right)$$

B : baseline

$B_\perp$: perpendicular baseline

θ : look angle

H_p : topographic height

Sensitivity to deformation 1000x higher than for topography

InSAR data processing

Coregistration principle

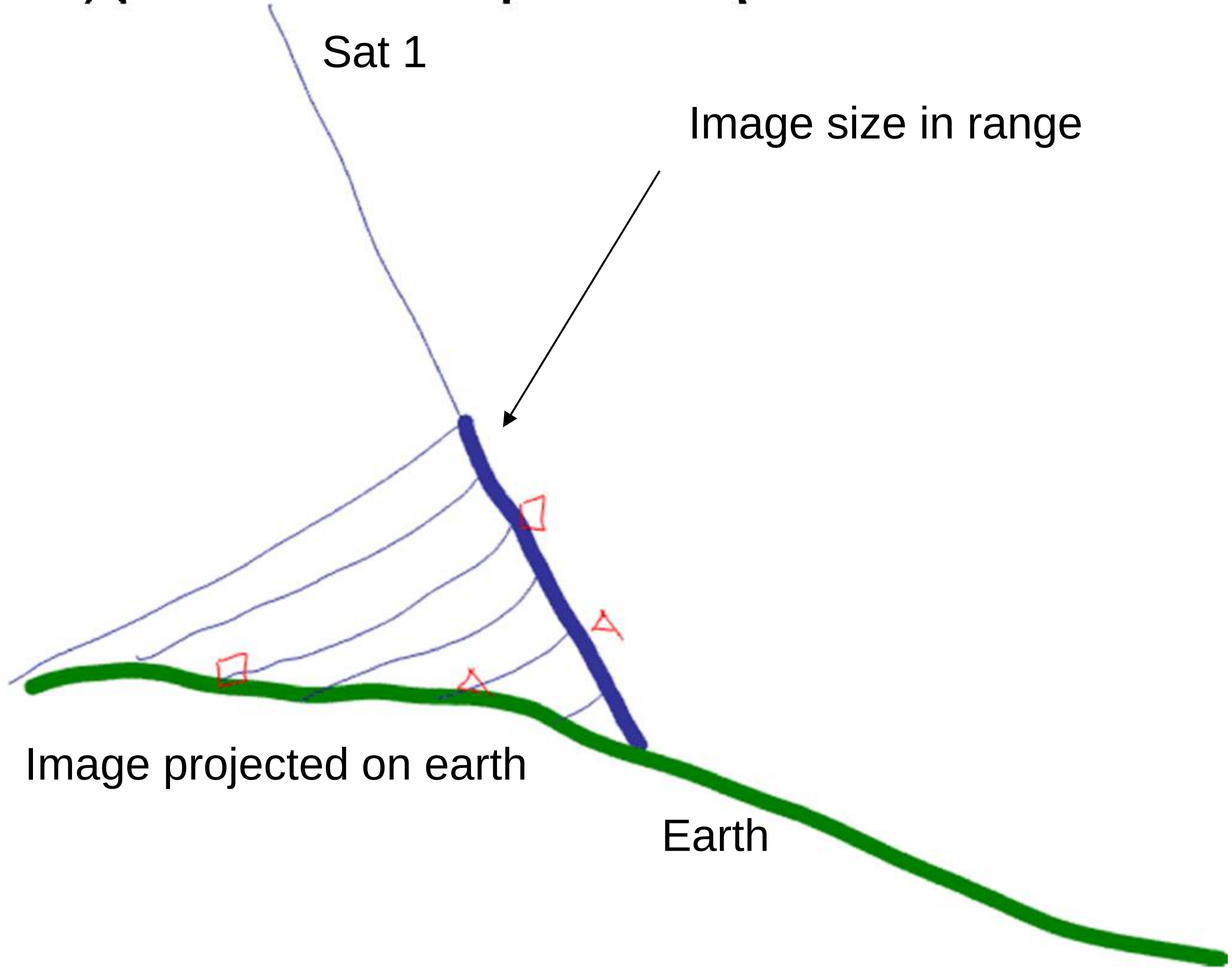

Coregistration principle

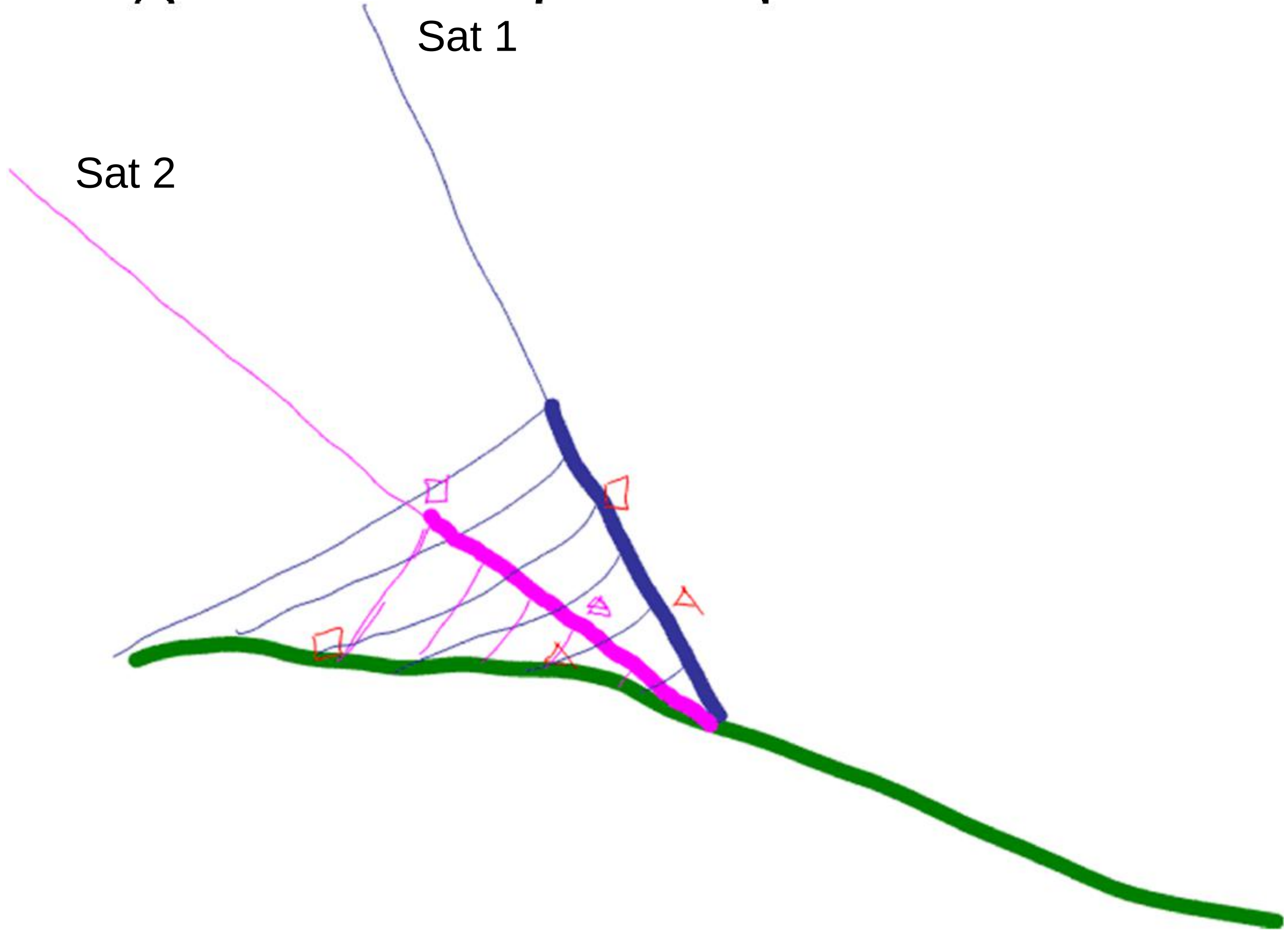

Coregistration principle

The images on your computer: equal size but not matching:

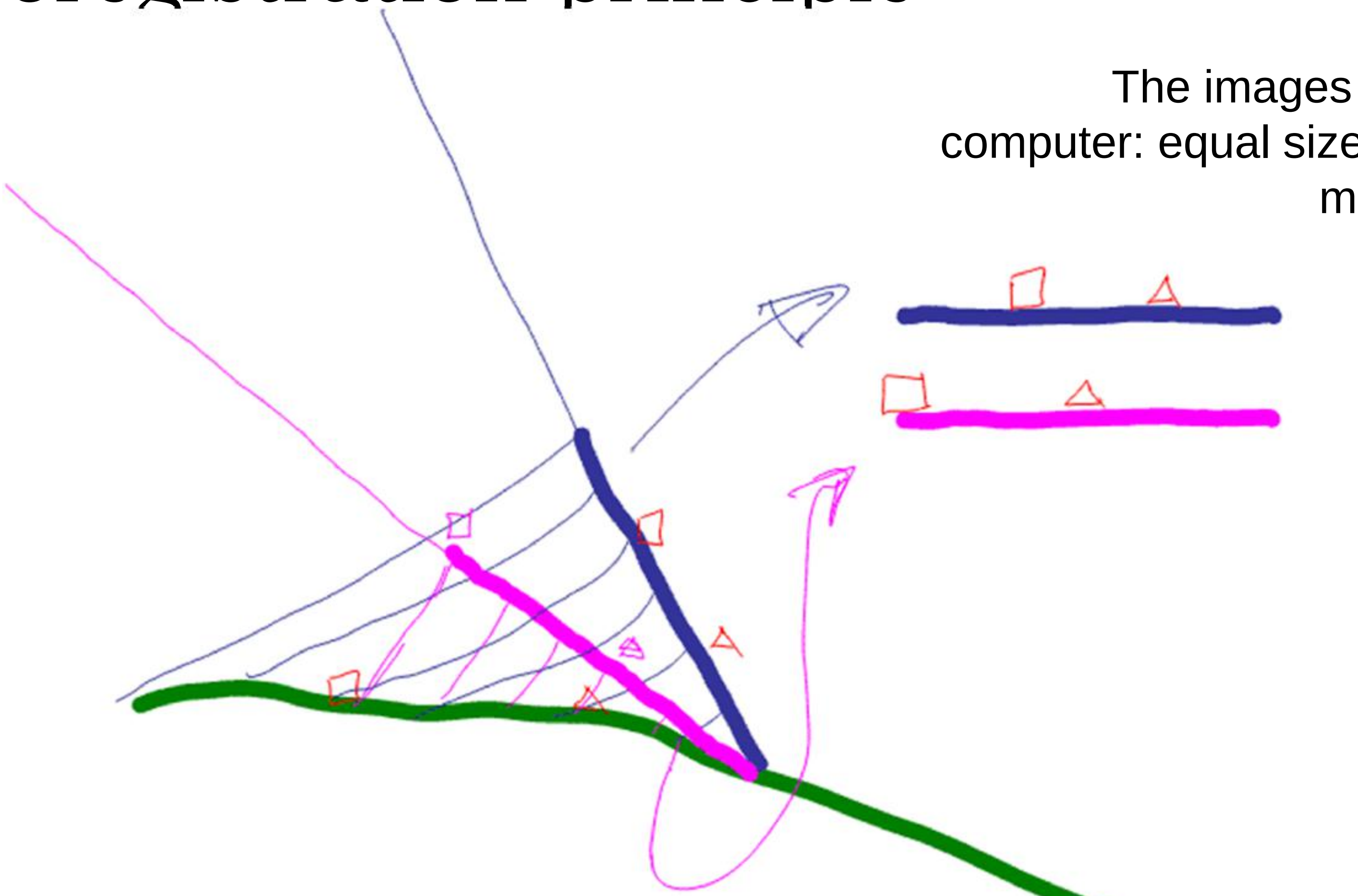

Coregistration principle

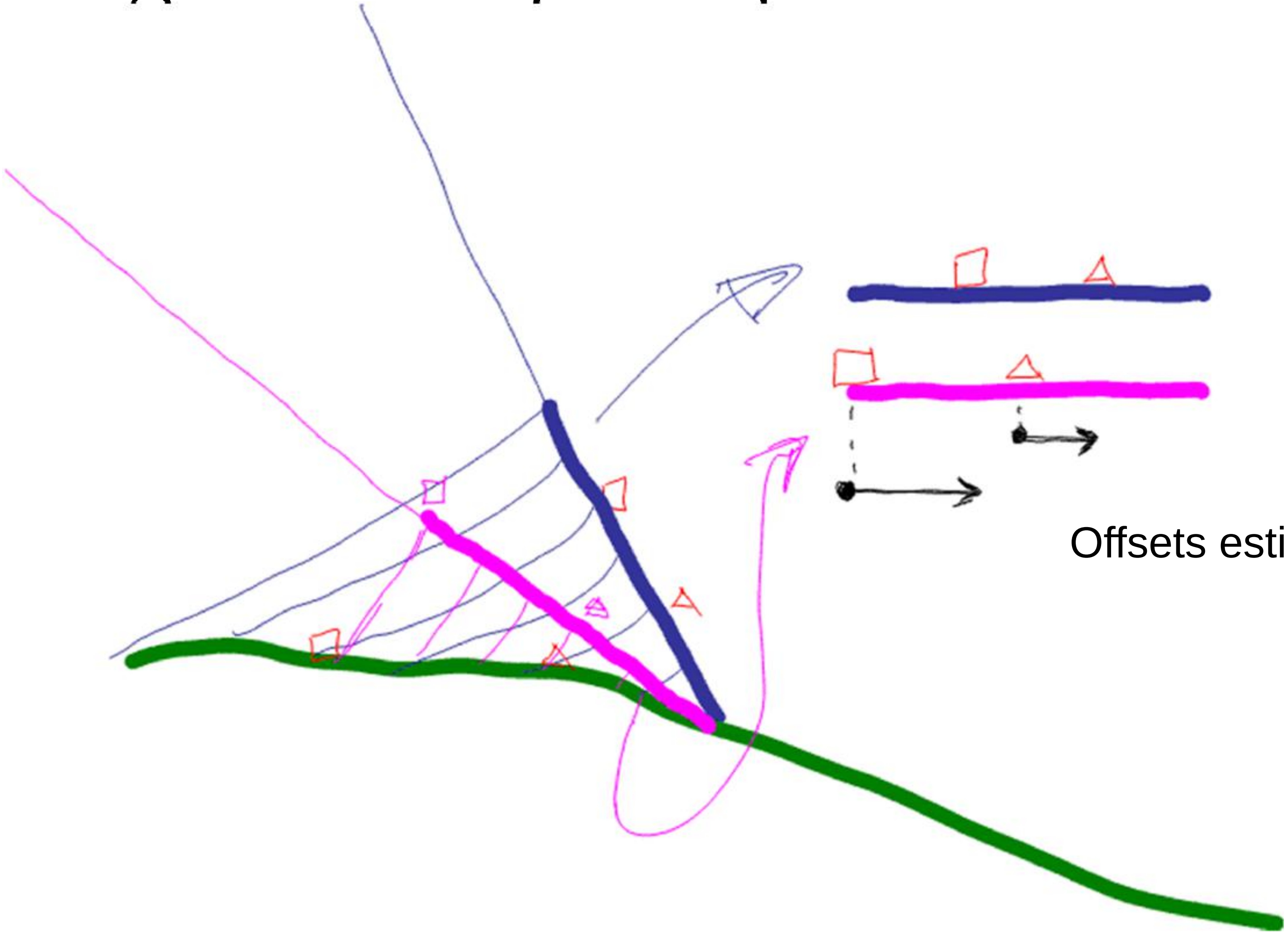

Offsets estimated

Coregistration principle

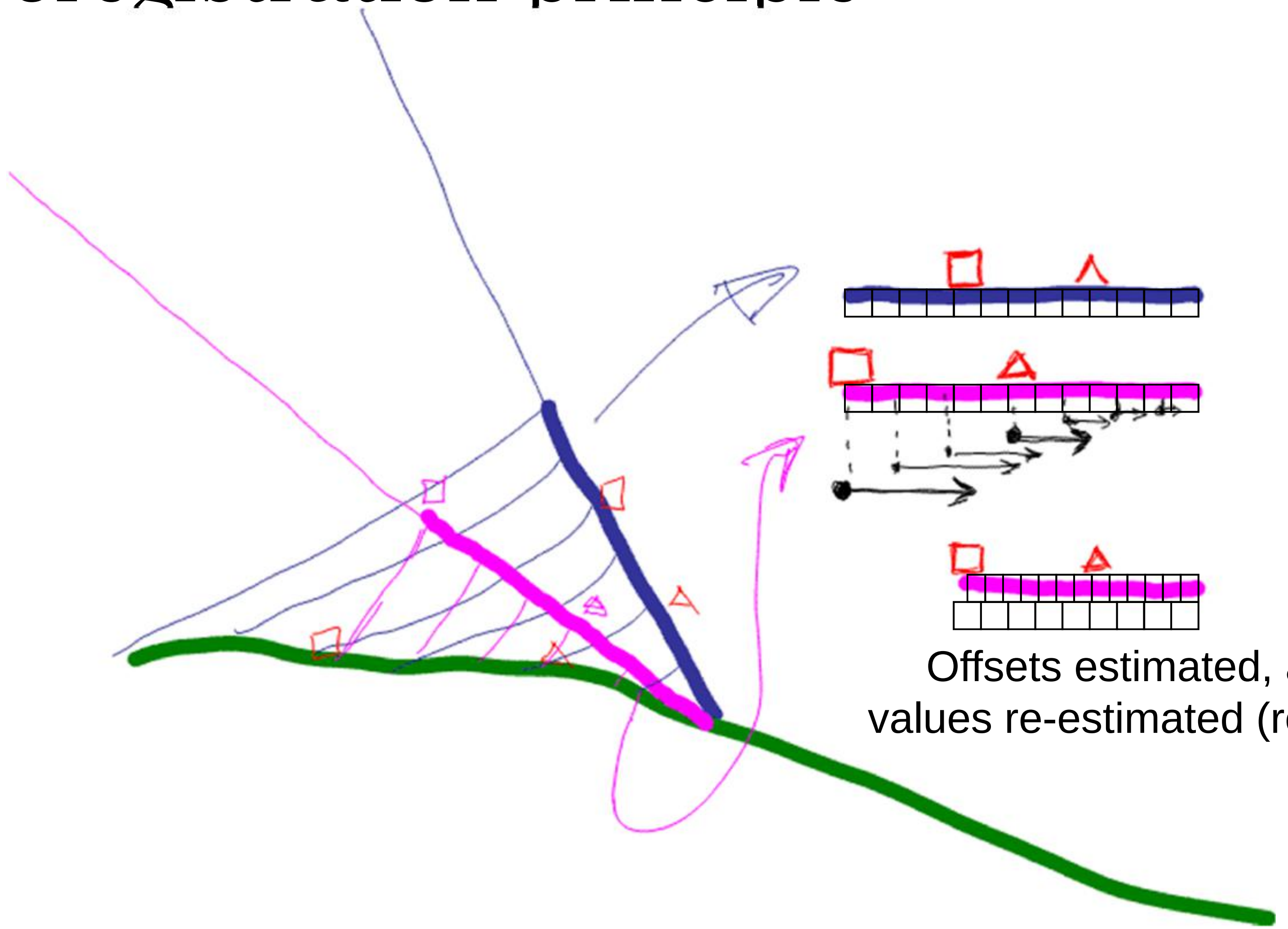

Offsets estimated, and image values re-estimated (resampled)

Offset vectors in 2D

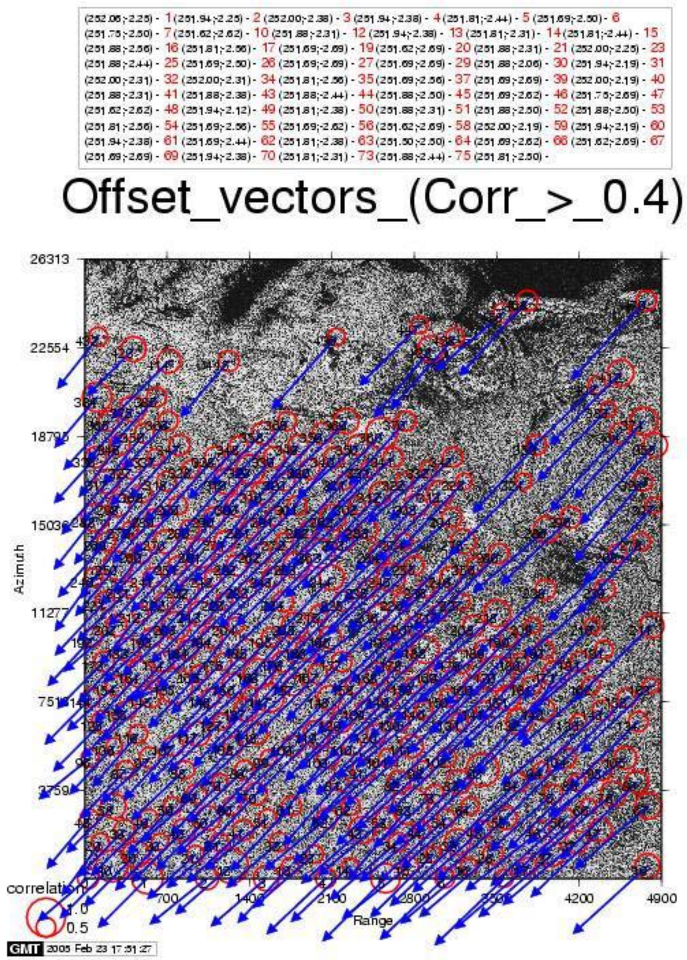

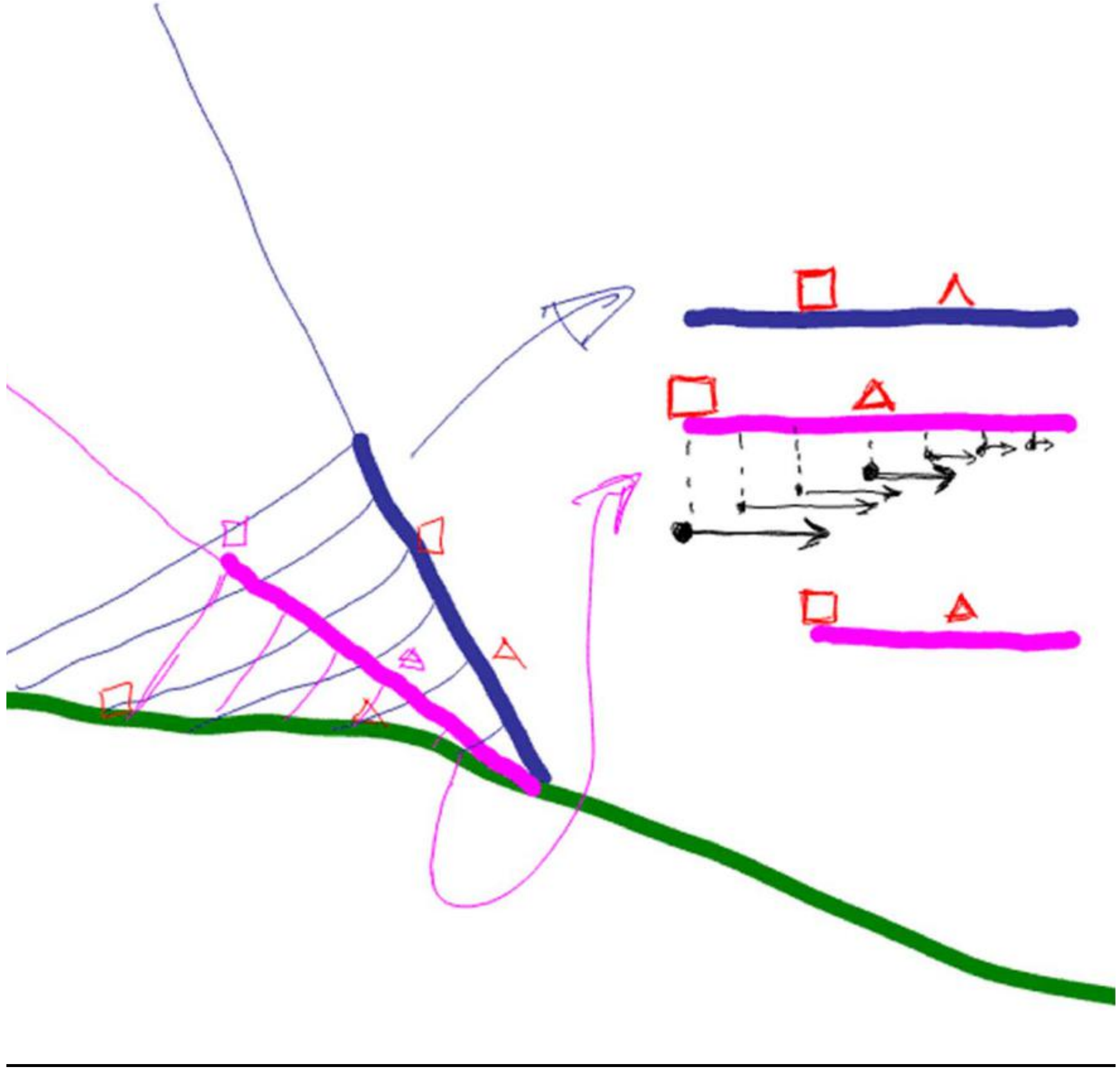

Step 1: orbit-based

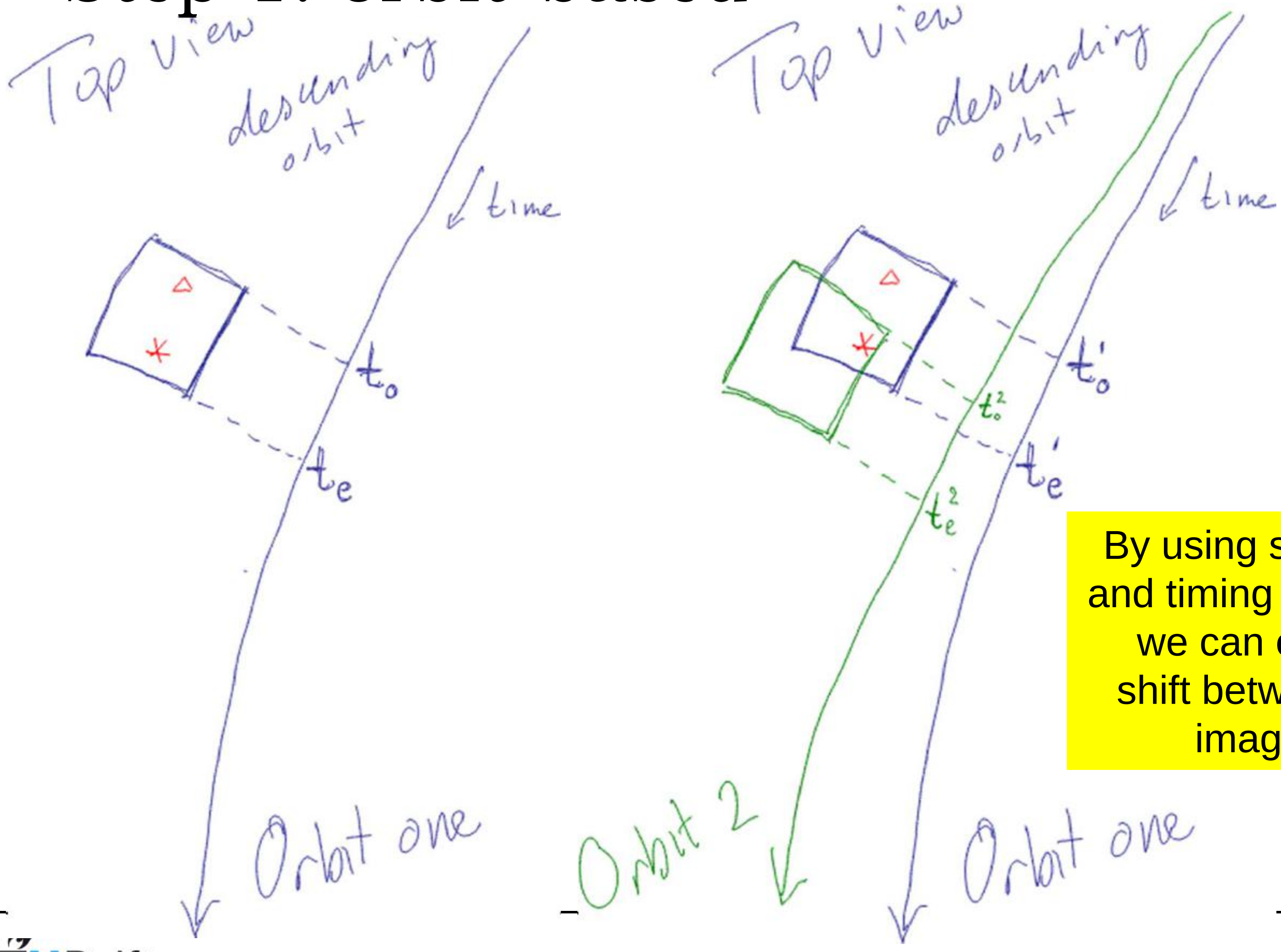

By using satellite orbit and timing information, we can estimate the shift between the two images (roughly)

Coregistration

- **Sampling is different for the two acquisitions**

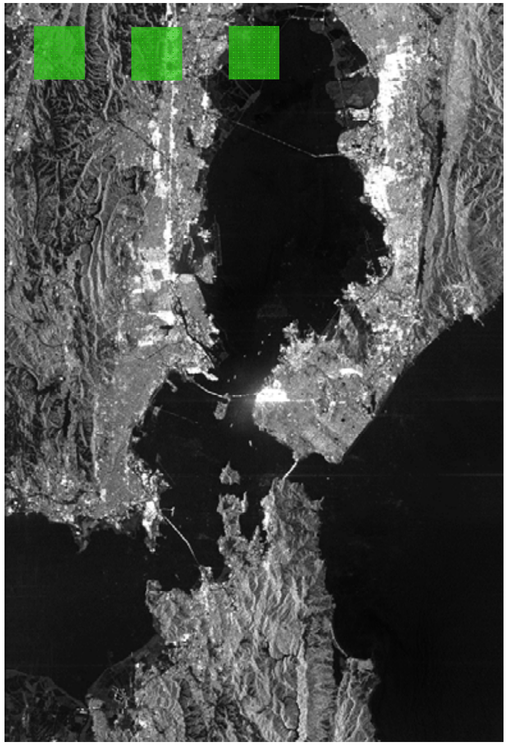

Master

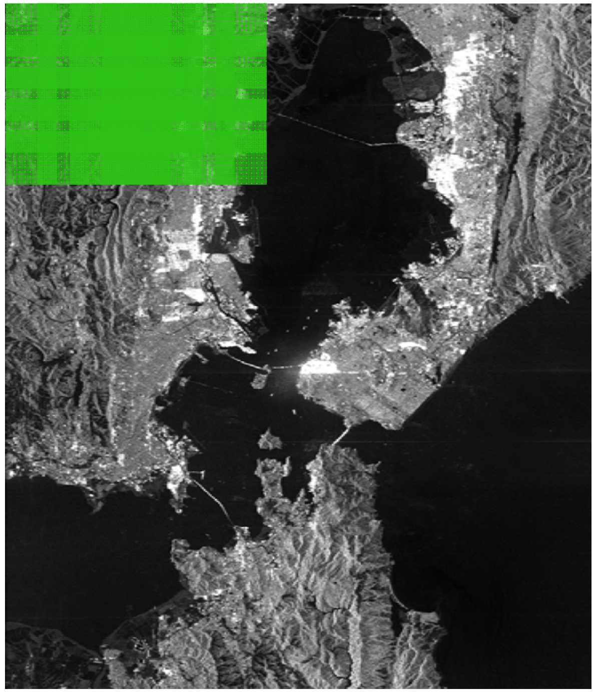

Slave

- **Use amplitude cross-correlation**

Master-Slave Offsets

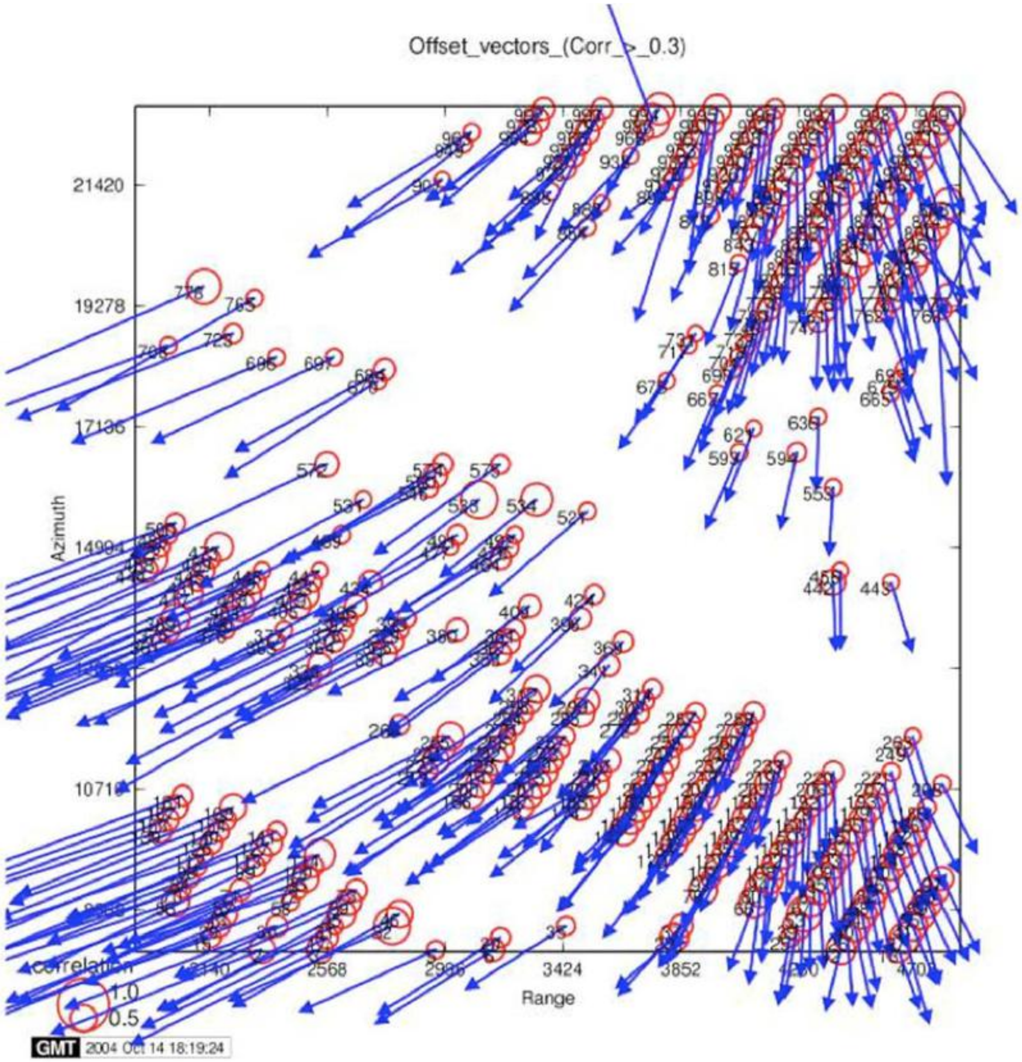

Fit a polynomial,
and remove outliers

Resampling

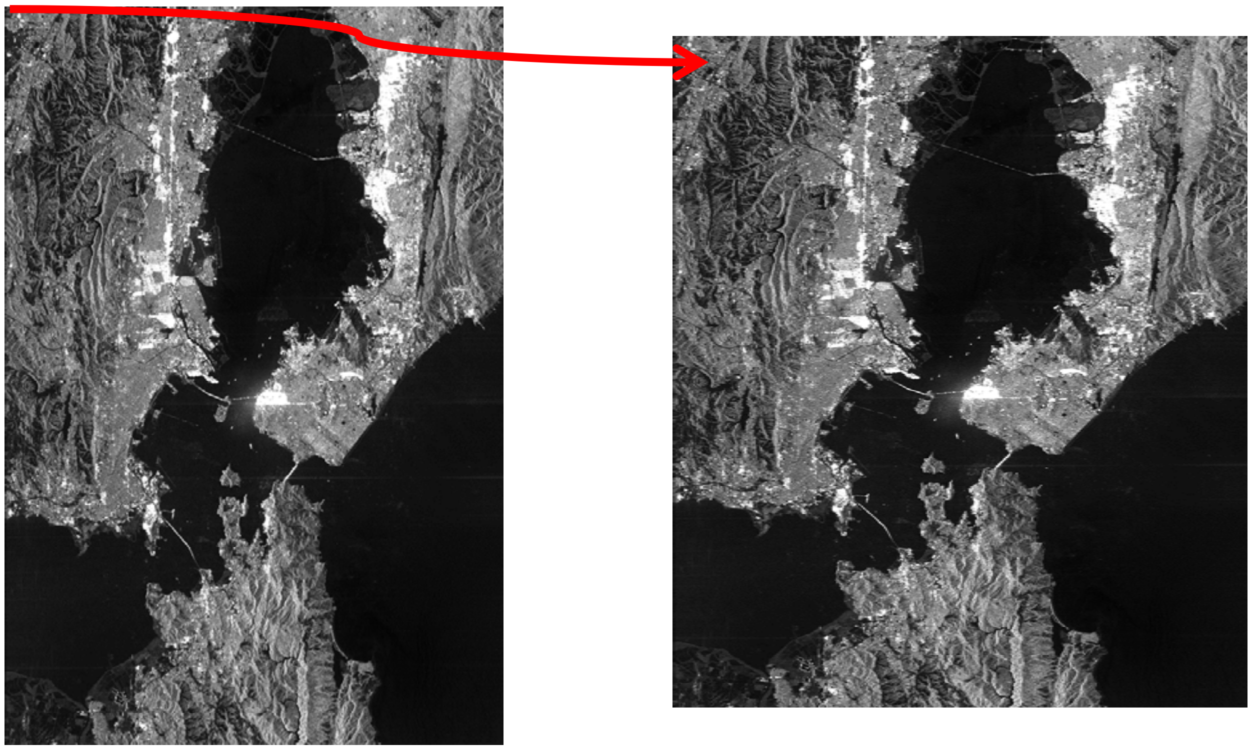

- Use polynomial to calculate position of each master pixel in slave
- Interpolate value in slave

Interpolation/resampling

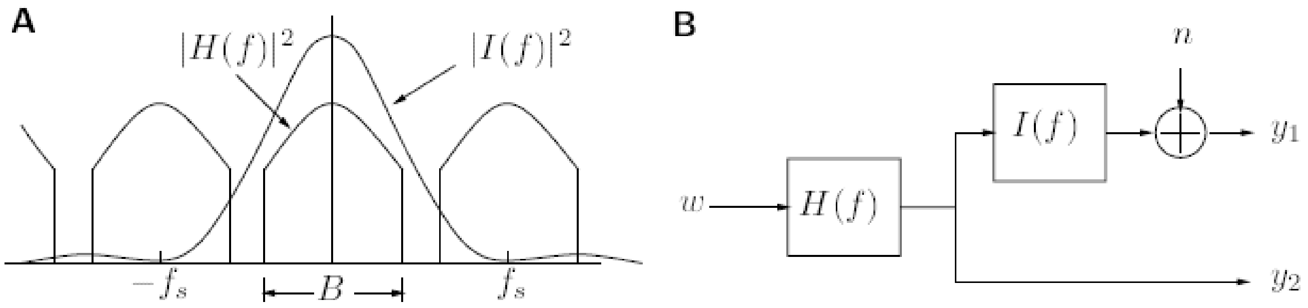

- Interpolation kernel should cover main spectrum, and minimal amount of replica's

Filtering - Range

- Required to remove non-overlapping spectral parts

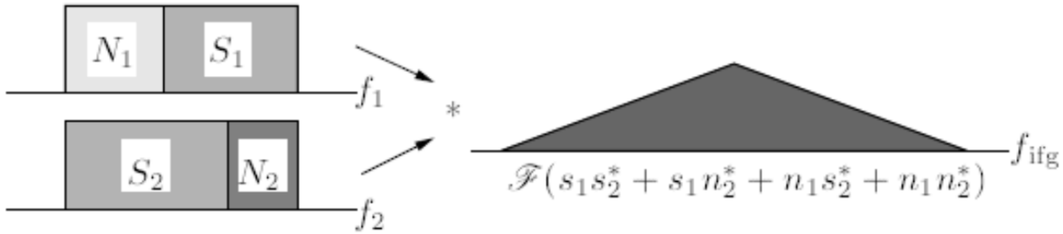

The convolution of two spectra with a distinct signal (S_1, S_2) and noise (N_1, N_2) component, where $\mathscr{F}(s_1) = S_1$. In the convolution (the product of the original data), the noise components n_1 and n_2 appear smeared over the spectrum.

- Wavenumber shift is baseline dependent

Interferogram formation

$$y_1 y_2^* = |y_1| e^{j\varphi_1} |y_2| e^{-j\varphi_2} = |y_1||y_2| e^{j(\varphi_1 - \varphi_2)}$$

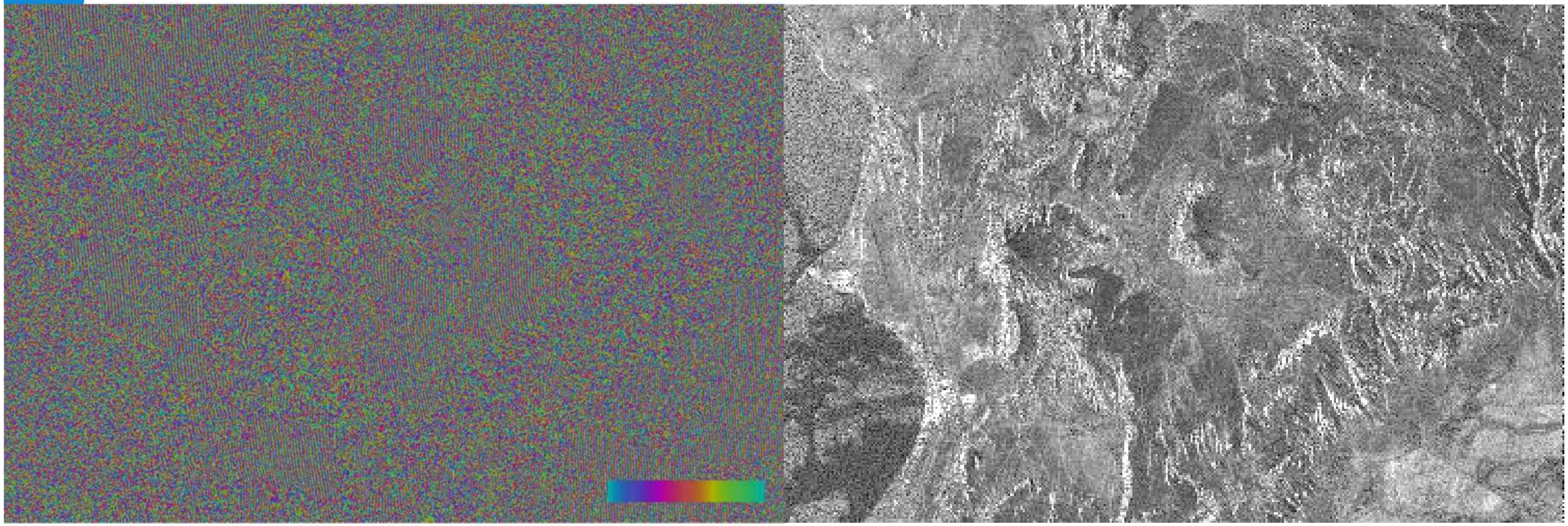

Phase contributions: reference surface+topography+deformation+atmosphere+noise

Subtract reference phase

Rule of thumb

Bperp=100m -> H_amb=100m

Bperp=200m -> H_amb=50m

Bperp=400m -> H_amb=25m

Topo-pair

- ref_phase   Bperp=380m ; H_amb=23m; Btemp=35days

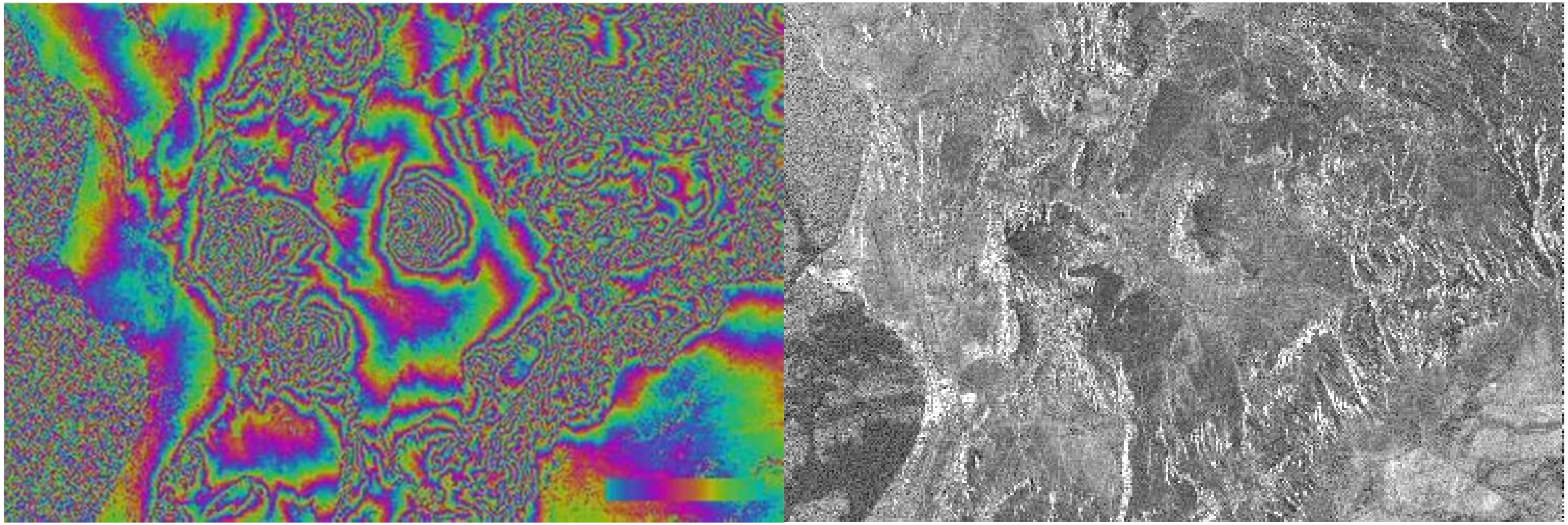

Phase contributions: **topography**+deformation+atmosphere+noise

Phase ambiguity estimation

(AKA Phase unwrapping. Essentially means counting fringes)

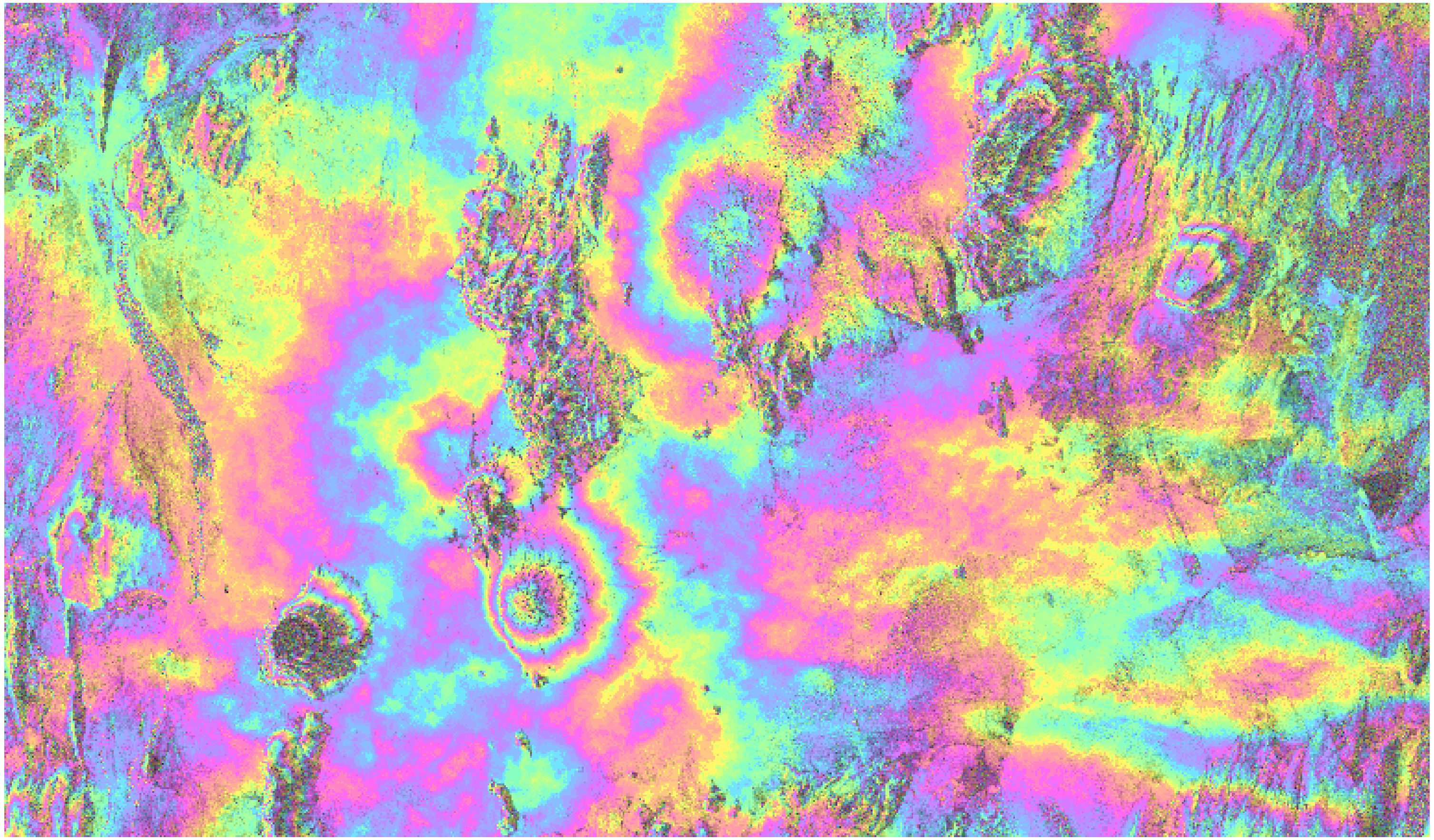

June 2, 2016

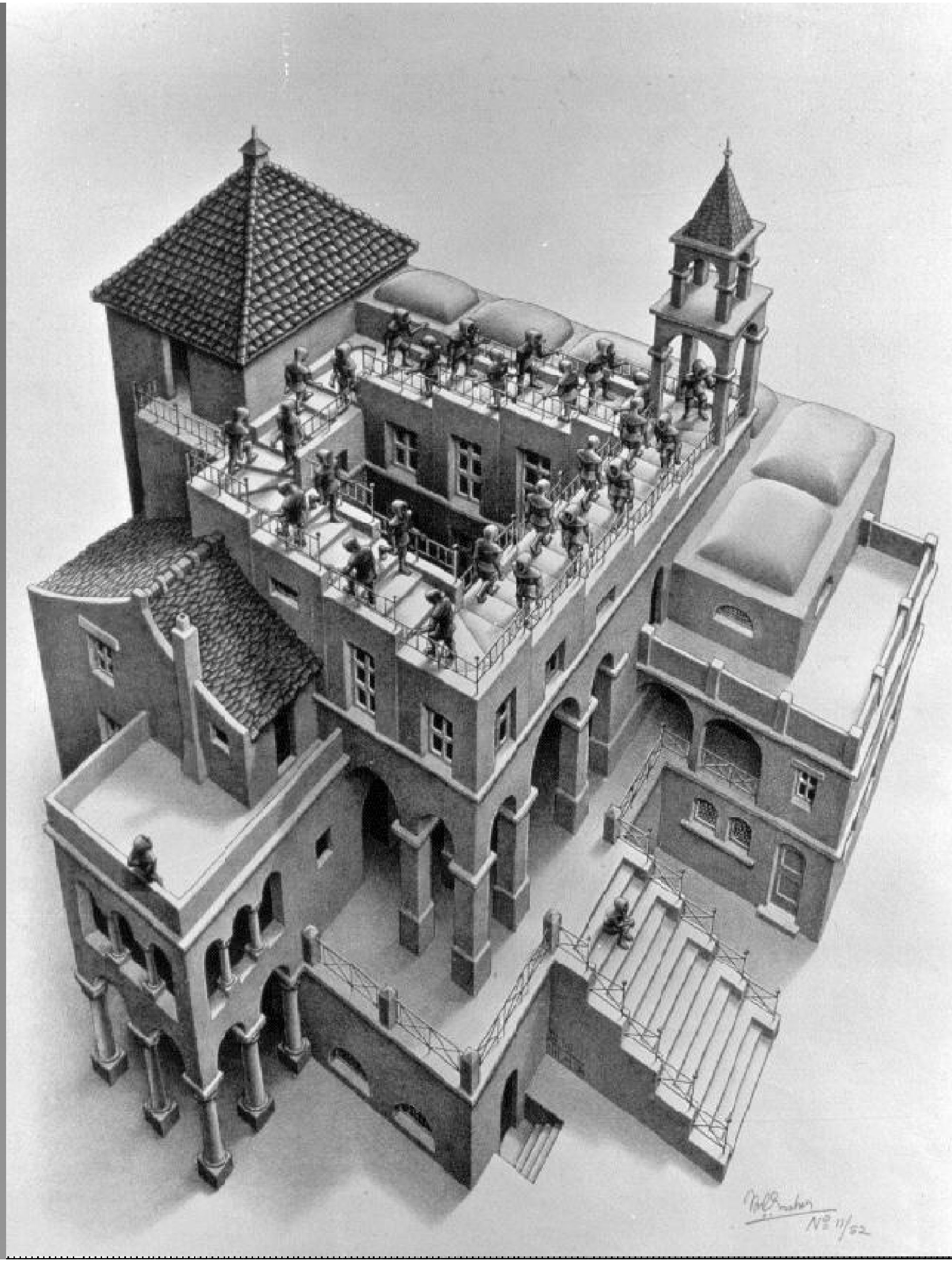

Unwrapping Phase Images

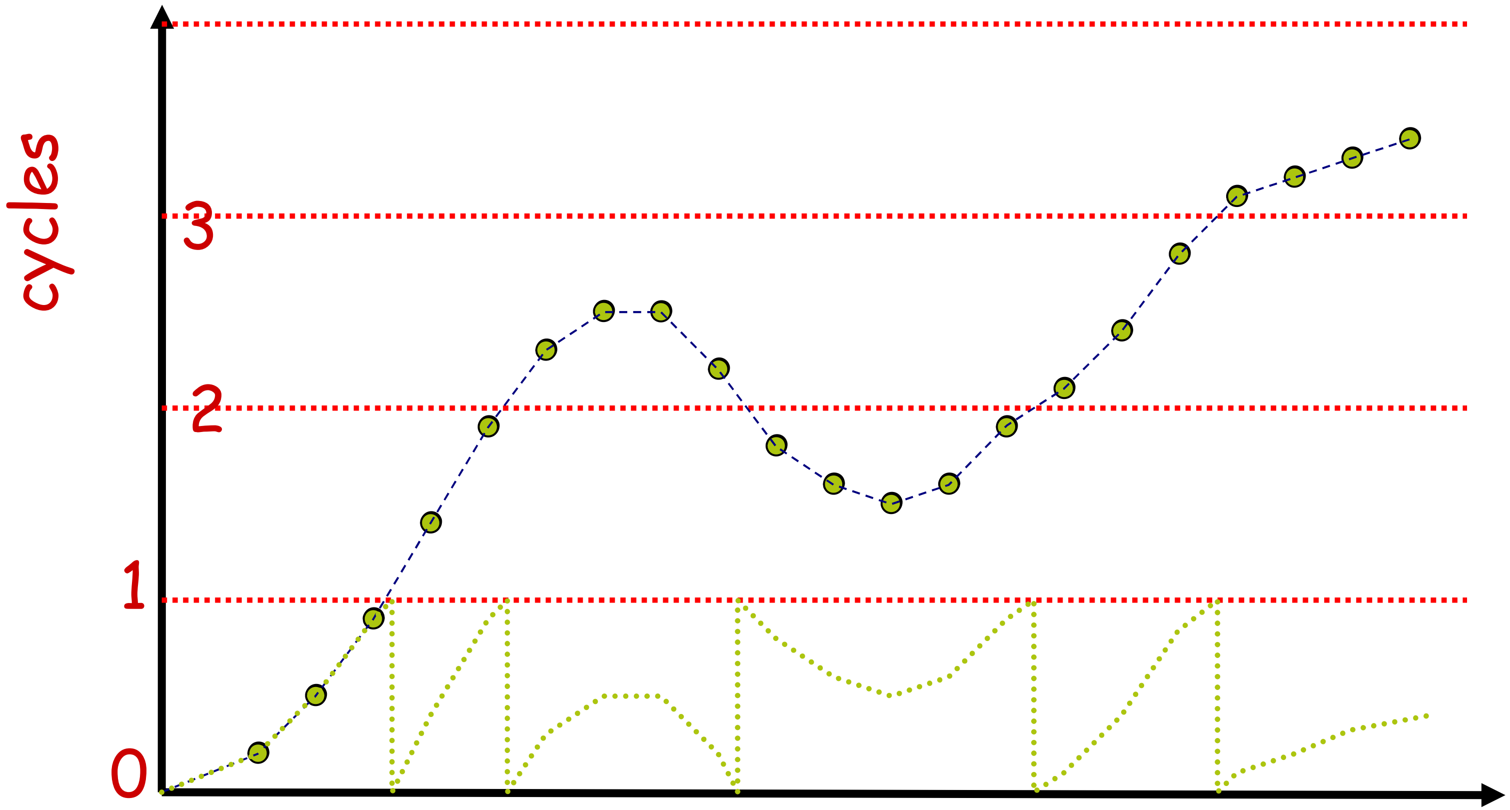

- Unwrapping involves finding (integer) *shift* values for each point.
- Unwrapping is simple in one dimension
  - One path through data
  - Use local gradient to estimate shift.
- For 2D images, the problem is more difficult (NP-hard)
  - Many paths through the data
  - Shifts along all paths must be consistent

General approach

- Strictly: phase unwrapping is ill-posed problem (not possible to obtain unique solution)
- Heuristic approach: assumption of Nyquist criterion:
  sampling rate is high enough to avoid aliasing
- In other words:
  True (unwrapped) phase values of neighboring pixels assumed to lie with one-half cycle

Heuristic approach: A method based on empirical information that has no explicit rationalization

Forward problem

- Define the Wrapping operator:

$$\boxed{\psi = W\{\phi\} = \text{mod}\{\phi + \pi, 2\pi\} - \pi \qquad \in [-\pi, \pi).}$$

Inverse problem

- Main condition for wrapped phase gradients:

$$\boxed{|\Delta\psi(x)| = |\ \psi(x+1) - \psi(x)\ | < \pi}$$

- Phase unwrapping is the integration of phase gradients

TUDelft

One-dimensional example

Nyquist criterion: phase differences between adjacent samples are element of [-0.5, 0.5) cycles

Wrapped data (modulo 1 cycle):

$\psi(x)$: 0.5 0.75 0.0 0.25 0.5 0.75 0.0 0.25

Gradient:

$\Delta\psi(x)$: 0.25 -0.75 0.25 0.25 0.25 -0.75 0.25

Wrapped differences of wrapped phases:

+1 +1

$\nabla\psi(x) \triangleq W\{\Delta\psi(x)\}$: 0.25 0.25 0.25 0.25 0.25 0.25 0.25

$\nabla\varphi \triangleq \nabla\psi(x)$

Integration:

$\varphi(x)$: 0.5 0.75 1.0 1.25 1.5 1.75 2.0 2.25

Possible solution that violates Nyquist criterion:

-0.5 -0.25 1.0 1.25 1.5 1.75 2.0 2.25

+1.25 !

- Key to phase unwrapping:
  - not: directly estimating unwrapped phase, but…
  - Estimating the phase differences between them (phase gradients)

- Problems occur due to additive phase noise (decorrelation) or high spatial frequency phase variation

2D phase unwrapping

define discrete equivalents to partial derivatives of a function F as

$$\Delta_i F(i,k) = F(i+1,k) - F(i,k)$$
$$\Delta_k F(i,k) = F(i,k+1) - F(i,k)$$

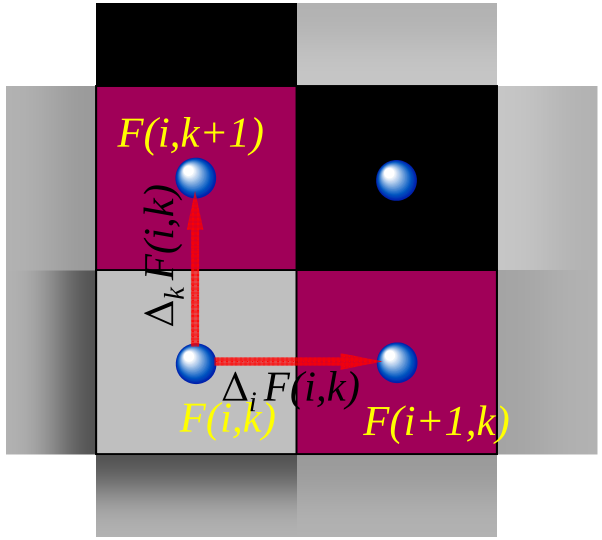

and compact them into *gradient* notation:

$$\nabla F(i,k) = \begin{pmatrix} \Delta_i F(i,k) \\ \Delta_k F(i,k) \end{pmatrix}.$$

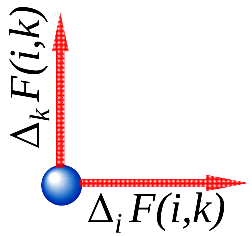

Suppose 2D vector field $\boldsymbol{A} = \begin{pmatrix} A_i \\ A_k \end{pmatrix}$

Definition of *curl :*

$$\begin{pmatrix} \Delta_i \\ \Delta_k \end{pmatrix} \times \begin{pmatrix} A_i(i,k) \\ A_k(i,k) \end{pmatrix} = \Delta_i A_k(i,k) - \Delta_k A_i(i,k)$$
$$= \left[A_k(i+1,k) - A_k(i,k)\right] - \left[A_i(i,k+1) - A_i(i,k)\right]$$
$$= A_k(i+1,k) - A_k(i,k) - A_i(i,k+1) + A_i(i,k)$$

Suppose 2D vector field $\boldsymbol{A} = \begin{pmatrix} A_i \\ A_k \end{pmatrix}$

$$\nabla F(i,k) = \begin{pmatrix} \Delta_i F(i,k) \\ \Delta_k F(i,k) \end{pmatrix}$$

Definition of *curl :*

$$\begin{pmatrix} \Delta_i \\ \Delta_k \end{pmatrix} \times \begin{pmatrix} A_i(i,k) \\ A_k(i,k) \end{pmatrix} = \Delta_i A_k(i,k) - \Delta_k A_i(i,k)$$
$$= \left[A_k(i+1,k) - A_k(i,k)\right] - \left[A_i(i,k+1) - A_i(i,k)\right]$$
$$= A_k(i+1,k) - A_k(i,k) - A_i(i,k+1) + A_i(i,k)$$

Assume that $\boldsymbol{A} = \nabla F$

From vector analysis (and potential field theory) it is known that the curl of a gradient field is equal to zero. The gradient field is therefore a **conservative field**.

$$\nabla \times \nabla F = 0$$

$$\nabla \times \nabla F =$$

$$\begin{pmatrix} \Delta_i \\ \Delta_k \end{pmatrix} \times \begin{pmatrix} \Delta_i F(i,k) \\ \Delta_k F(i,k) \end{pmatrix} = \Delta_i \Delta_k F(i,k) - \Delta_k \Delta_i F(i,k)$$

$$= \left[\Delta_k F(i+1,k) - \Delta_k F(i,k)\right] - \left[\Delta_i F(i,k+1) - \Delta_i F(i,k)\right]$$

$$= \Delta_k F(i+1,k) - \Delta_k F(i,k) - \Delta_i F(i,k+1) + \Delta_i F(i,k) = 0$$

∇F :

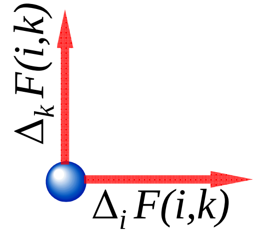

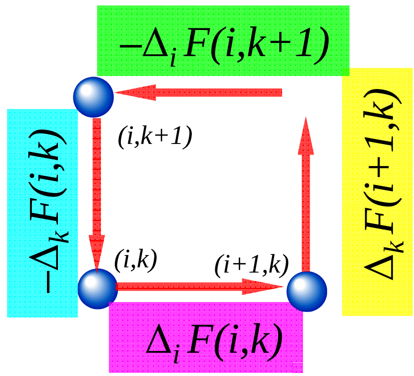

$-\Delta_i F(i,k+1) = -[\, F(i+1,k+1) - F(i,k+1)]$

$\Delta_k F(i+1,k) = \ [\, F(i+1,k+1) - F(i+1,k)]$

$\Delta_i F(i,k) \ = \ F(i+1,k) - F(i,k)$

$-\Delta_k F(i,k) \ = -[\, F(i,k+1) - F(i.k)]$

Curl of vector gradient of scalar potential F is identically zero.

- In phase unwrapping: the vector gradient field of the *unwrapped phase* is necessarily zero (every closed loop integral is zero)

$$\nabla \times \nabla F = 0$$

- The unwrapped phase field is thus completely specified, up to an additive constant

- However, the vector gradient field of the wrapped phase can be non-conservative (closed-loop integrals can give non-zero results)

$$\nabla \times \hat{\nabla} \psi \neq 0$$

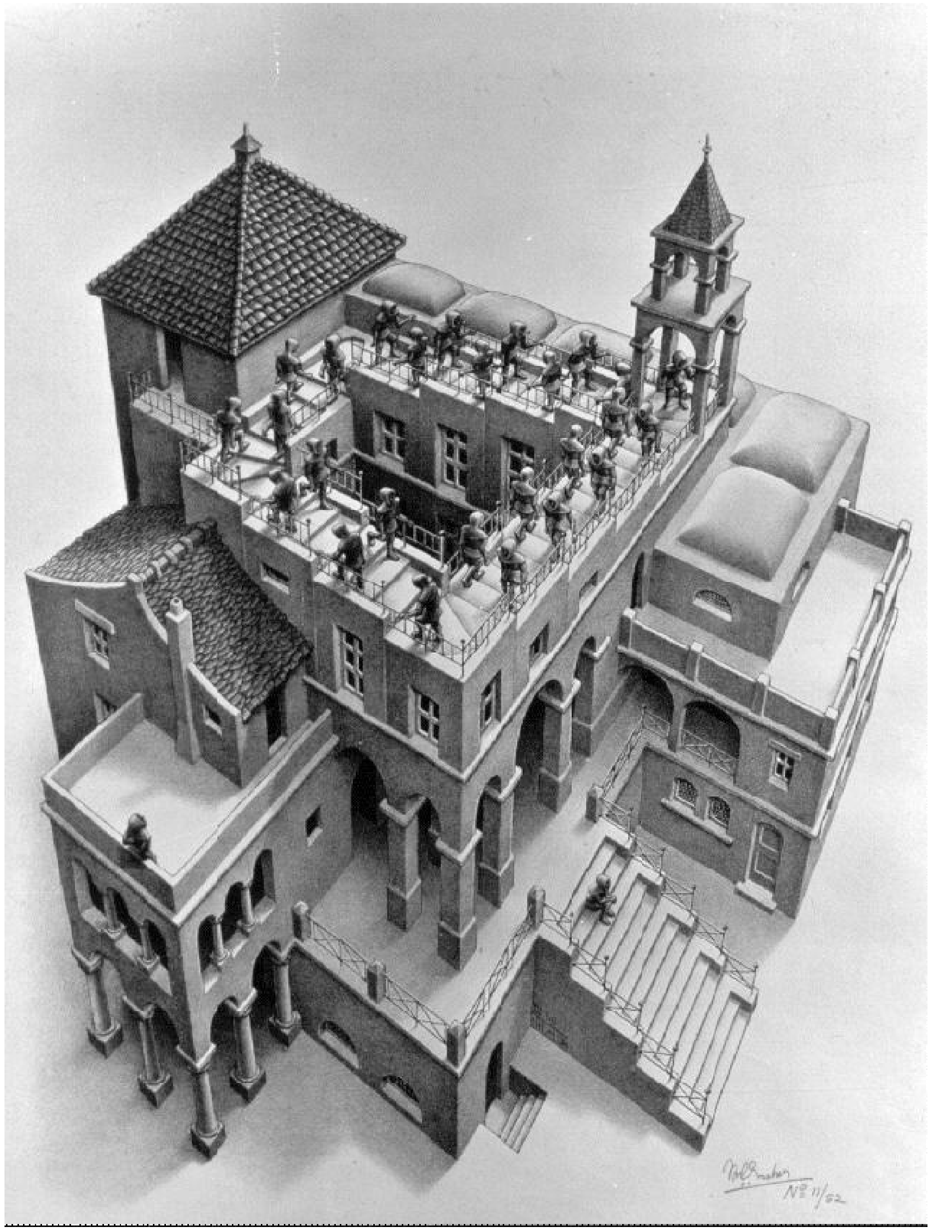

Ascending and descending, by M.C. Escher

e.g. a true gradient outside [−π,+π) interval will be wrapped into it

Example

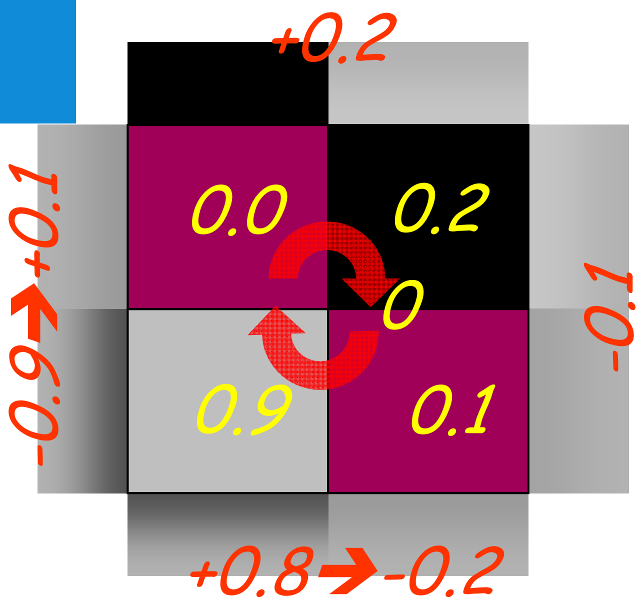

Neutral

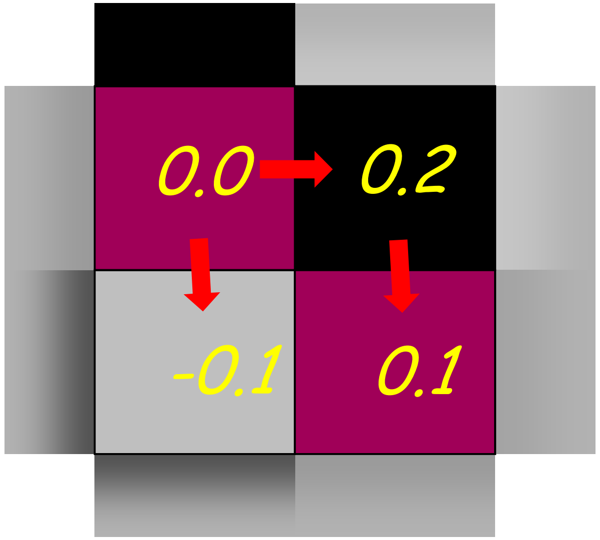

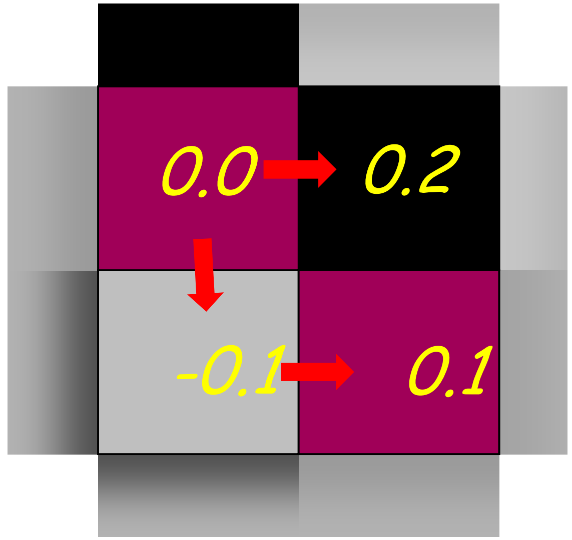

Result is path independent

Example residue

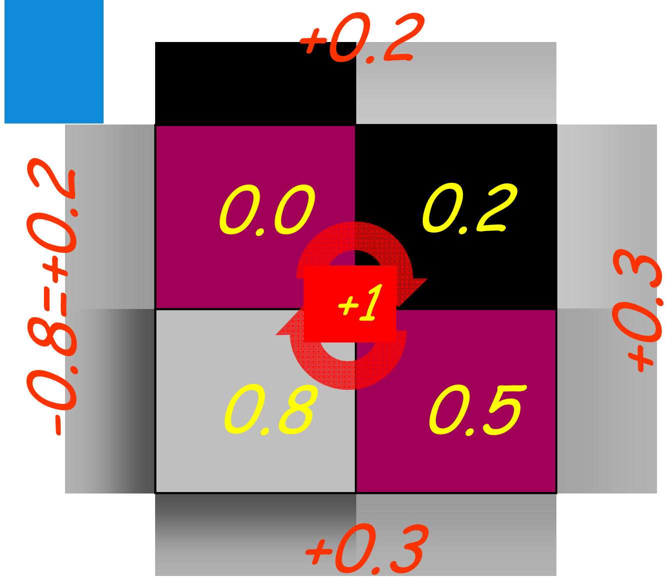

Positive residue

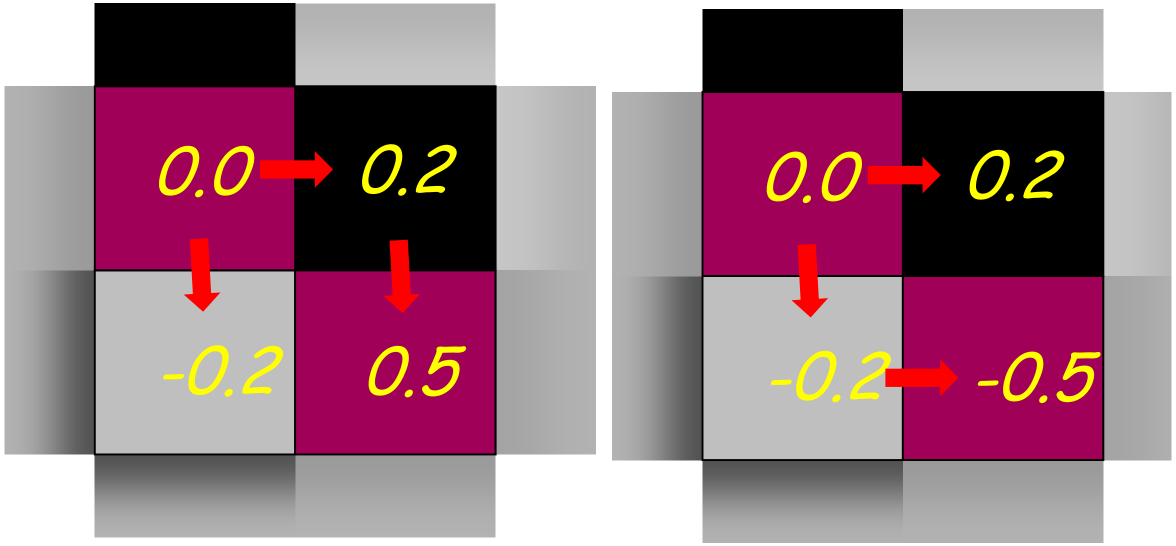

Result is path dependent

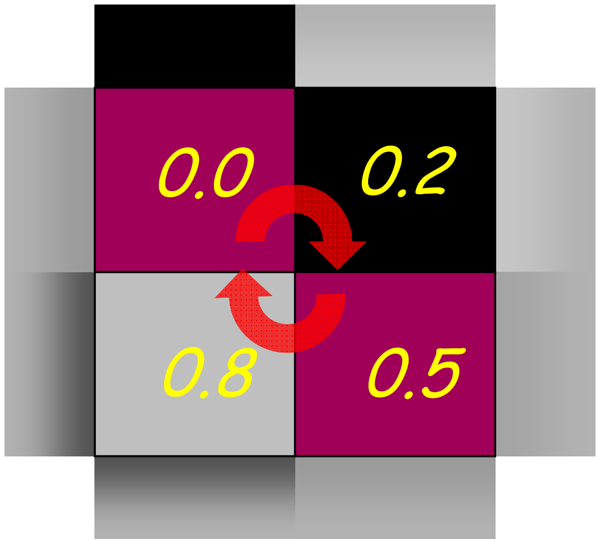
0.0
0.2
0.8
0.5

Example branch cut

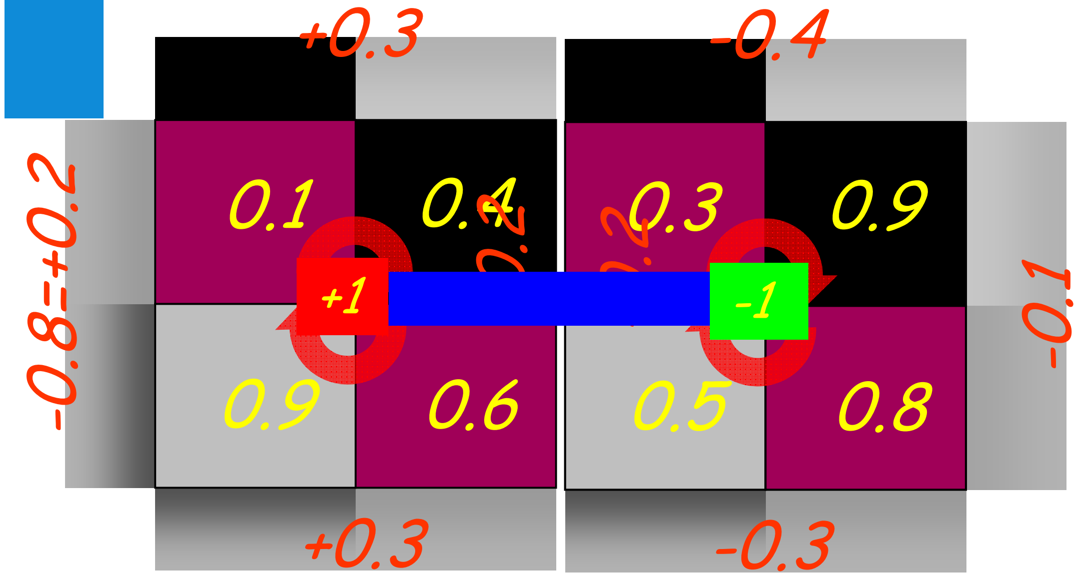

Unloaded residue pair

Positive residue Negative residue

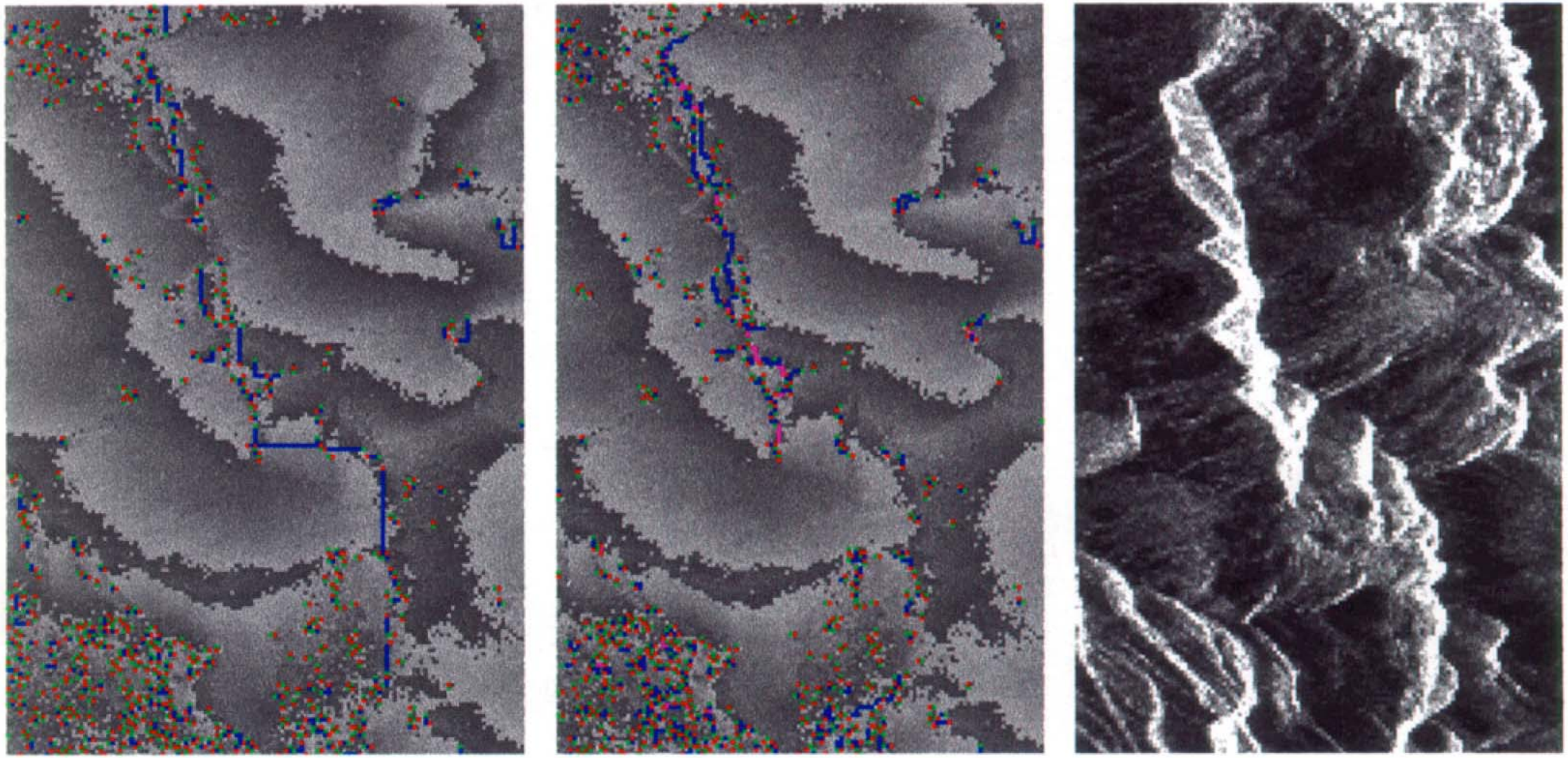

Figure 11. Wrapped phase (grey), residues (green, red), and branch-cuts (blue, multiple cuts: pink) found by a minimum cost flow algorithm. Left: minimization of total branch-cut length (constant costs); note the unrealistic long straight branch-cuts. Centre: minimization of a cost function derived from the phase gradient and its variance; the branch-cuts are guided along the ridges of the mountains (visible as bright areas in the intensity SAR image of the same area (right)).

Terrain motion

Ramon Hanssen

2-6-2016

Previous lecture: Learning objectives

- Interferometry: intuitive approach, physical approach
- Understanding sensitivity
- Basic observables and variables, concepts
- Practical data processing
- Quality control

Learning objectives 2nd lecture

- Interferogram interpretation
- Quality control InSAR
- Time series techniques: PSI, SBAS
- PSI interpretation and example HB

Interferogram interpretation

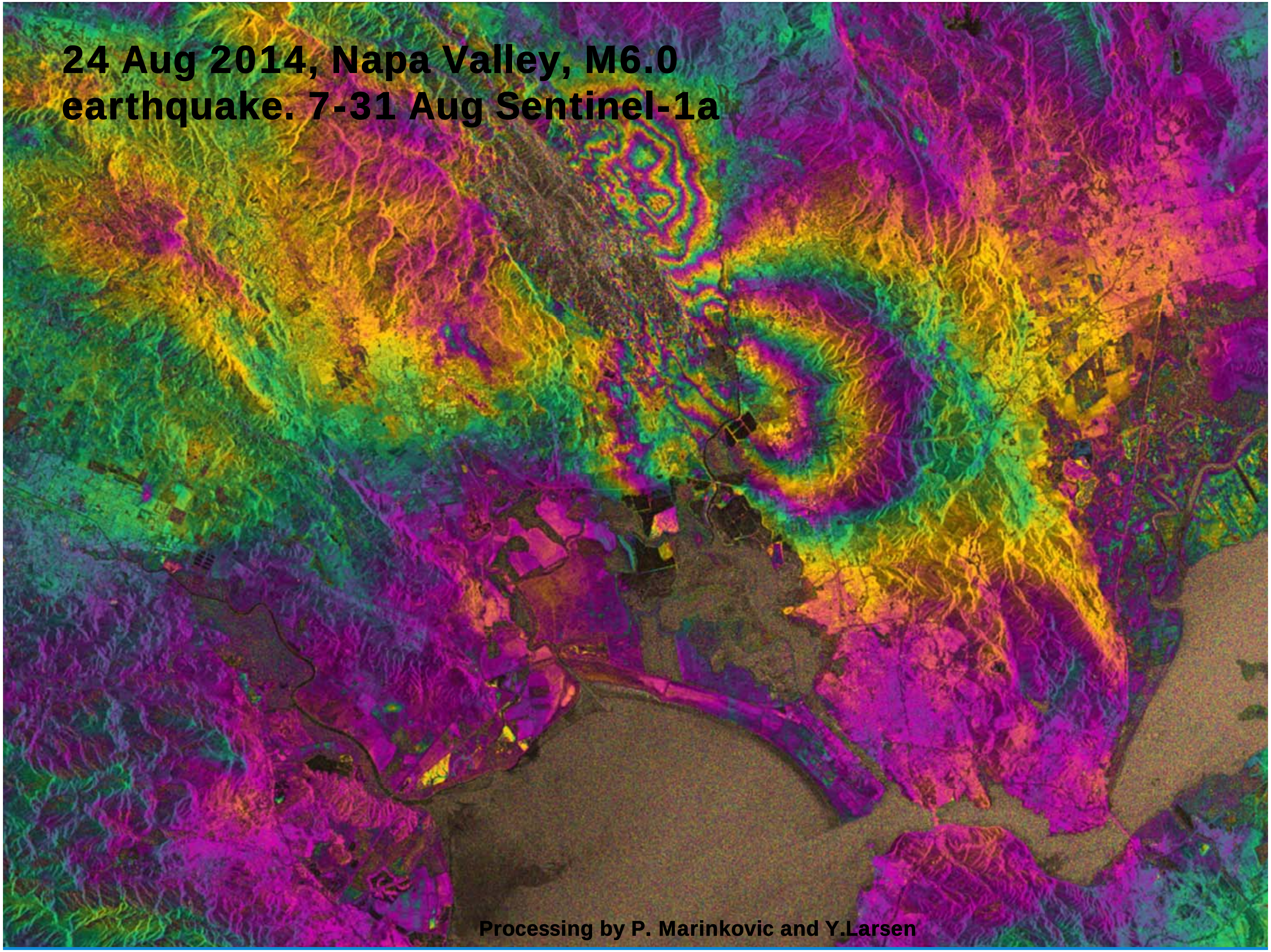
24 Aug 2014, Napa Valley, M6.0
earthquake. 7-31 Aug Sentinel-1a
Processing by P. Marinkovic and Y.Larsen

Radar image datum and geometry

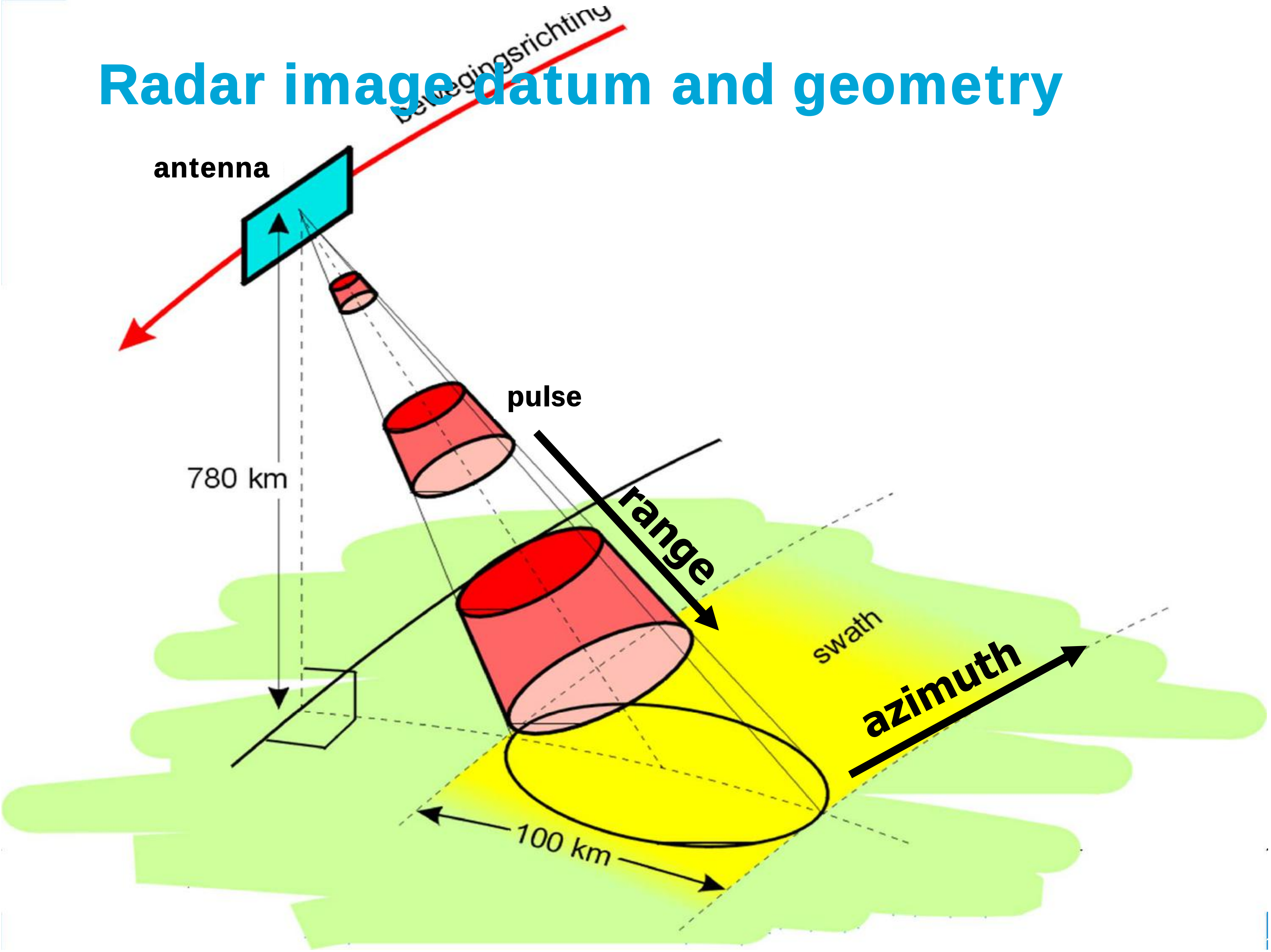

Right-looking radar system

Internal datum:

Radar coordinate system

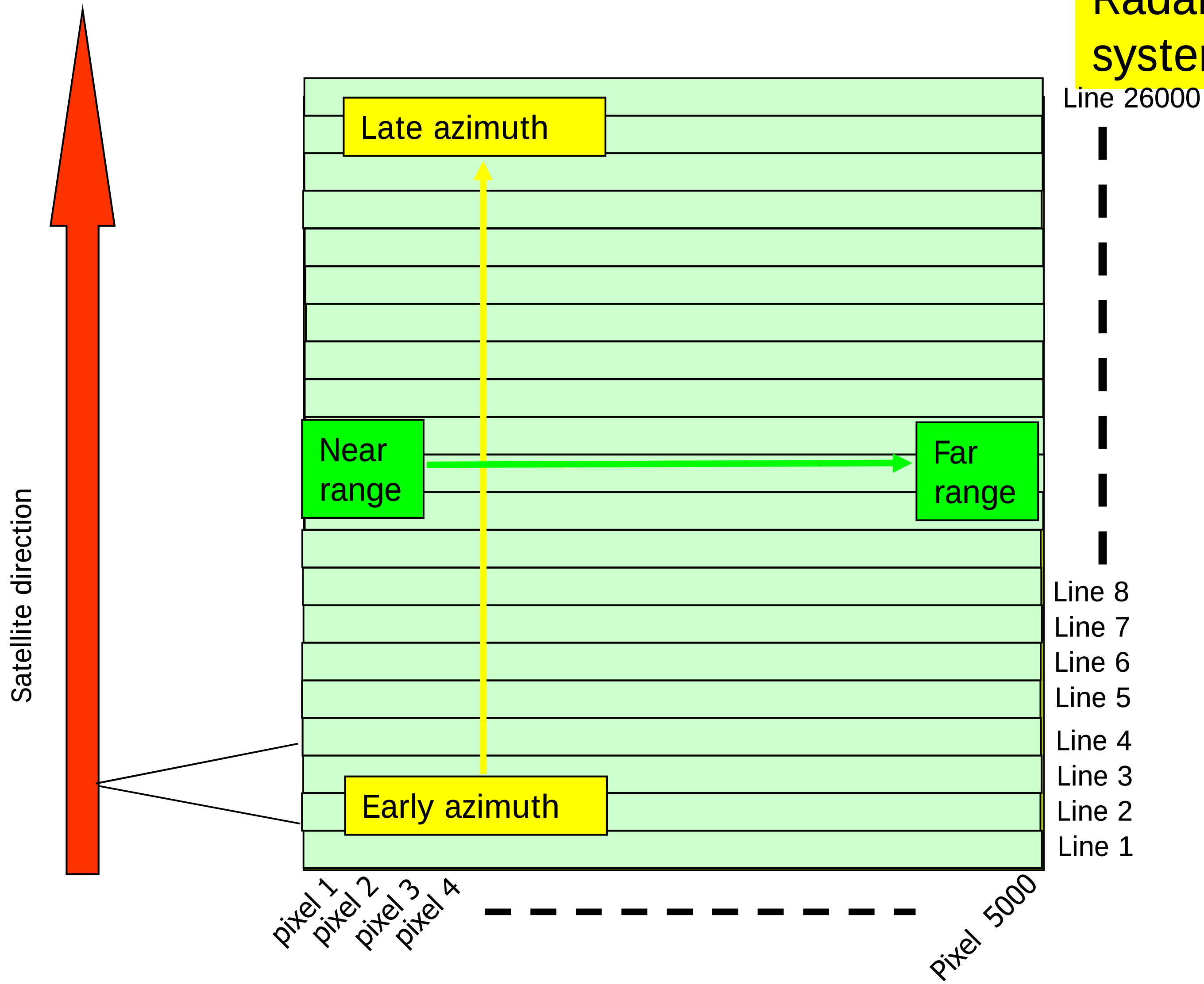

Binary data file

‘Computer’ datum:

Data file / matrix

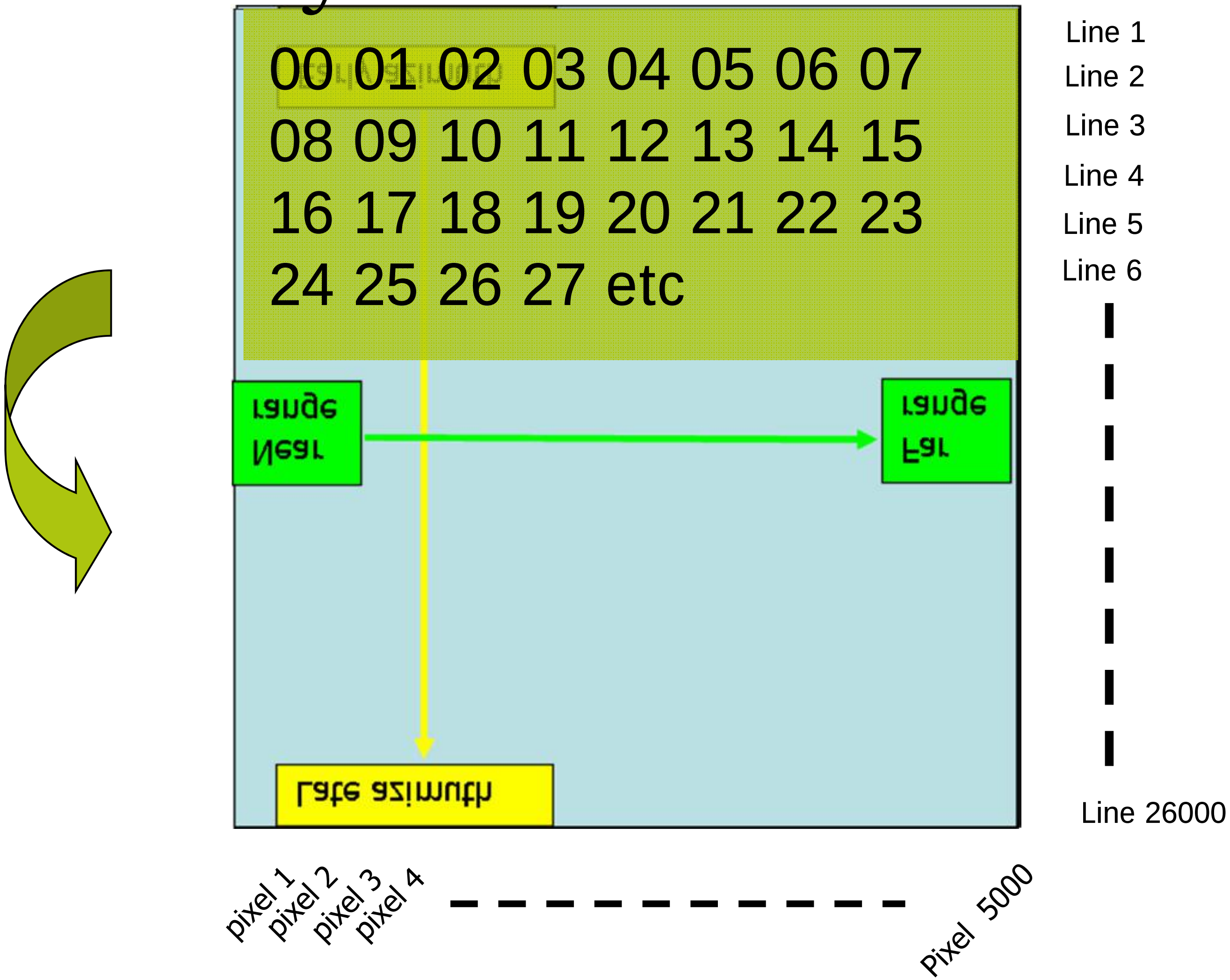

Geographic datum: ascending

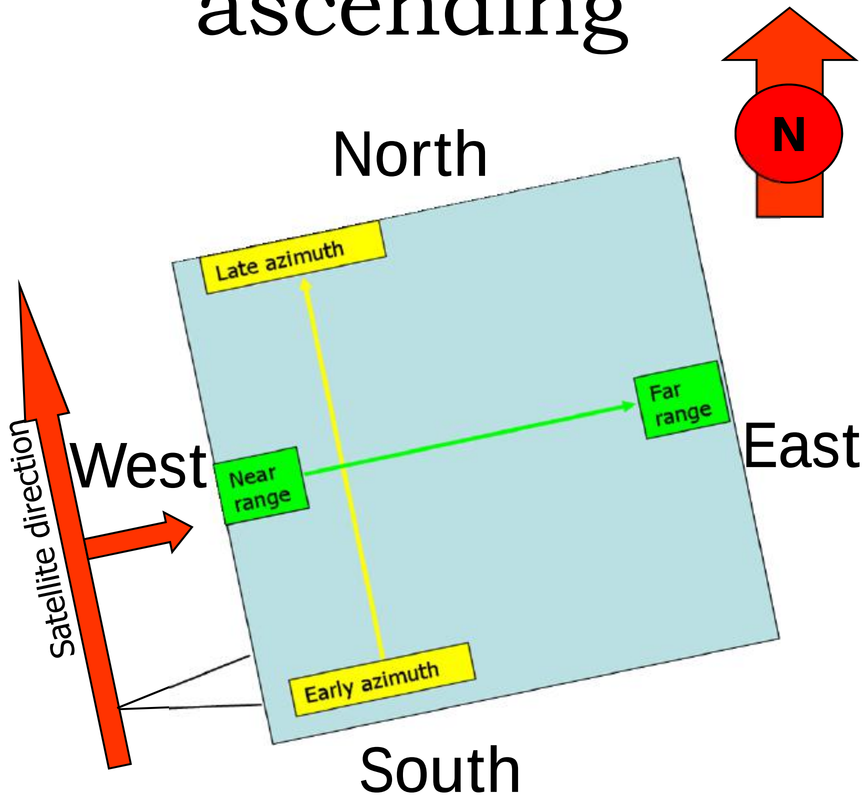

Geograpic datum

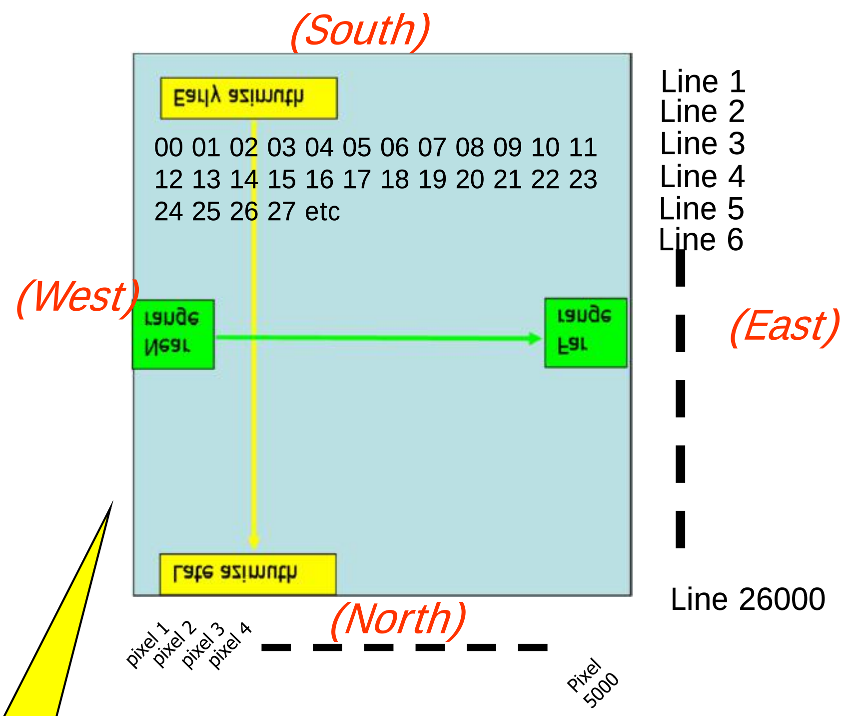

'Computer' datum

Image is upside-down !!!

Geographic datum: descending

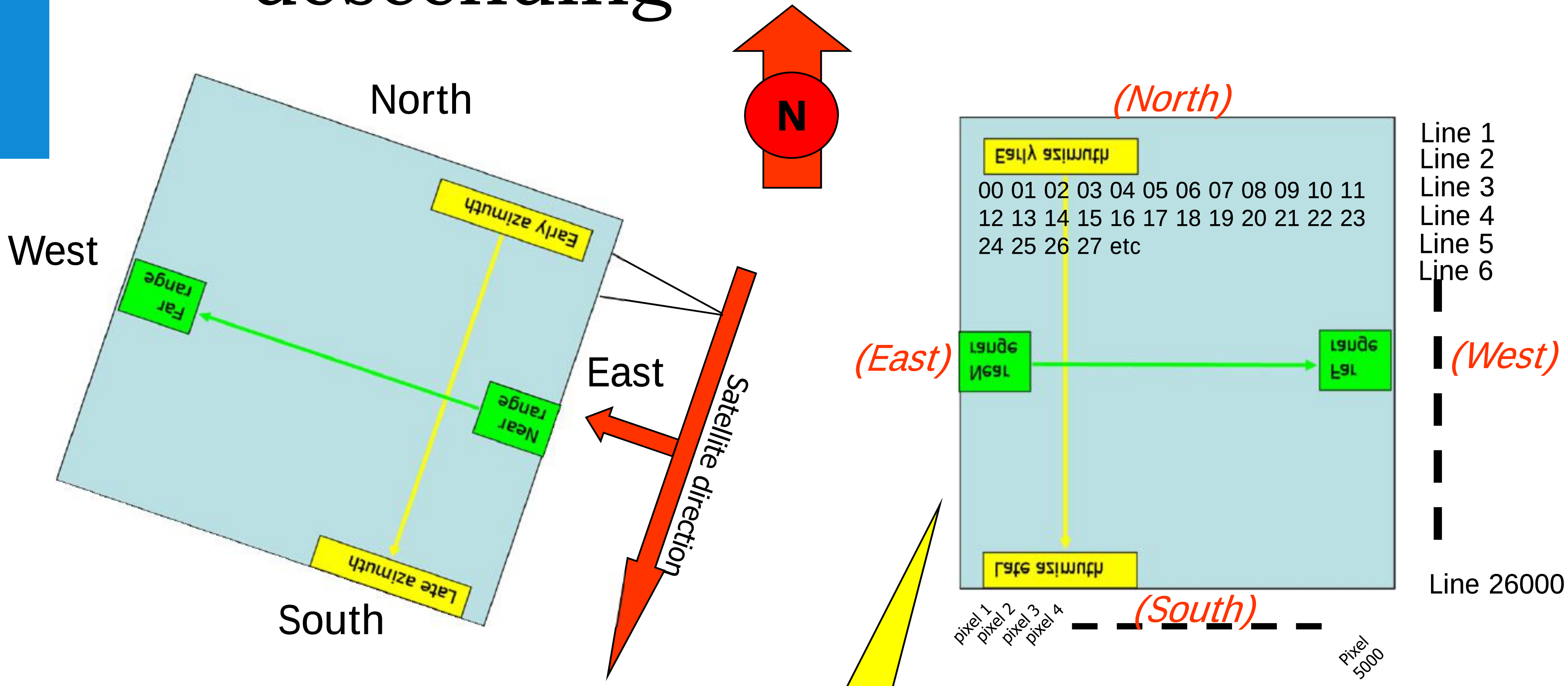

Geograpic datum

'Computer' datum

Image is flipped left-right !!!

Summary

- Descending image (morning acquisitions) are **flipped left-right!**
- Ascending image (evening acquisitions) are *flipped up-down!*

TU Delft

Interpretation: On the sign of the phase

-image on the right is standard output Doris (independent of descending or ascending image)

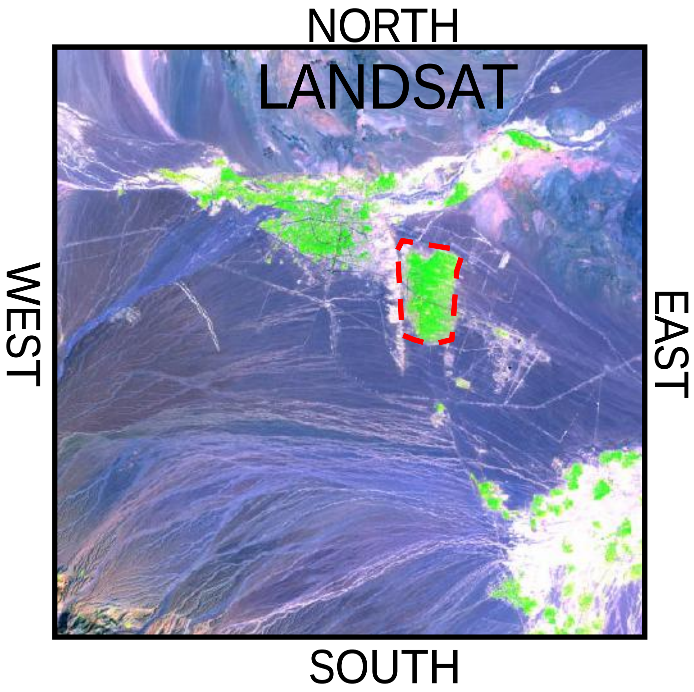

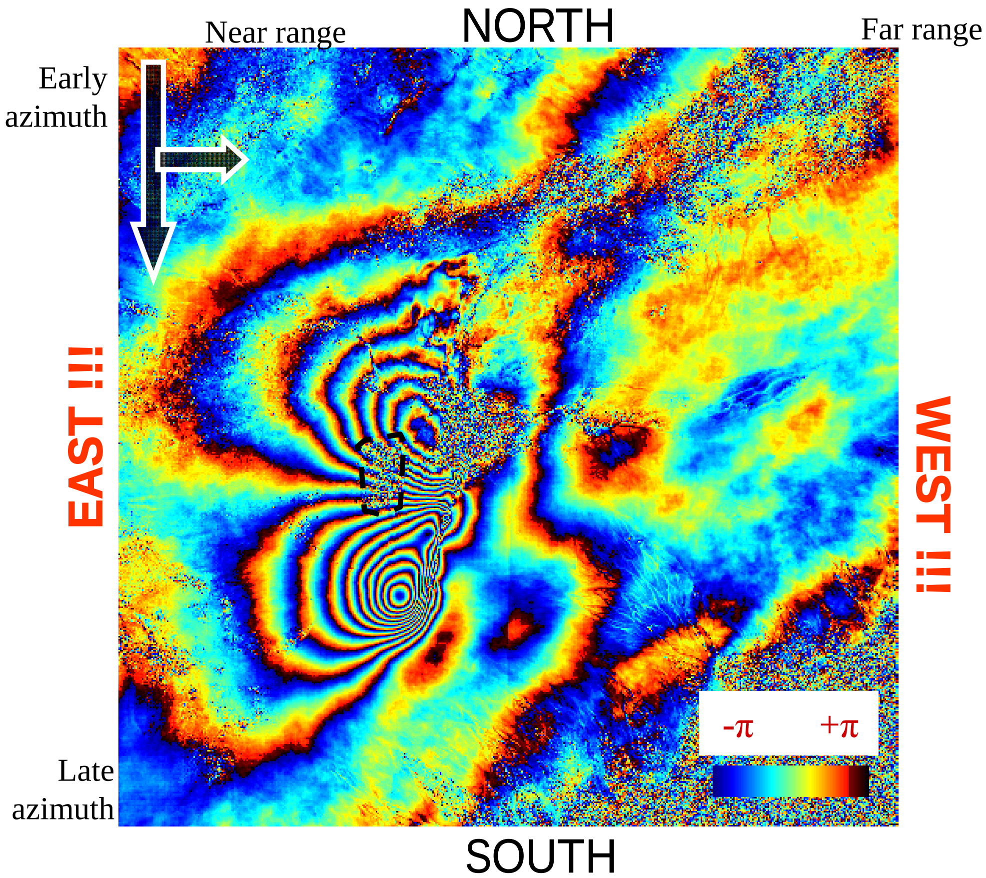

96

Phase-deformation relationship

$$\frac{2R_1}{\lambda} = \frac{\psi_1}{2\pi}$$

$$\psi_1 = -\frac{4\pi}{\lambda}R_1$$

$$\psi_2 = -\frac{4\pi}{\lambda}R_2$$

$$R_2 = R_1 + D_p$$

$$\phi_p = \psi_{1p} - \psi_{2p} = -\frac{4\pi(R_1 - R_2)}{\lambda} =$$

$$\boxed{\phi_p = -\frac{4\pi}{\lambda}D_p}$$

D_p : line-of-sight deformation

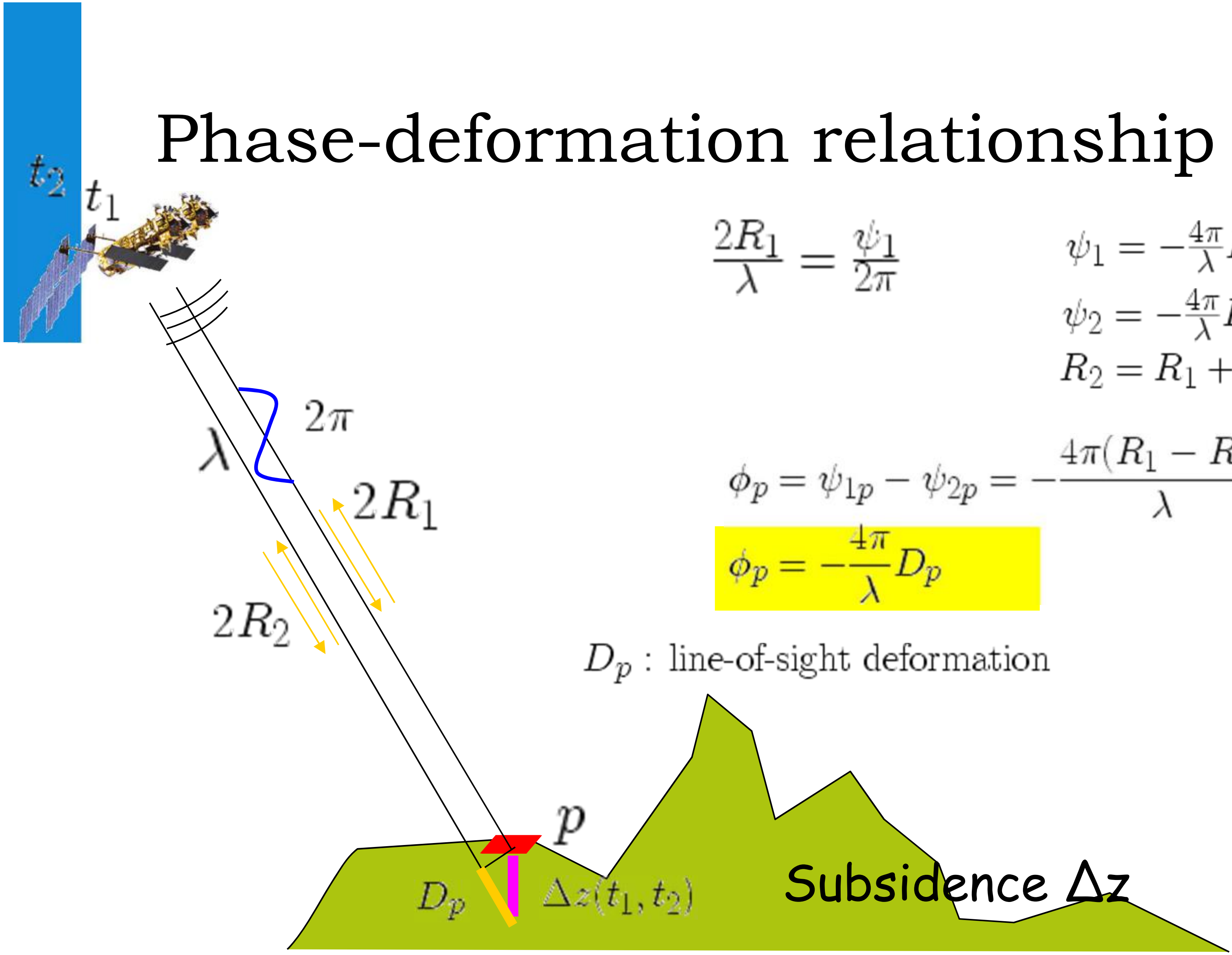

97

Interpretation: On the sign of the phase

FIRST, consider the TIMES of the images!!!

We perform: MASTER – SLAVE

CHECK: $t_{master} < t_{slave}$

If YES: range increase ($\mathbf{R}_{t1} < \mathbf{R}_{t2}$)

→ phase decrease ($\varphi_{t1} > \varphi_{t2}$)

→interferometric phase increase ($\varphi_{t1} - \varphi_{t2} > \mathbf{0}$)

$$D = -\frac{\lambda}{4\pi}\phi$$

98

Interpretation: On the sign of the phase

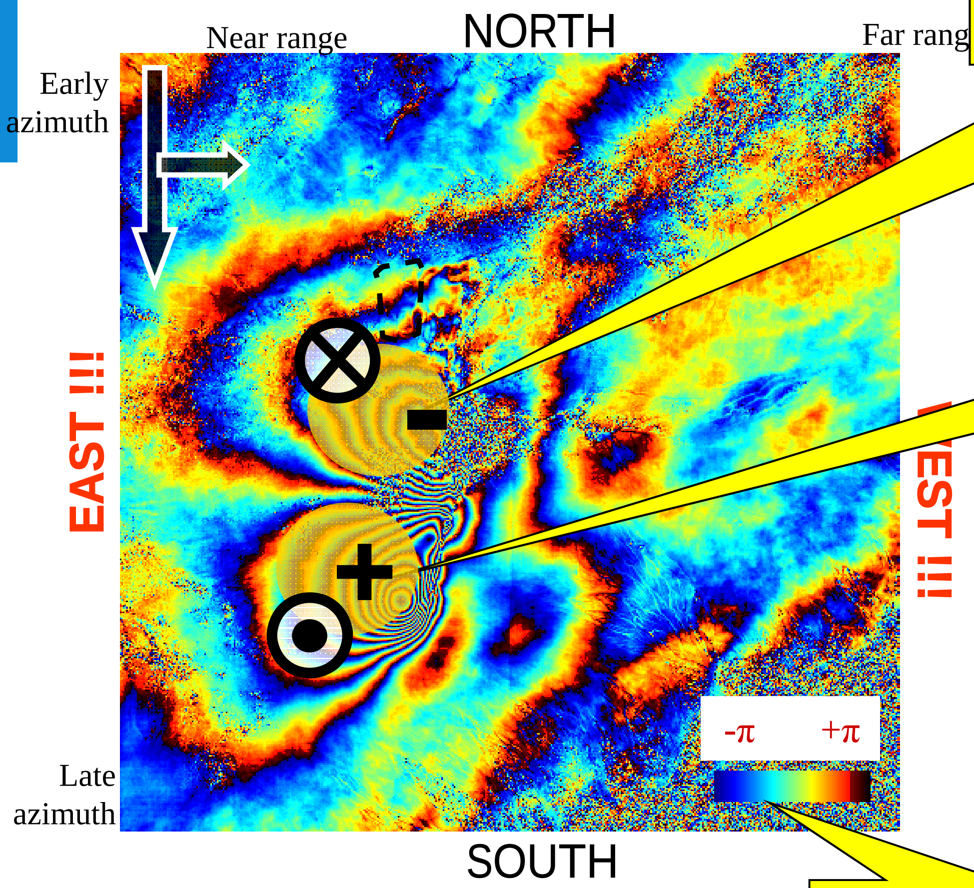

Towards center: BYR: increasing interferometric phase→ increasing range to satellite

$$D = -\frac{\lambda}{4\pi}\phi$$

Towards center: BRY: decreasing interferometric phase→ decreasing range to satellite

Colorbar BYR: increasing interferometric phase

Interpretation: On the sign of the phase

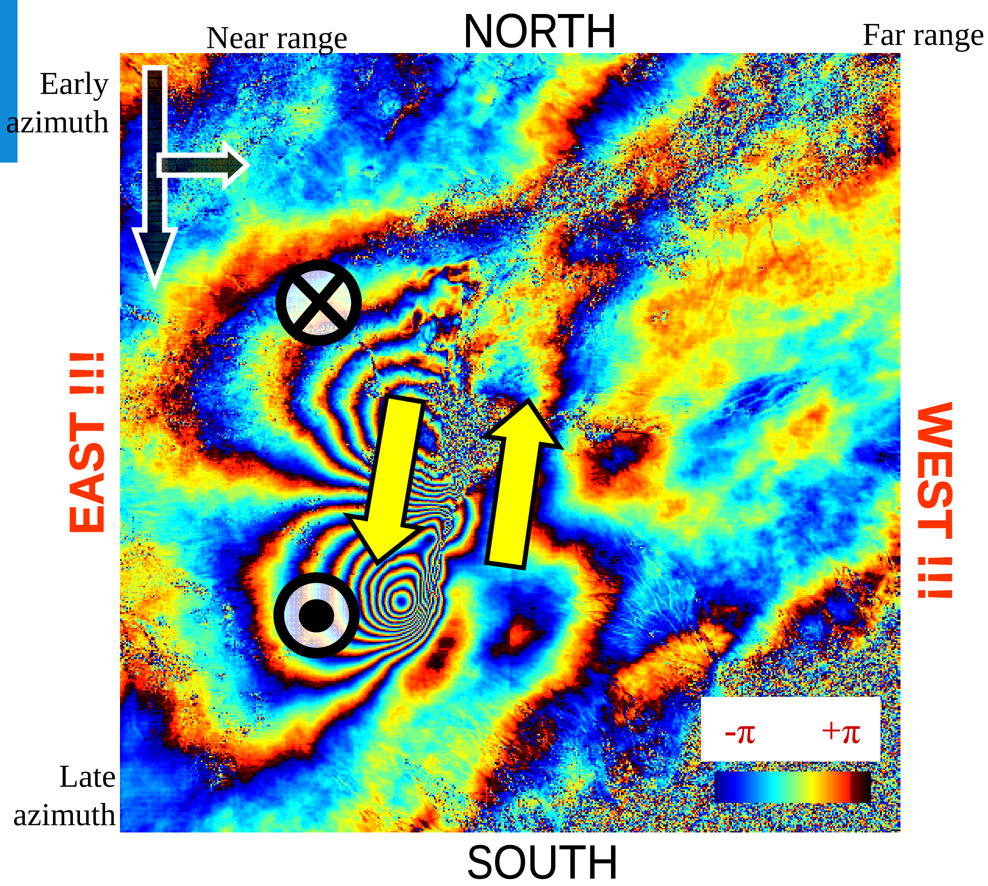

100

Interpretation: On the sign of the phase

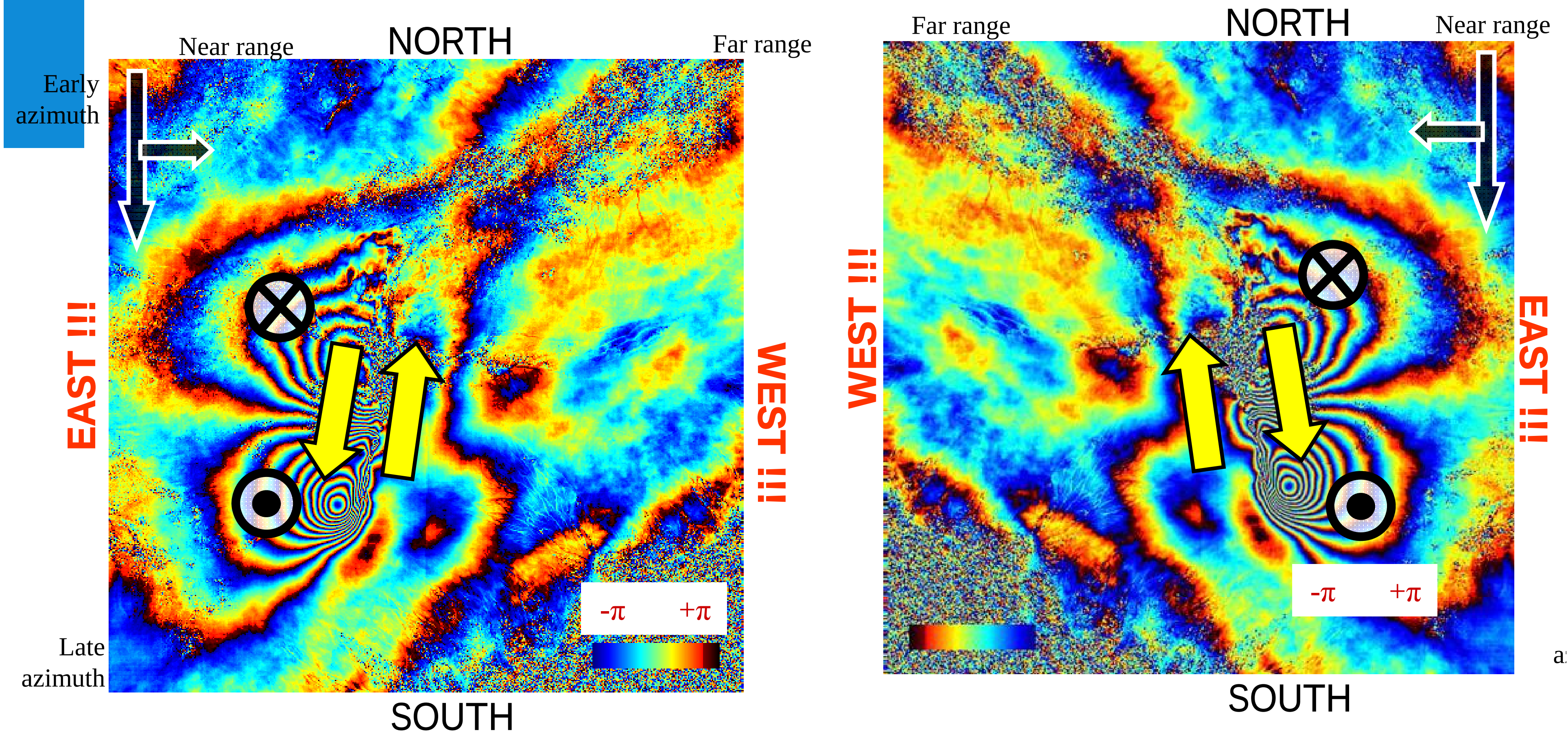

CONCLUSION: Right lateral
(strike slip)

101

Quality control

- The Stochastic Model for InSAR

Model of observation equations (1)

Functional model:

$$\partial\phi_p = -\frac{4\pi}{\lambda}\left(D_p + \frac{B_\perp}{R_1 \sin\theta^\circ} H_p\right)$$

Observation

Unknowns

Rank deficiency!

Often treated opportunistically

Stochastic model:

$$Q_\phi = \sigma^2_\phi I_n$$

Based on thermal (instrumental) noise

This is too much simplified, let's make it more realistic!

Model of observation equations (2)

- **Add unknown parameter:**
  - Phase ambiguity

Integer valued unknown

$$\boxed{\partial\phi_p} = -\frac{4\pi}{\lambda}\left(\boxed{D_p} + \frac{B_\perp}{R_1 \sin\theta^\circ}\boxed{H_p}\right) + 2\pi\,\boxed{k}$$

- **Add error signal to stochastic model:**
  - Atmosphere (troposphere, ionosphere)
  - Orbit errors
  - Decorrelation
    - Geometric
    - Temporal

Spatial varying disturbance

~trend

Pixel-based noise

Spatially ~constant

Spatially varying

Main condition for interferometry

Coherence!

Coherence (Complex Correlation)

- Definition:

$$\gamma = \frac{E\{y_1 y_2^*\}}{\sqrt{E\{|y_1|^2\} \cdot E\{|y_2|^2\}}}$$

- Estimation of coherence magnitude:

$$|\hat{\gamma}| = \frac{\left|\sum_{n=1}^{N} y_1^{(n)} y_2^{(n)} \cdot e^{-j\phi^{(n)}}\right|}{\sqrt{\sum_{n=1}^{N} |y_1^{(n)}|^2 \sum_{n=1}^{N} |y_2^{(n)}|^2}}$$

- Coherence magnitude is a measure of the correlation (values 0 – 1)

Coherence loss as function of time

1 day interval

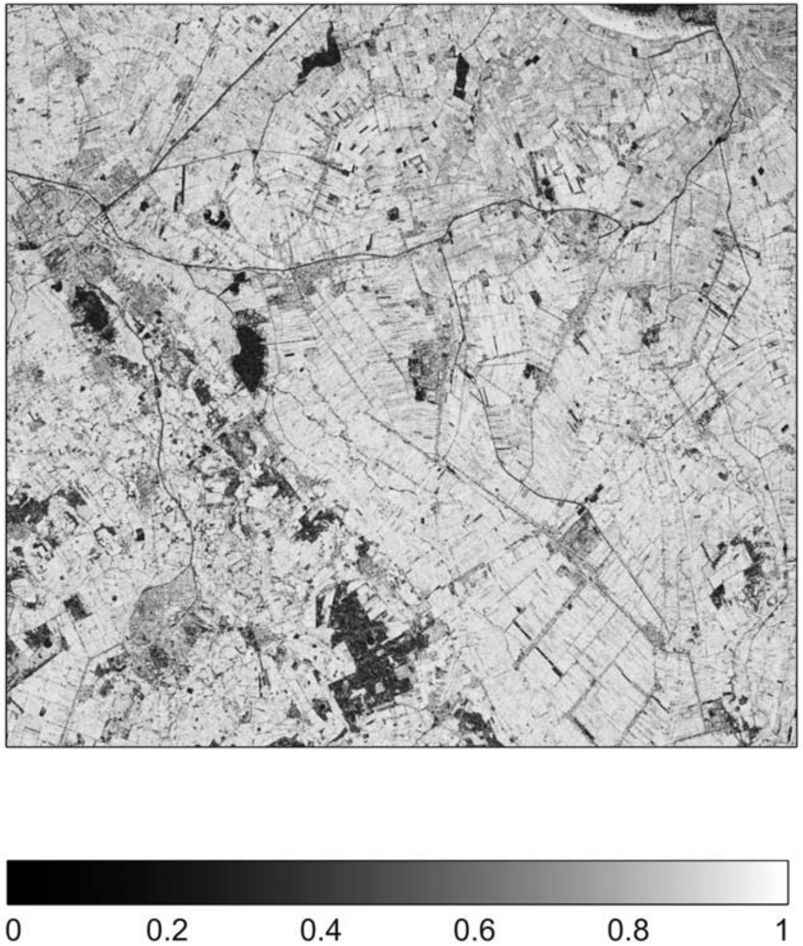

3.5 year interval

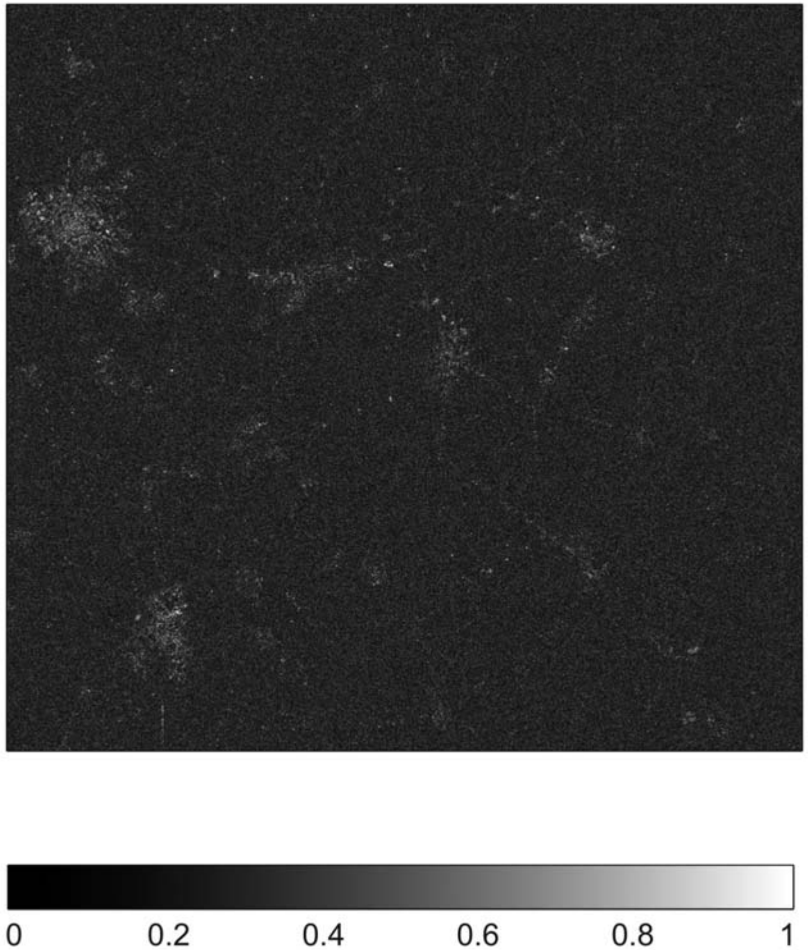

Anthropogenic features remain coherent over long time intervals

Coherence, multilooks, and phase PDF

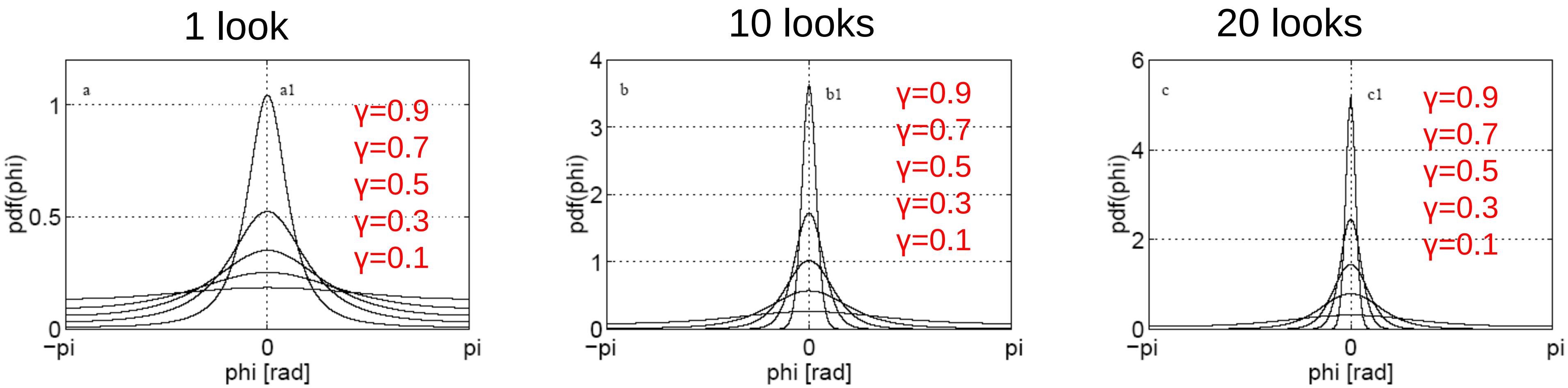

Temporal Decorrelation

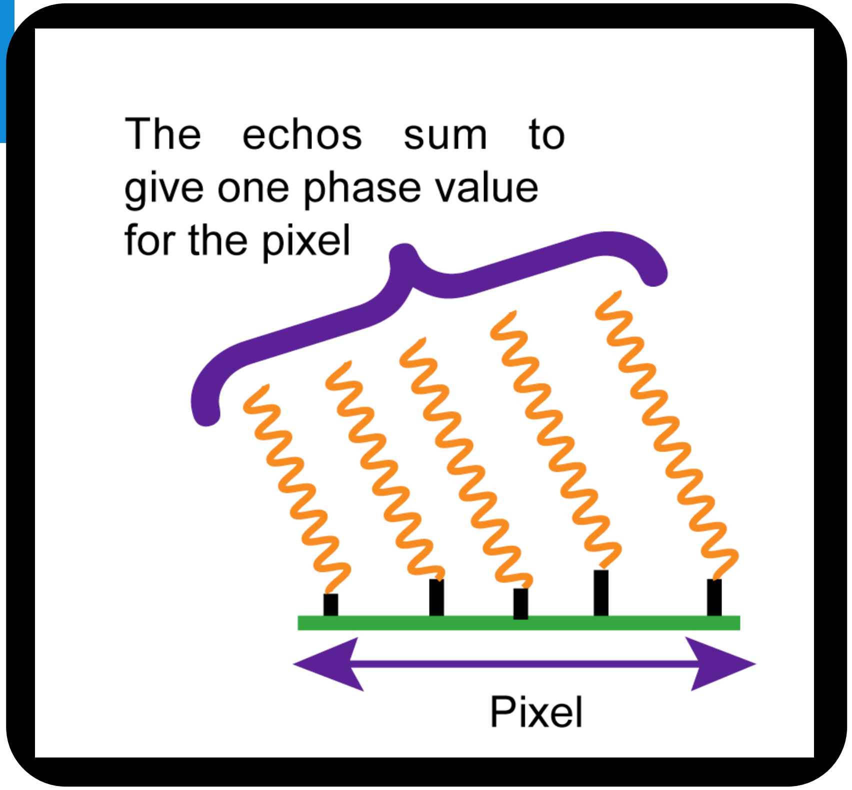

Distributed scatterer pixel

If scatterers move with respect to each other, the phase sum changes

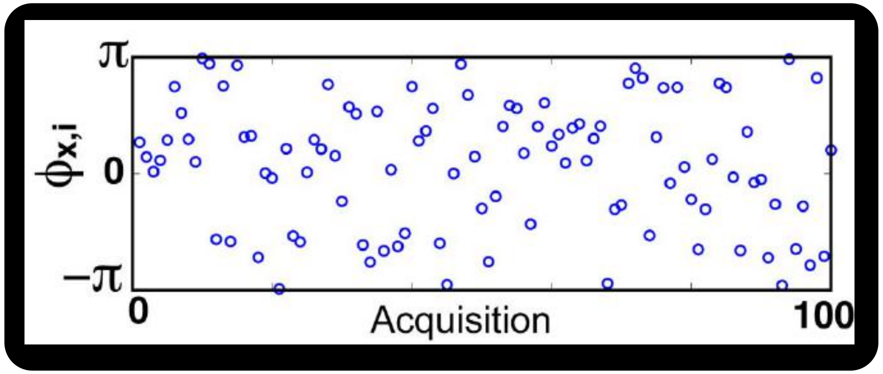

Temporal decorrelation

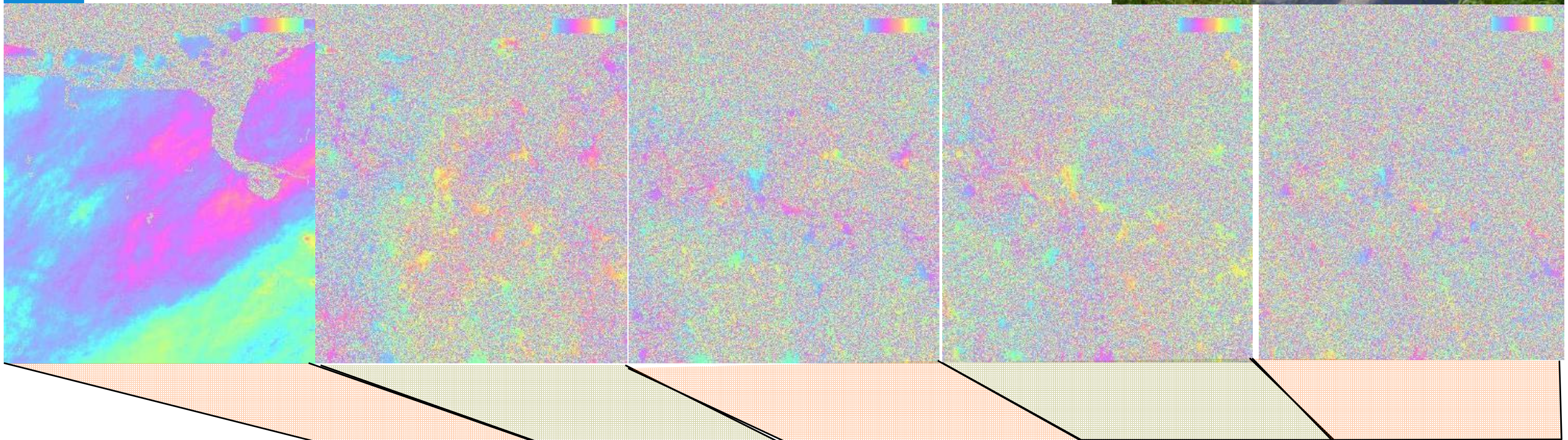

Time interval	1 day	1 year	2 year	3 year	6 year

Coherence and wavelength

Loss of correlation is due to:

- volume of vegetation
- movement of vegetation
- dielectric change (moisture)

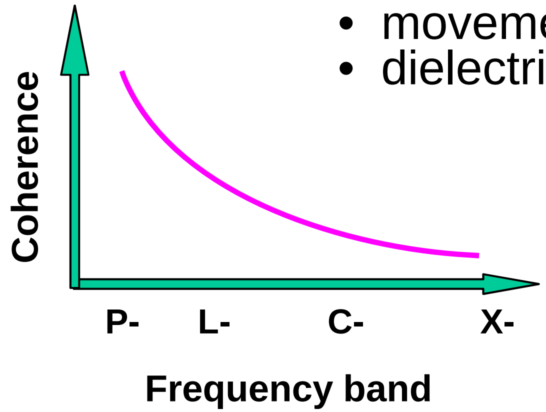

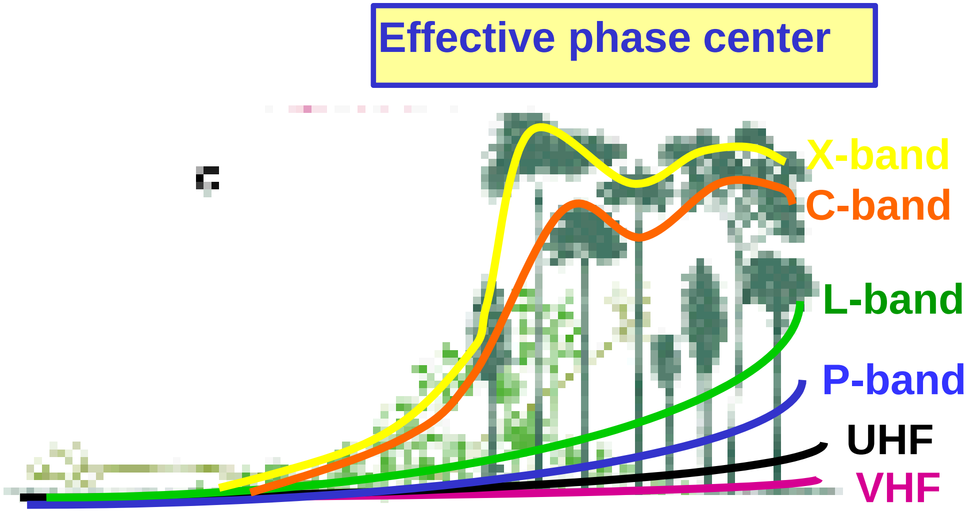

Source: H.Zebker

Coherence as function of wavelength

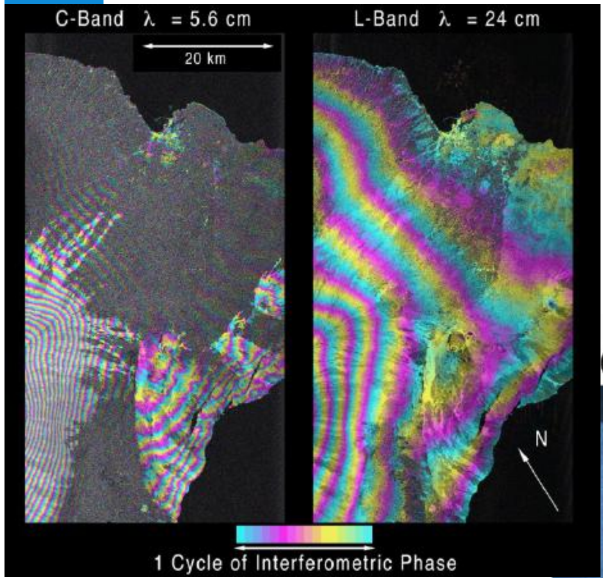

Results SIR-C mission,
Simultaneous C and L band
ΔT=6 months

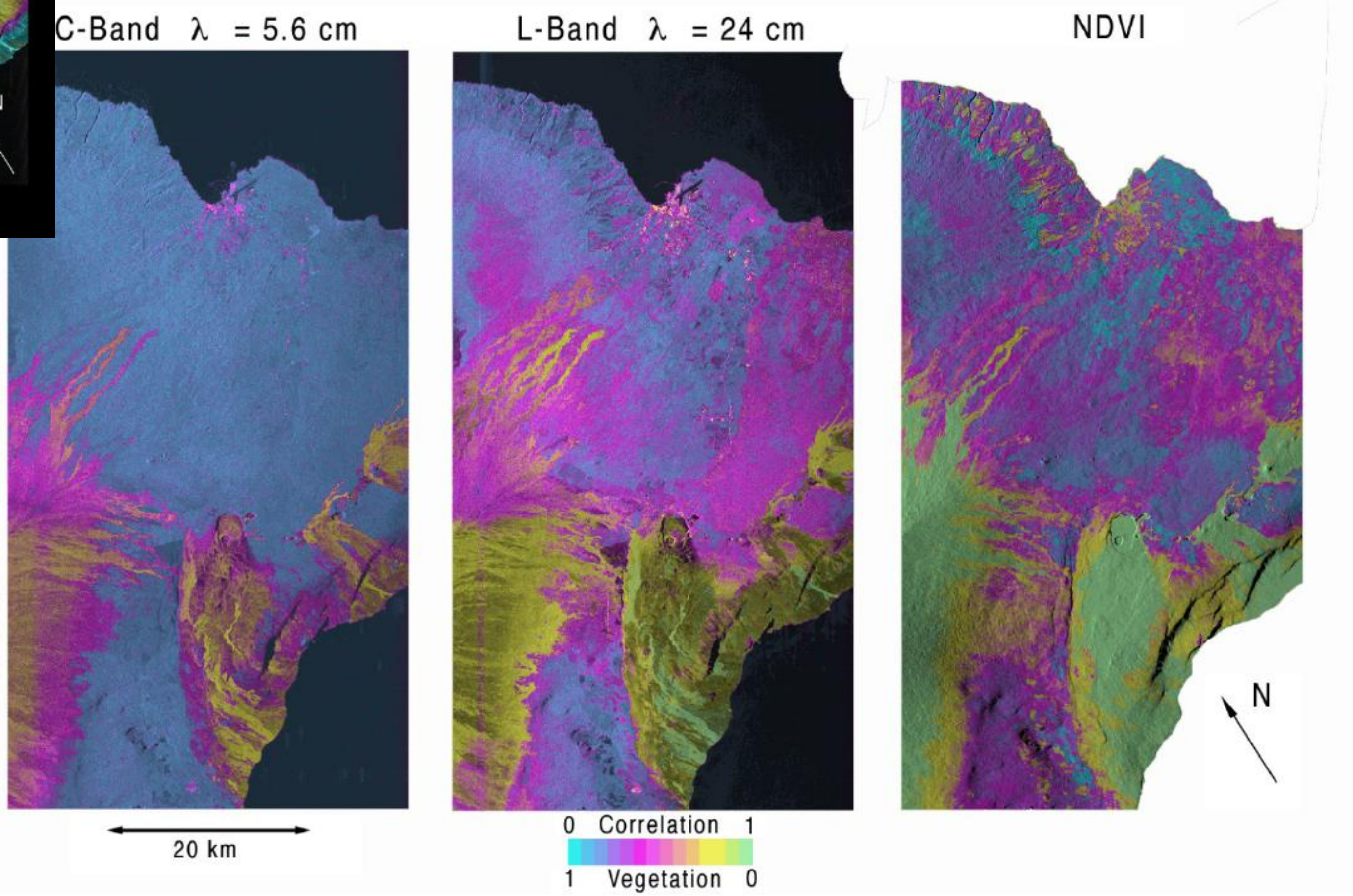

Source: H.Zebker

Error sources

- Decorrelation
- Atmosphere
- Orbit error
- DEM error

Structure of Atmosphere

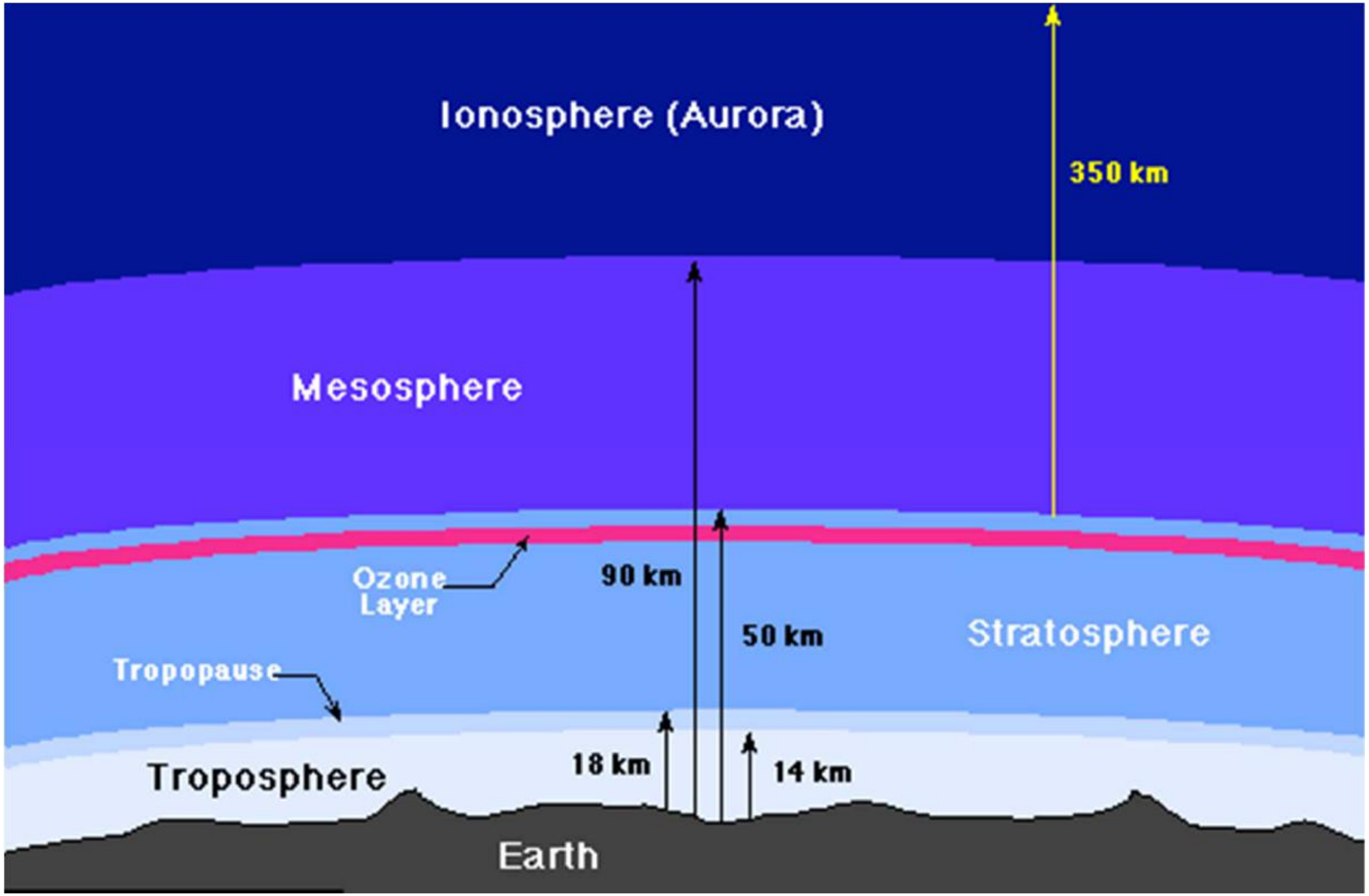

Ionospheric refractivity

$$N(x,z,t) = -4.03 \bullet 10^7 \; n_e / f^2$$

n_e = number of electrons
f = electromagnetic frequency

- Delay due to free electrons
- Dispersive (frequency-dependent):
  - ✓ How many times worse is L-band than C-band?

Ionospheric Delay

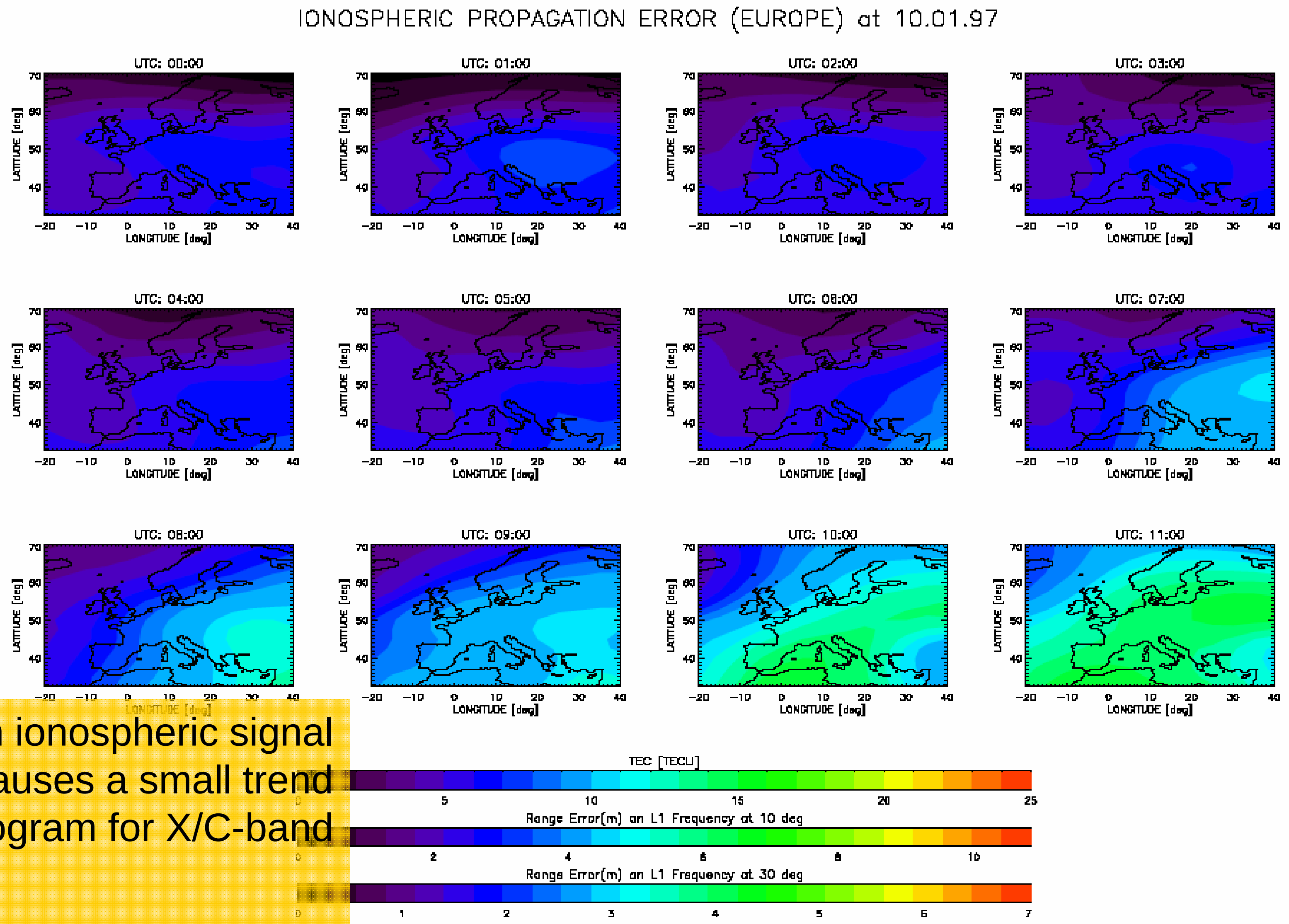

Main ionospheric signal usually causes a small trend in interferogram for X/C-band

TU Delft

Wenchuan Earthquake, L-Band

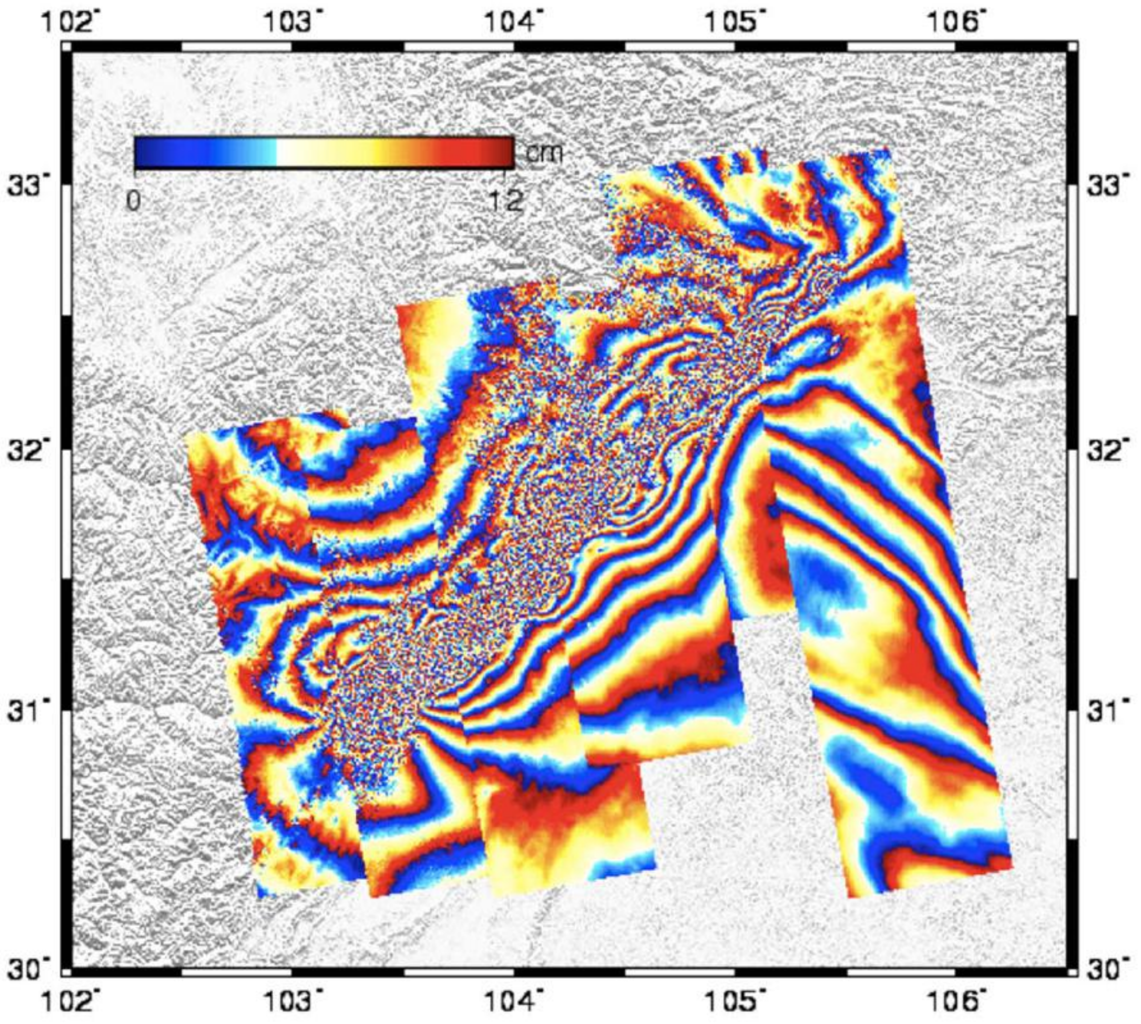

Ionospheric fringes?

Ding et al, ALOS Symposium, 2008

Coregistration Offsets

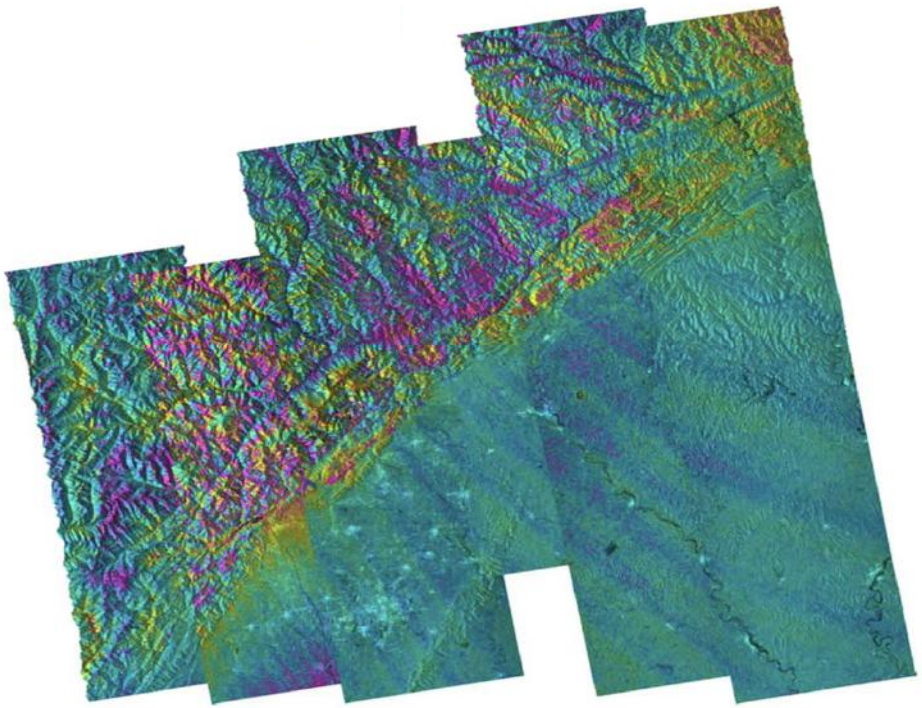

Range offsets

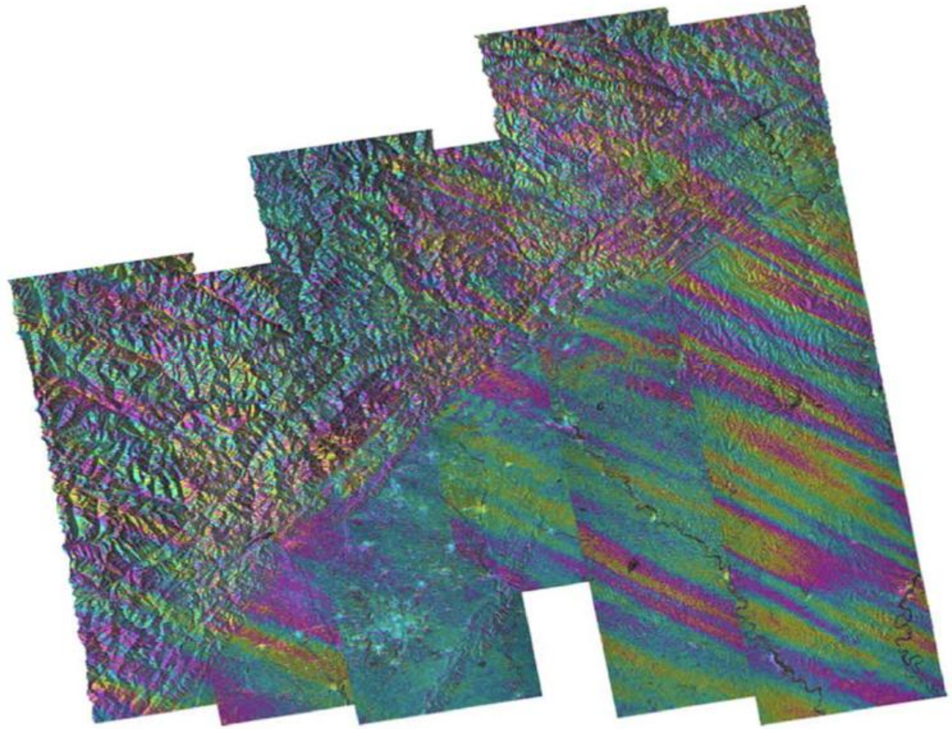

Azimuth offsets

Ding et al, ALOS Symposium, 2008

High-Latitude Azimuth offsets

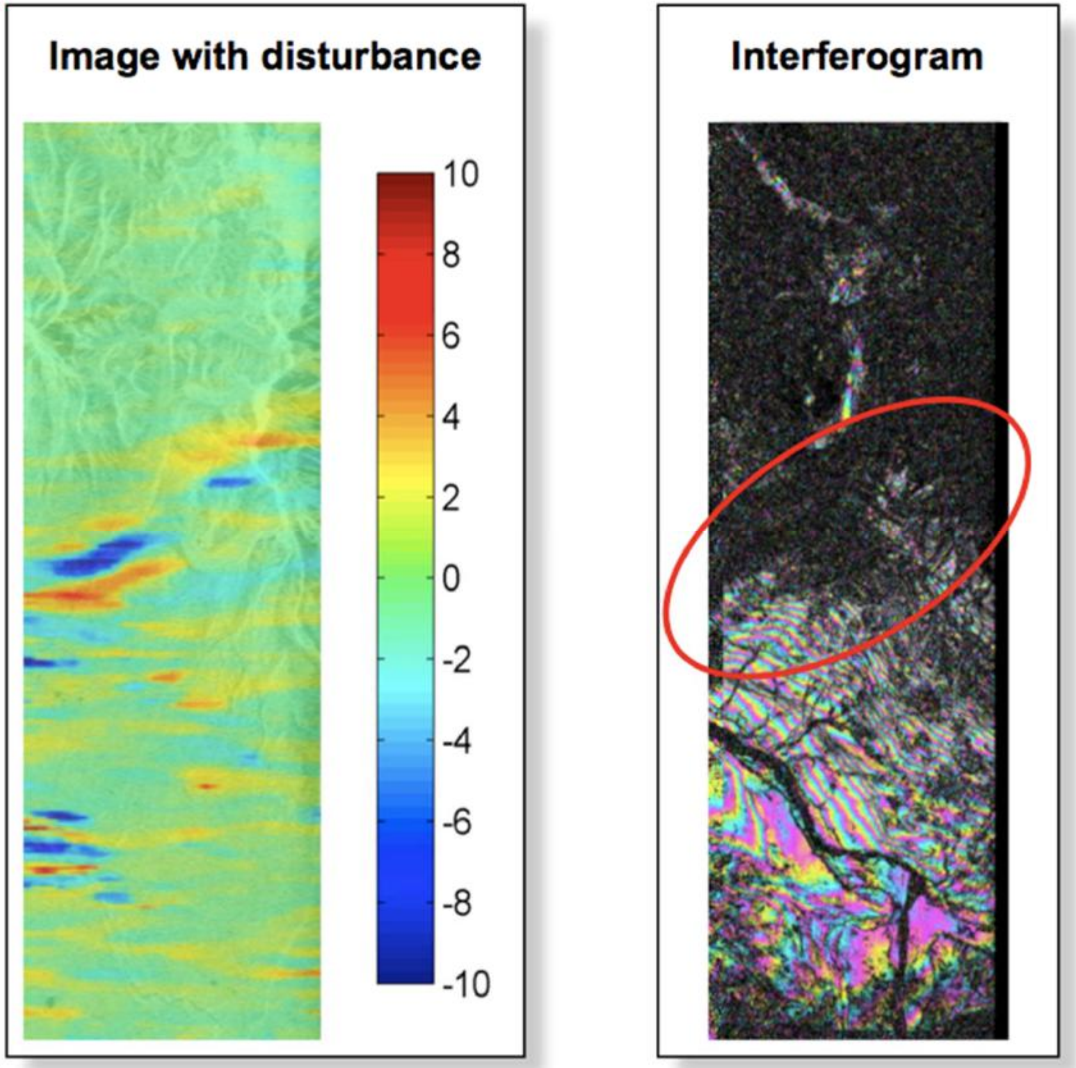

Meyer and Nicoll,
Fringe 2007

Structure of Atmosphere

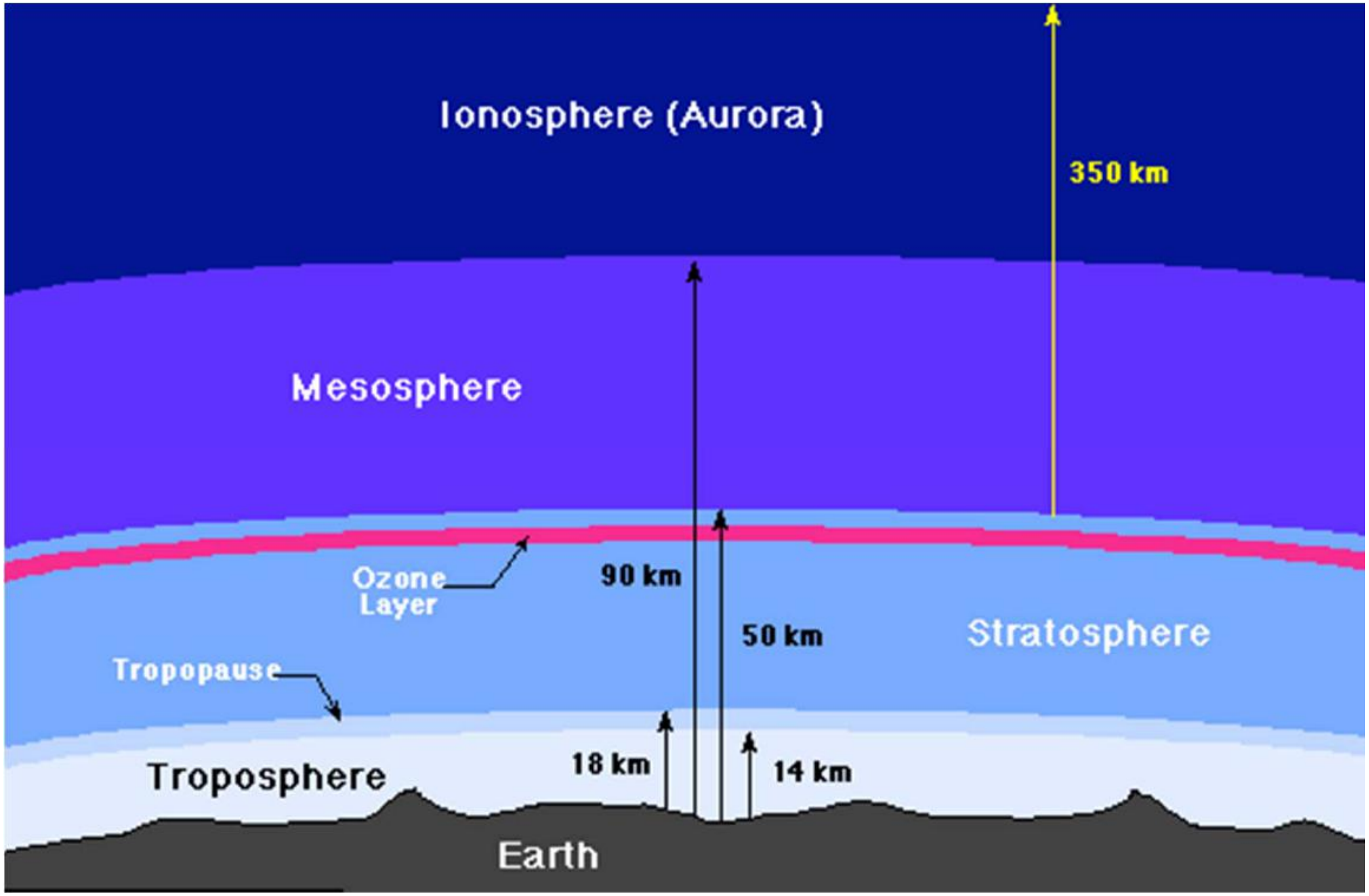

Tropospheric Refractivity

$$N(x,z,t) = k_1 \frac{P}{T} + \left(k_2' \frac{e}{T} + k_3 \frac{e}{T^2} \right) + 1.4W$$

Most spatial variability

- P=Pressure
- T=Temperature
- e=Partial water vapour pressure
- W=Liquid water

- Hydrostatic term from surface measurements
- Wet delay term (sensitivity 4-20 times higher for WV than for T)
- Liquid term limited (<5%)

Water vapor

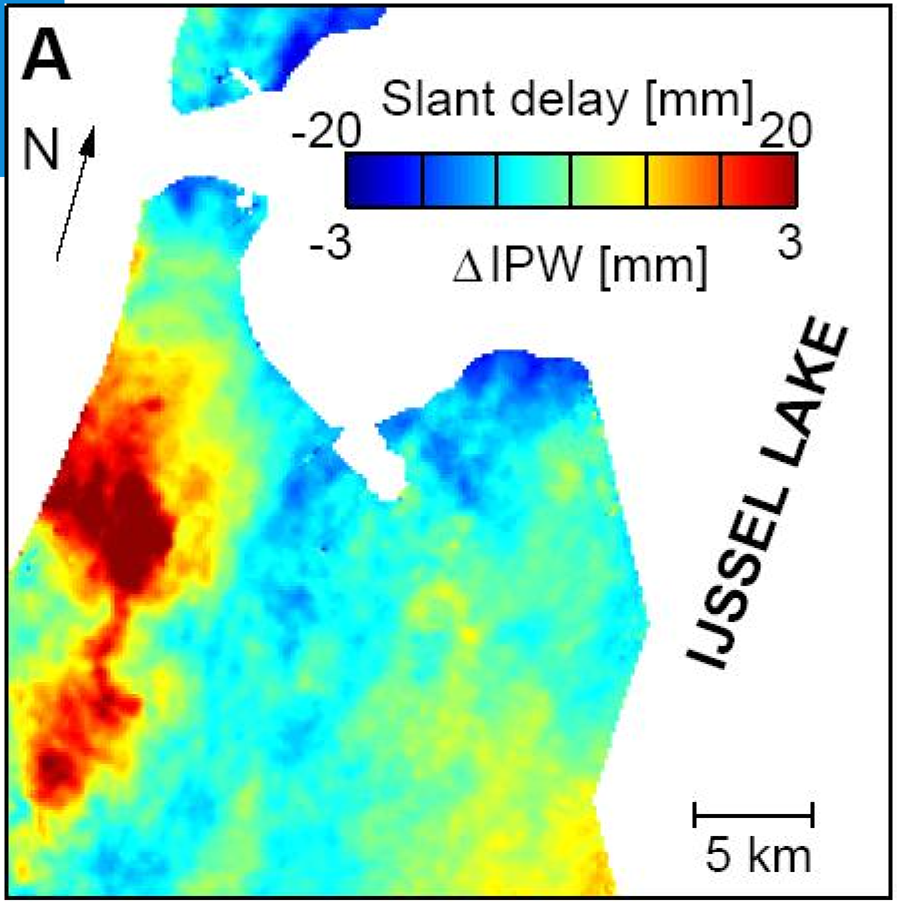

Spatial variability of water vapour

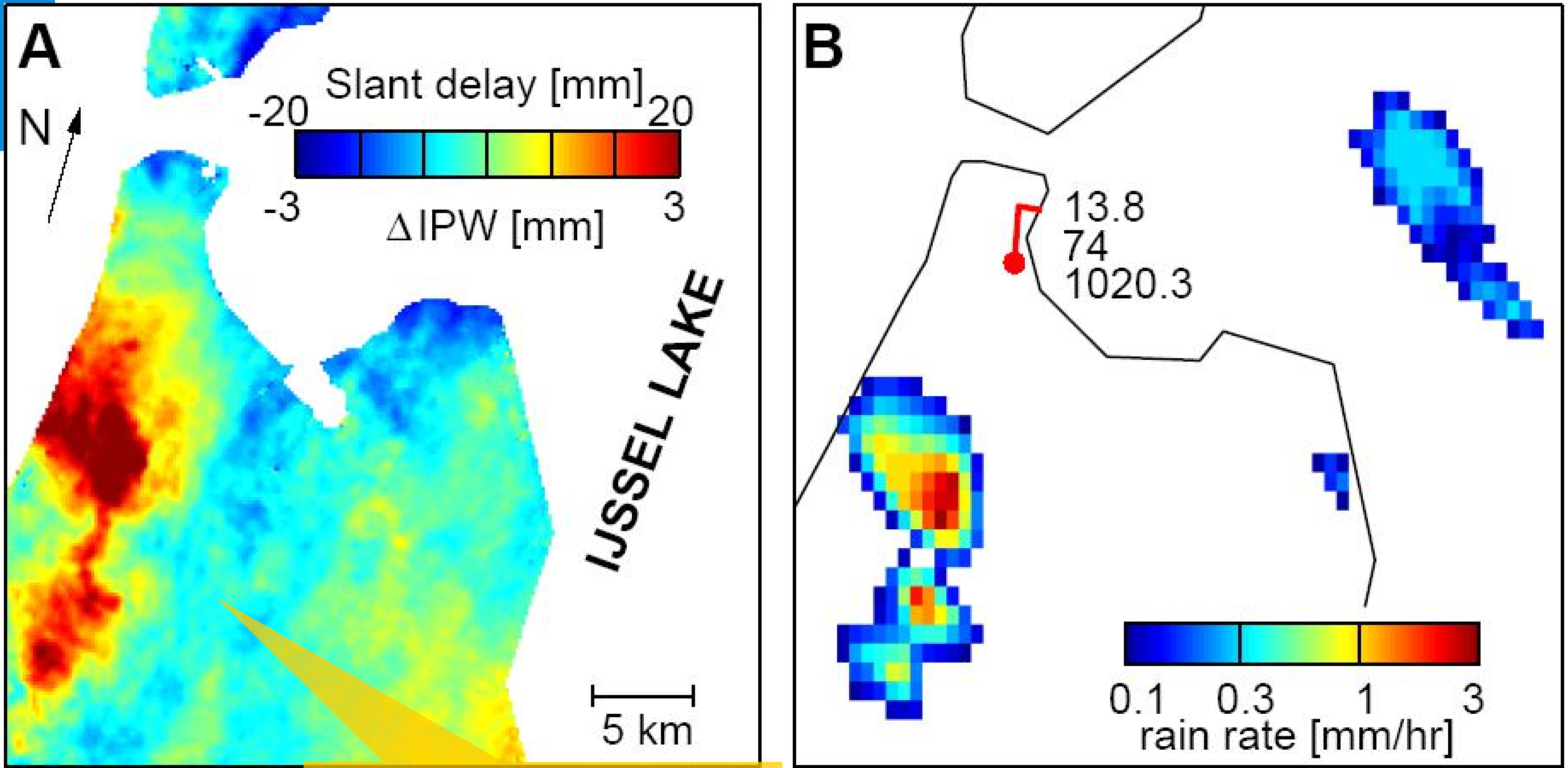

260 million liter excess water in cloud system

Tropospheric signal

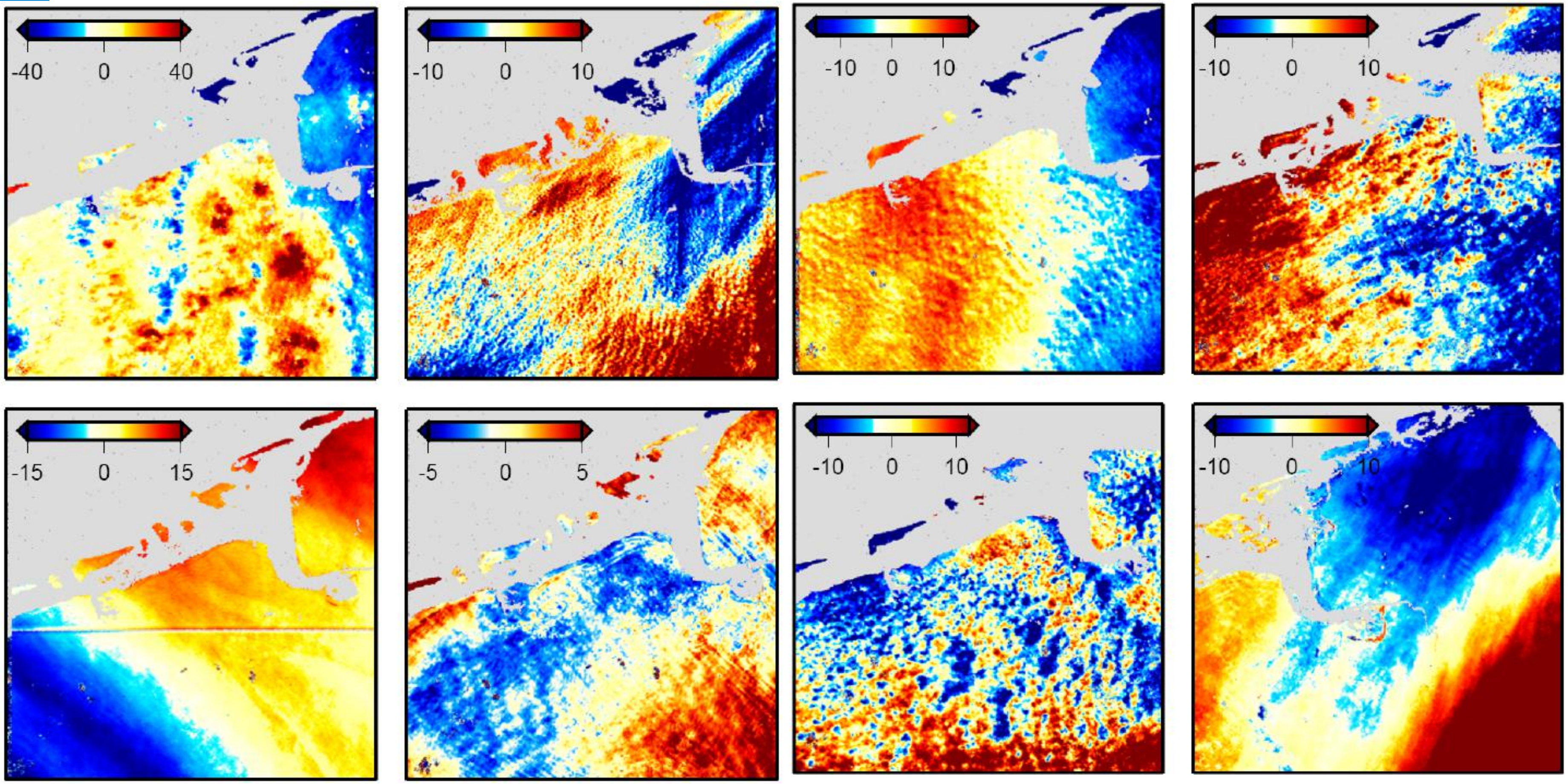

Temporal variability in water vapour

In the presence of topography, changes in the refractivity between the two acquisitions will cause an interferometric phase even if no spatial variability

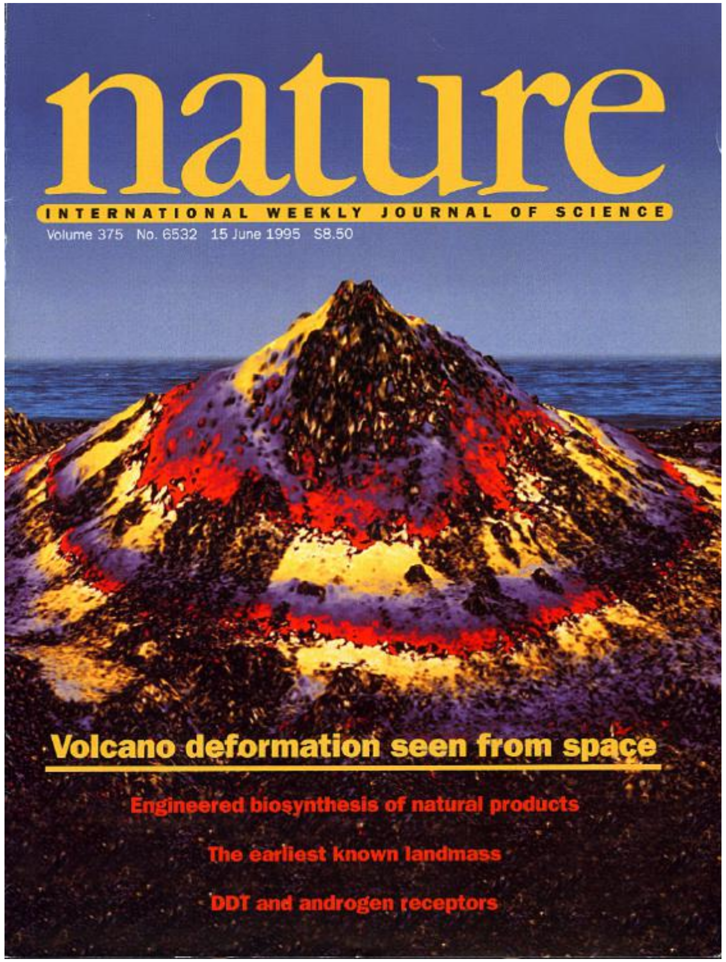

Change in refractivity profile

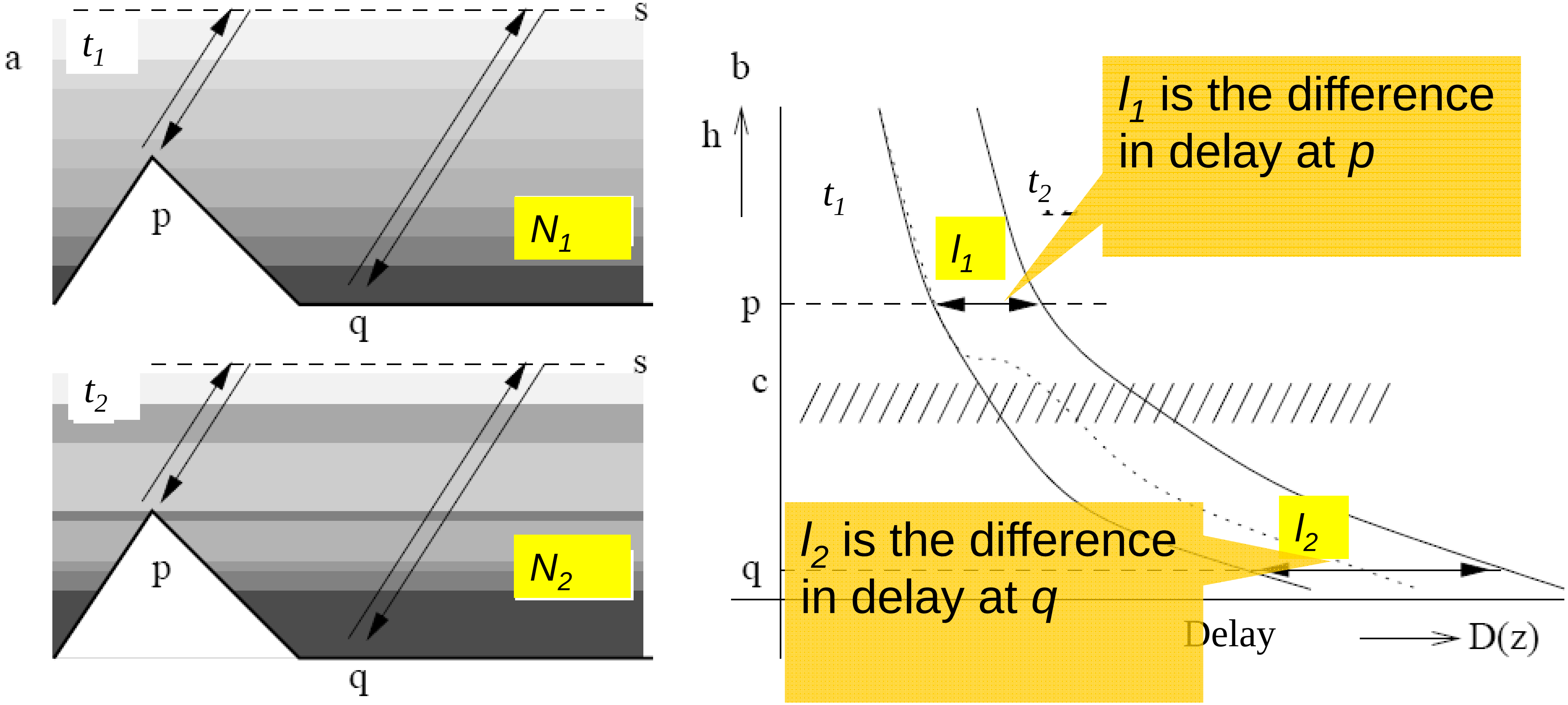

✓ A difference between l_2 and l_1 will result in a phase offset between p and q

Error sources

- Decorrelation
- Atmosphere
- Orbit error
- DEM error

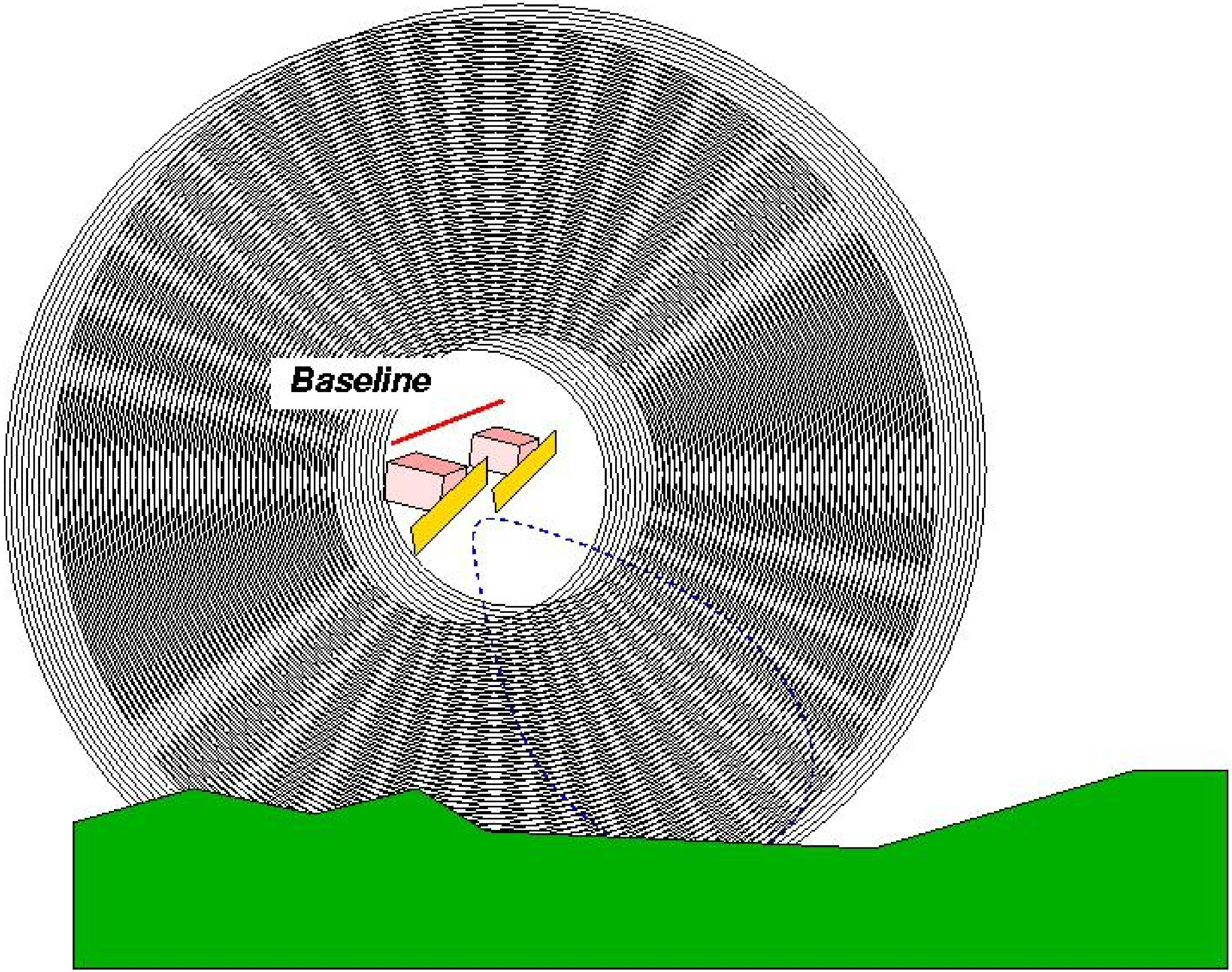
Baseline

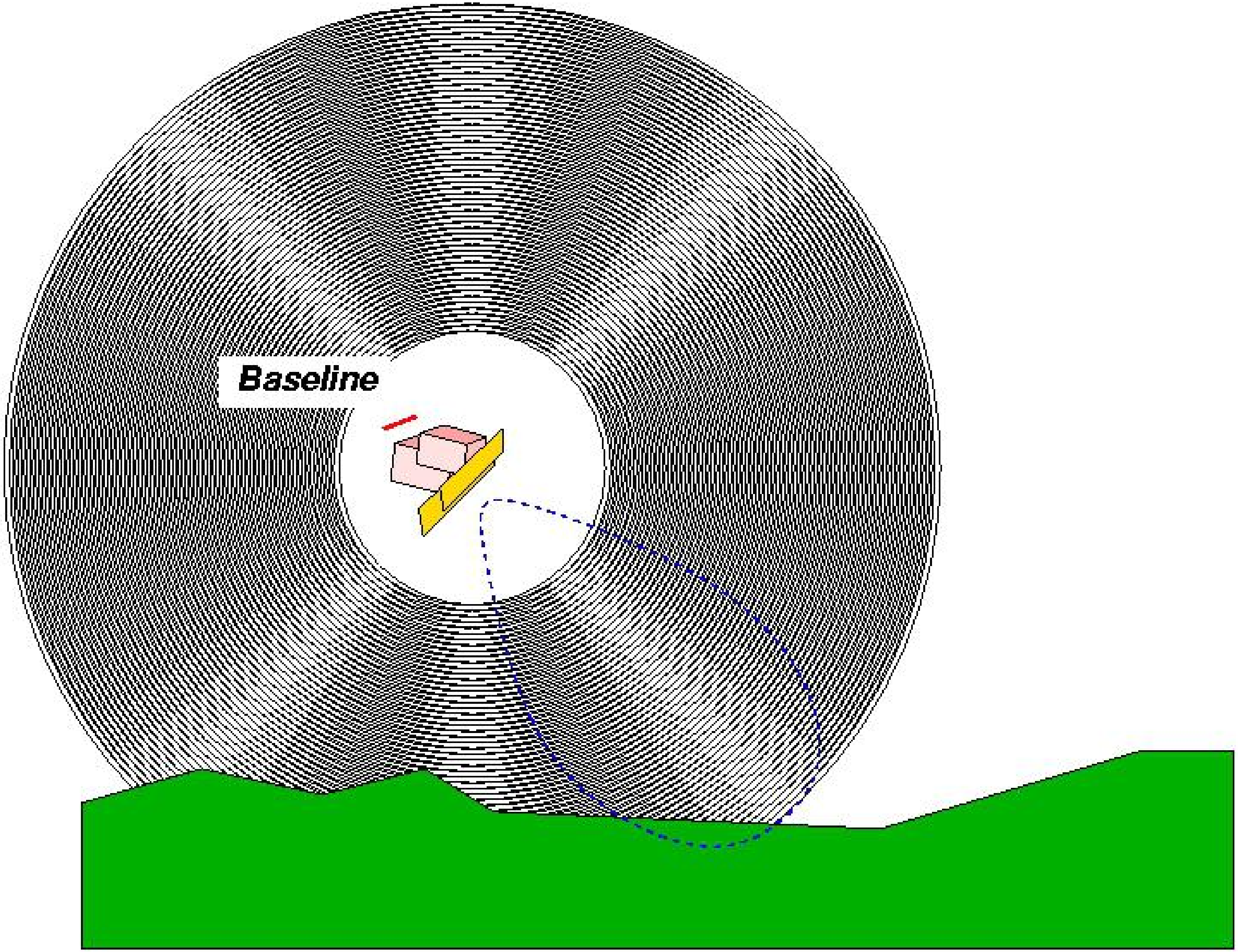
Baseline

Orbit Error Components

$dB_{\parallel}$

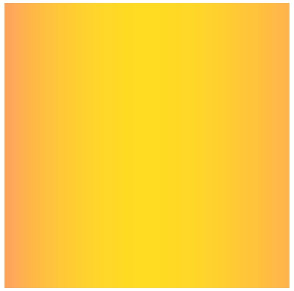

$dB_{\perp}$ **(nearly linear)**

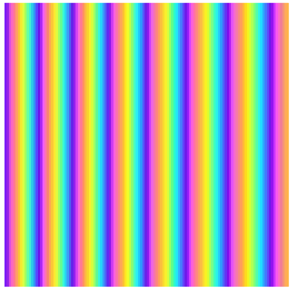

2 m

$d\frac{\partial B_{\parallel}}{\partial t}$ **(linear)**

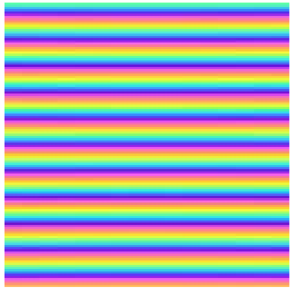

$d\frac{\partial B_{\perp}}{\partial t}$

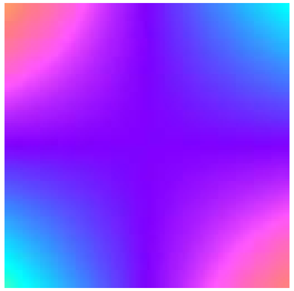

2 cm/s

$d\frac{\partial^2 B_{\parallel}}{\partial t^2}$

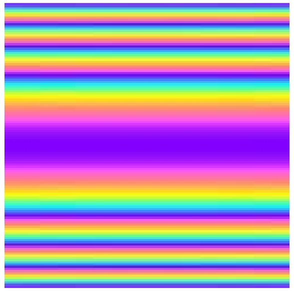

D omponents

$d\frac{\partial^2 B_{\perp}}{\partial t^2}$

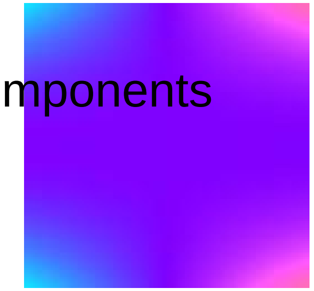

2 mm/s²

Courtesy Herman Baehr

Orbit Error Correction

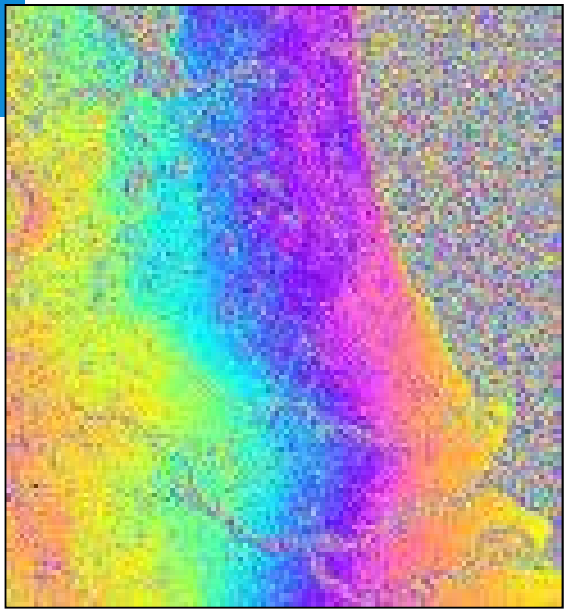

Interferogram

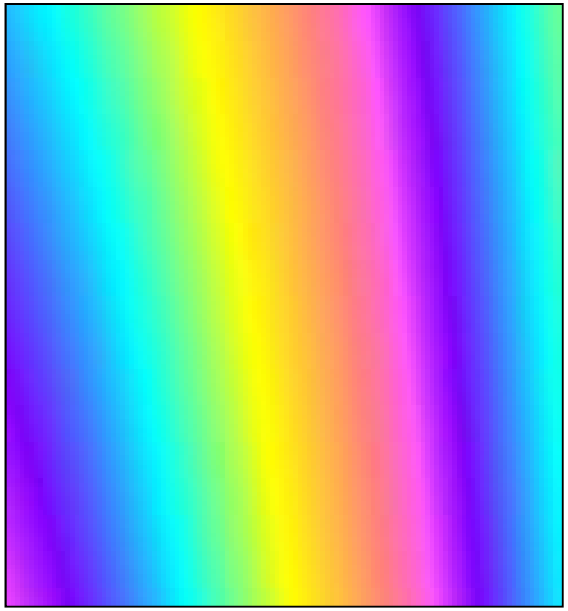

Orbit Correction Estimate

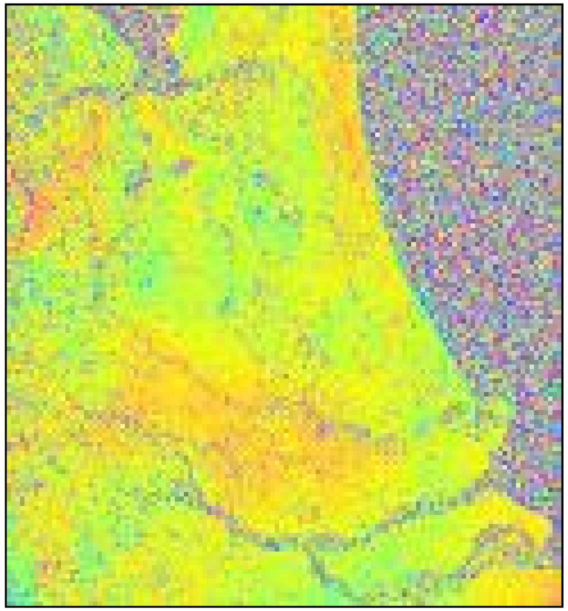

Remaining Phase

Courtesy Herman Baehr

Persistent Scatterer Interferometry

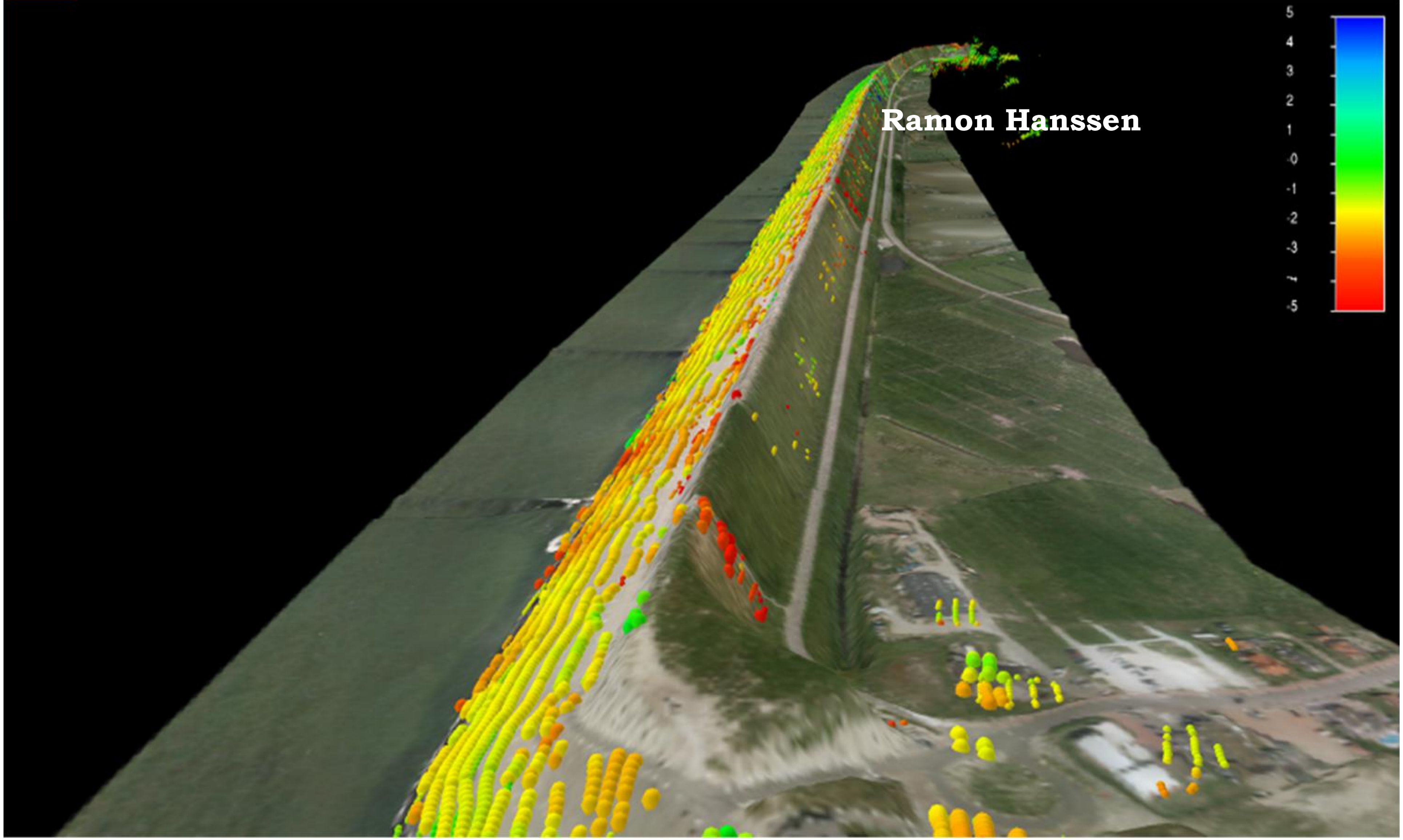

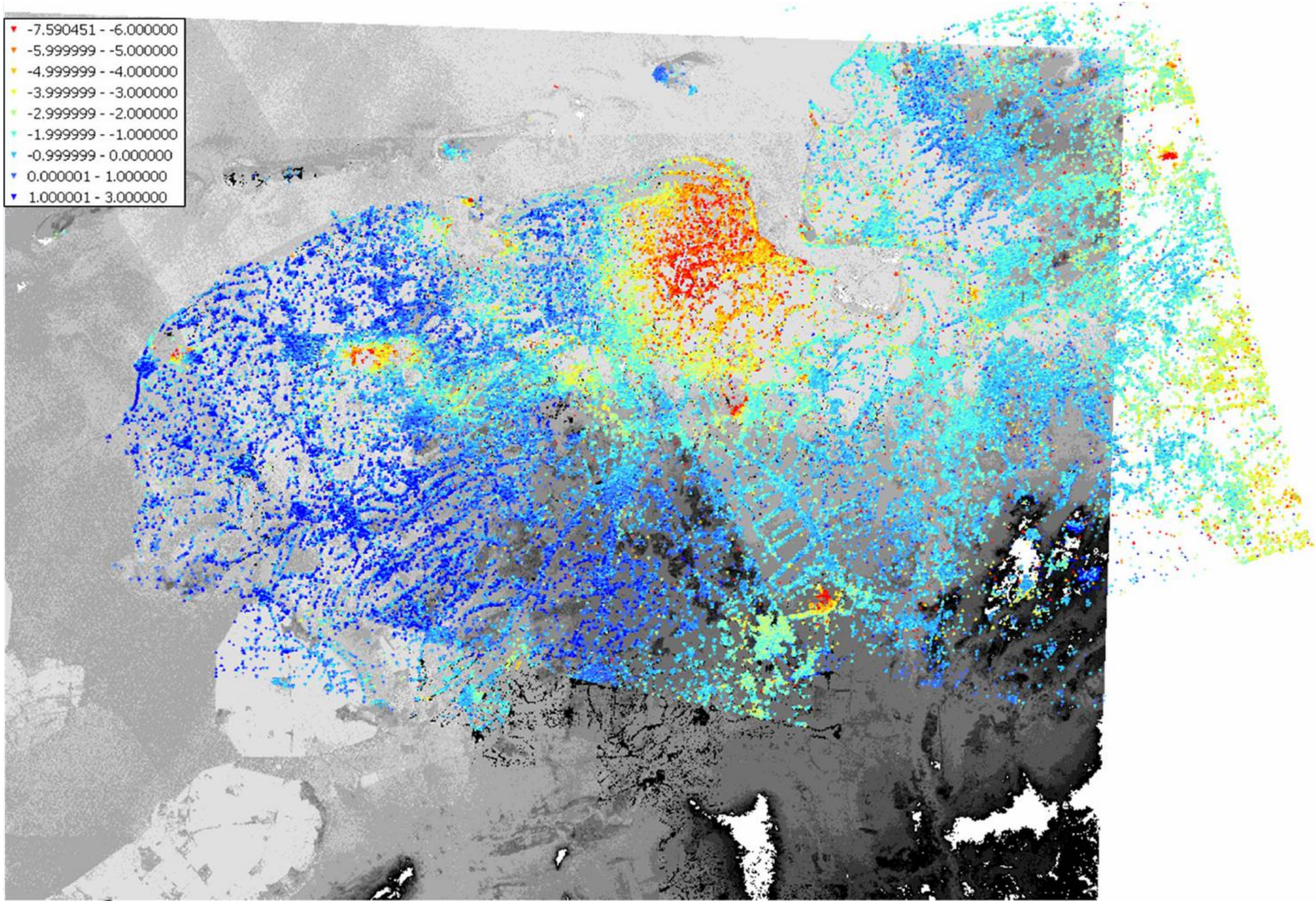
-7.590451 - -6.000000
-5.999999 - -5.000000
-4.999999 - -4.000000
-3.999999 - -3.000000
-2.999999 - -2.000000
-1.999999 - -1.000000
-0.999999 - 0.000000
0.000001 - 1.000000
1.000001 - 3.000000

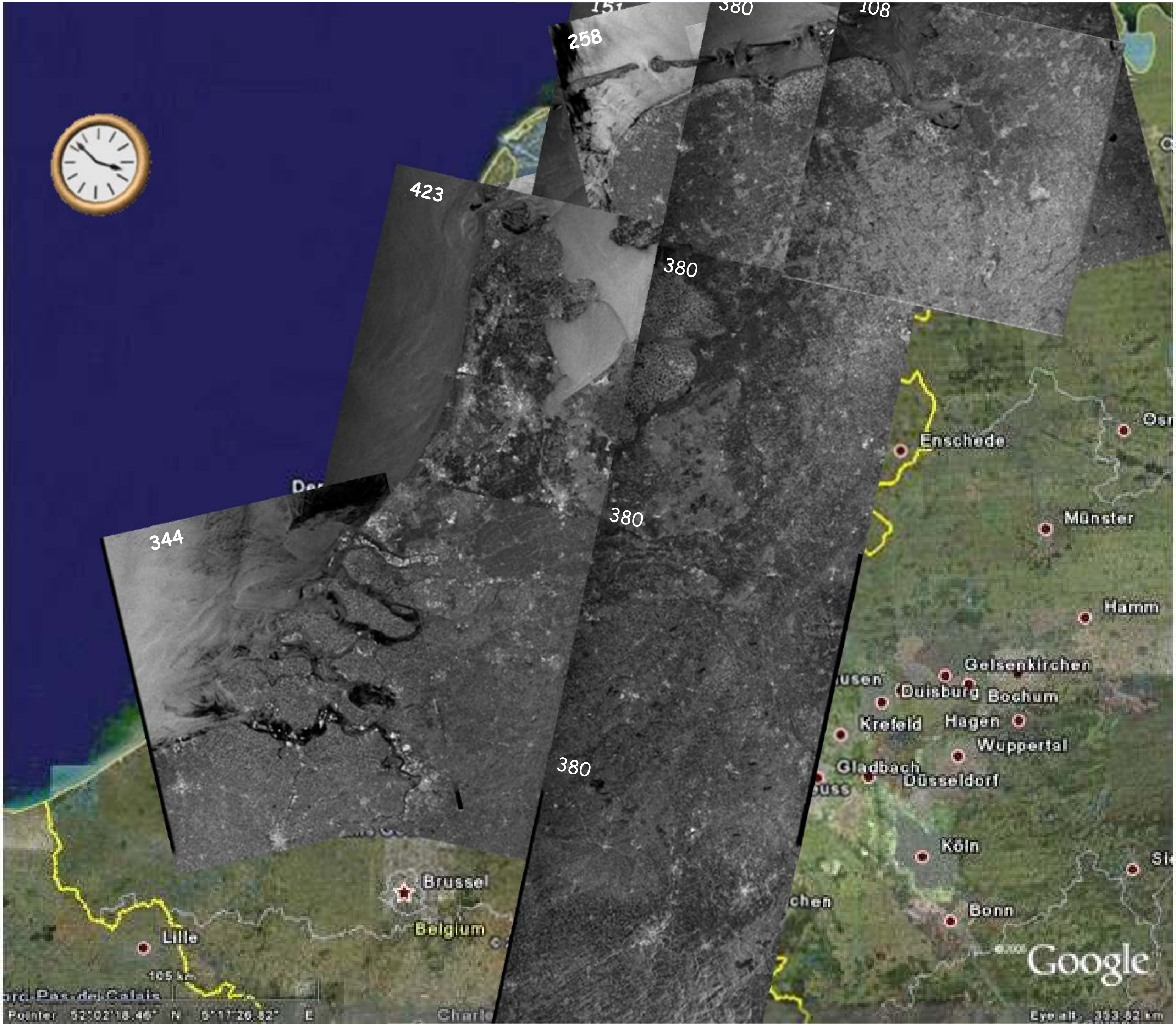

258
108
423
380
380
344
380
Enschede
Münster
Hamm
Gelsenkirchen
Duisburg
Bochum
Krefeld
Hagen
Wuppertal
Gladbach
Düsseldorf
Köln
Bonn
Brussel
Belgium
Lille
Google

Time-Series approach: Persistent Scatterers

- Pixels with strong and consistent (coherent) reflections in time.
- Multi-pass InSAR – time series
- Estimate atmospheric signal, ambiguities, topography, displacement

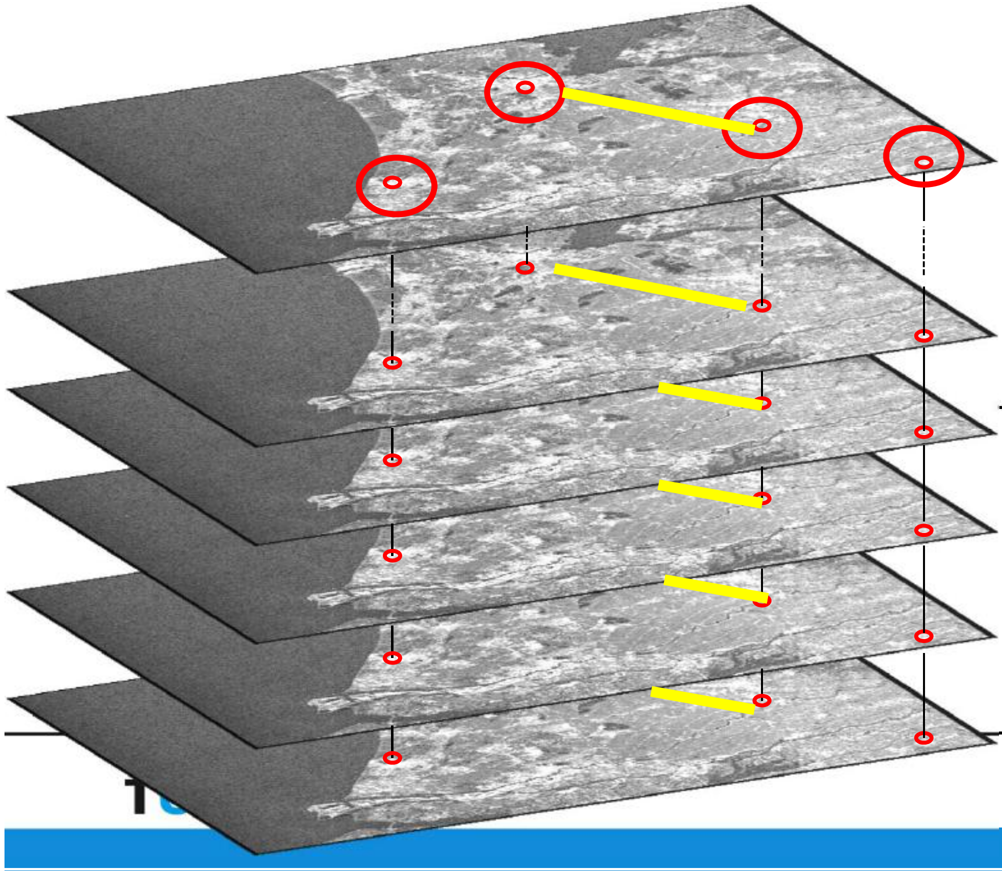

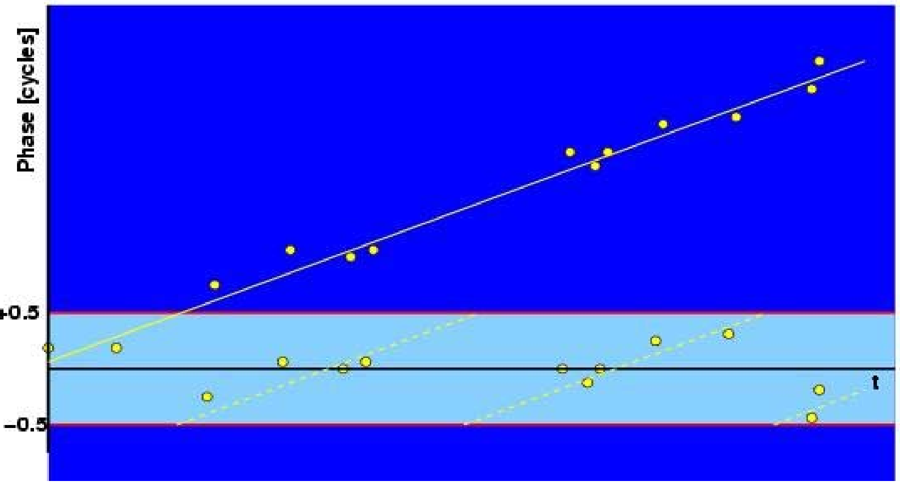

Validation experiment

- 5 (4) reflectors, ~200 m spacing
- Monitored March 2003 – now
- 3.5 years: ~40 Envisat and ~40 ERS-2 images
- Spirit leveling performed at every acquisition

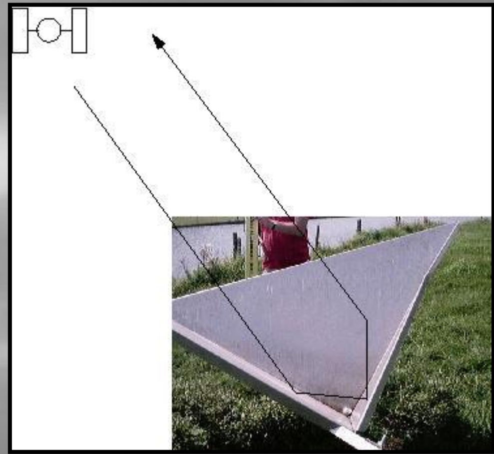

140

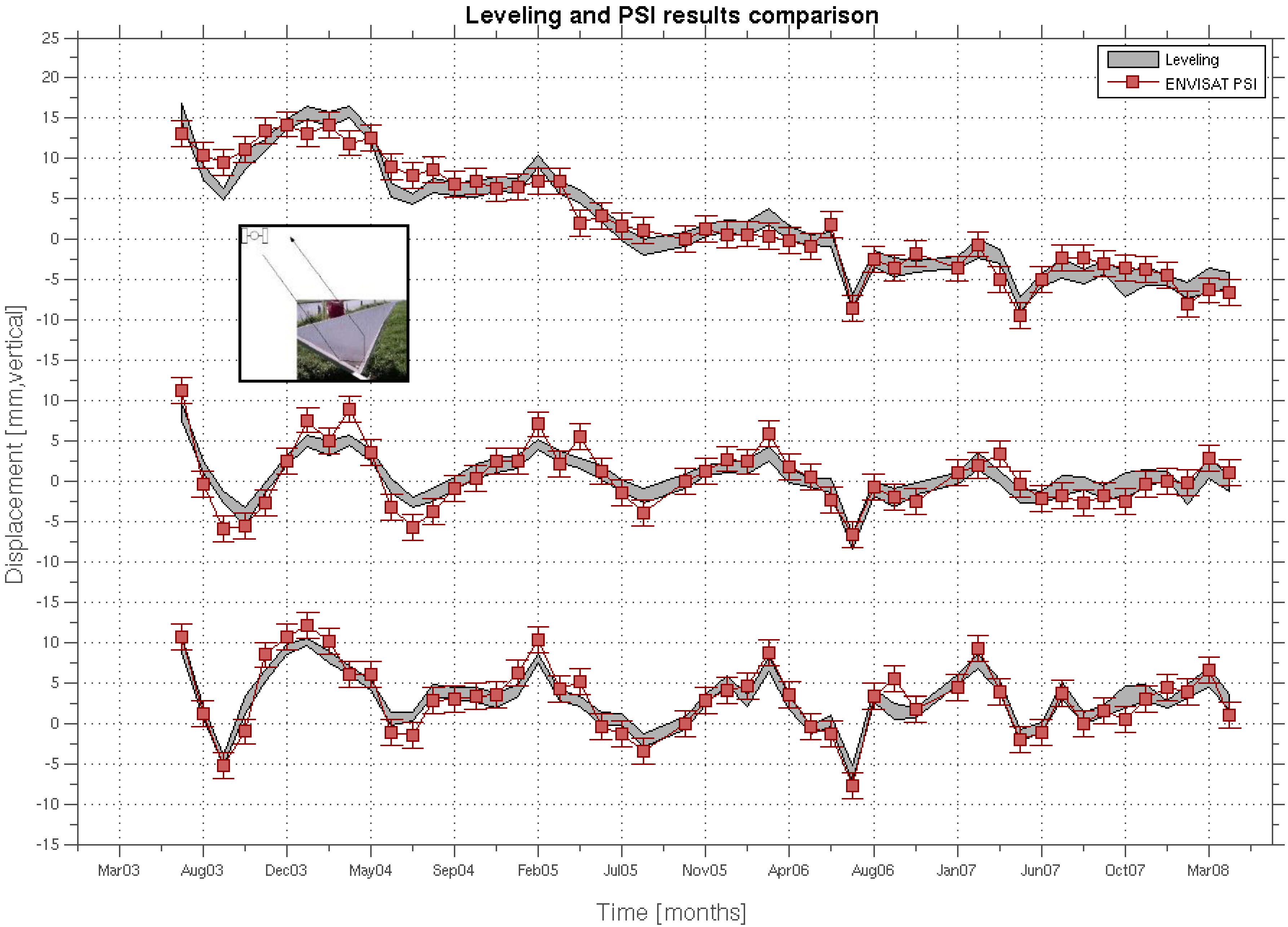
Leveling and PSI results comparison
Leveling
ENVISAT PSI
Displacement [mm,vertical]
Time [months]
Mar03
Aug03
Dec03
May04
Sep04
Feb05
Jul05
Nov05
Apr06
Aug06
Jan07
Jun07
Oct07
Mar08
25
20
15
10
5
0
-5
-10
-15

Deformation measurements: time-series approaches

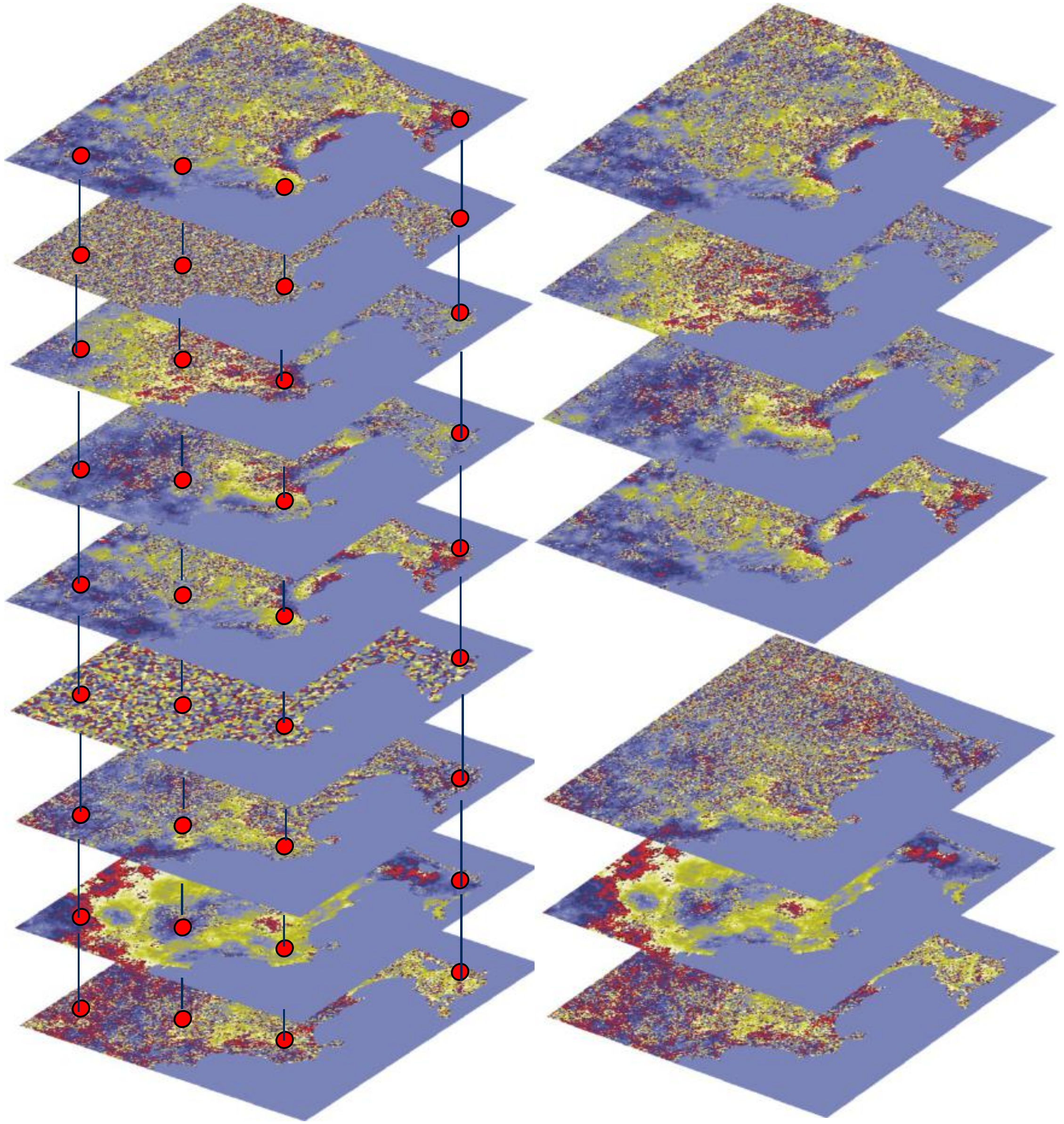

- Evaluation per point: double-differences
- Opportunistic subsets

Image F. Serafino, Napels University

Subsets vs Single-master stack

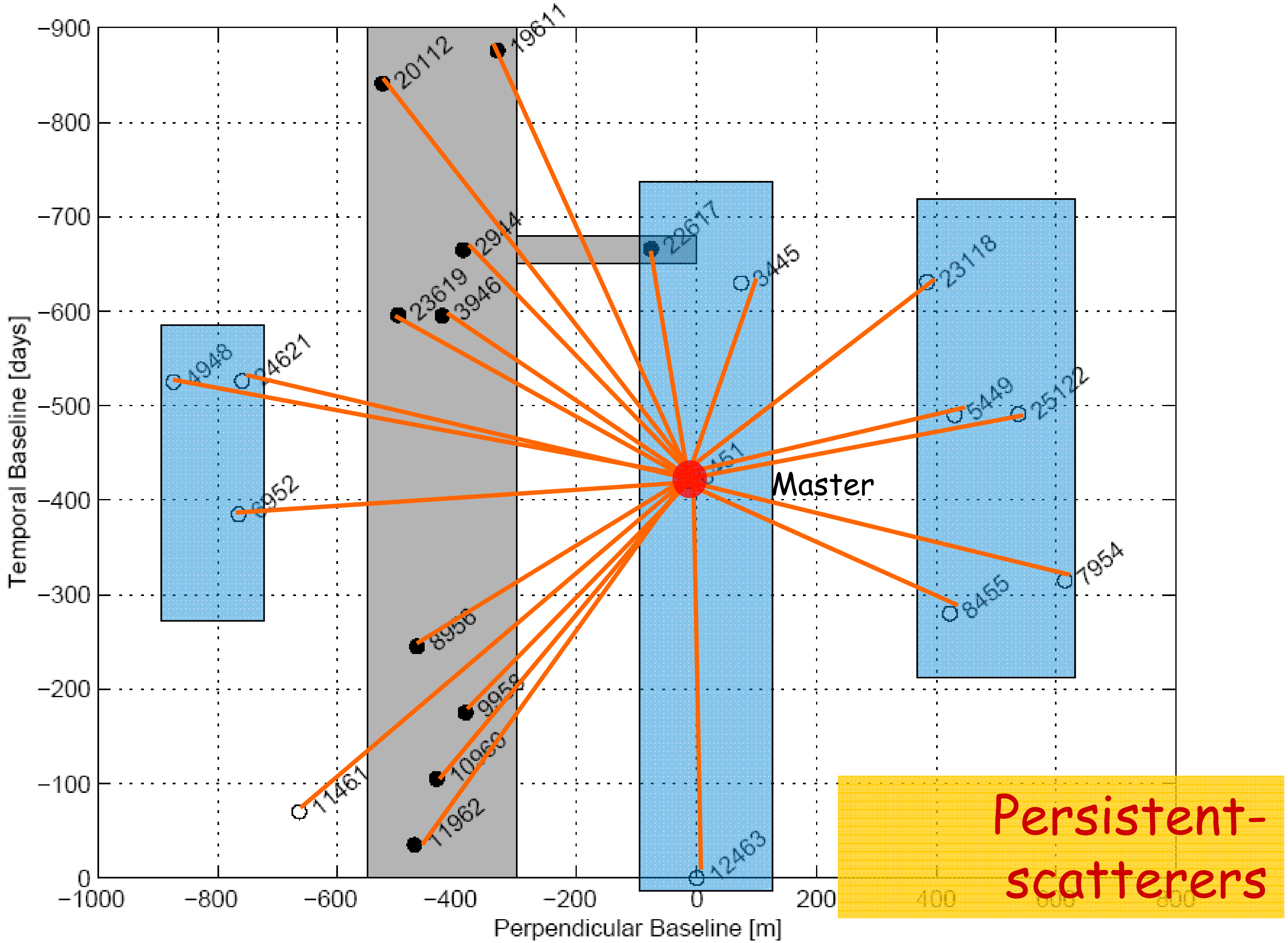

Rotterdam time series

Perpendicular baseline 72 m

Temporal baseline 35 days

ΔDoppler = 37 Hz

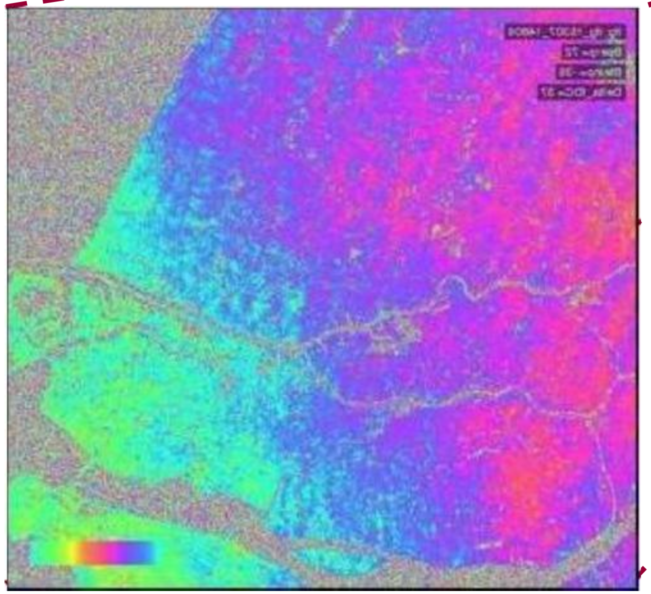

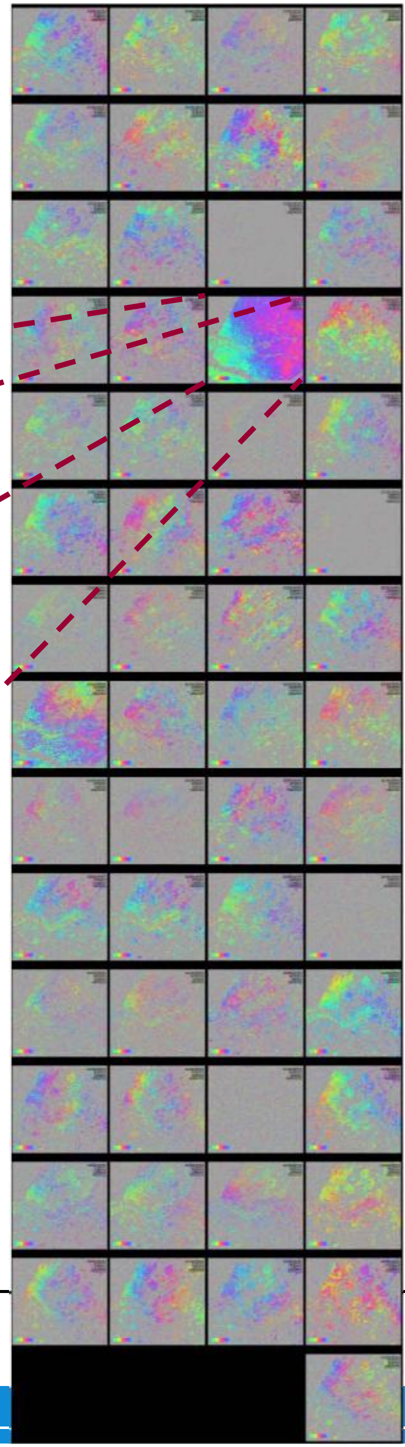

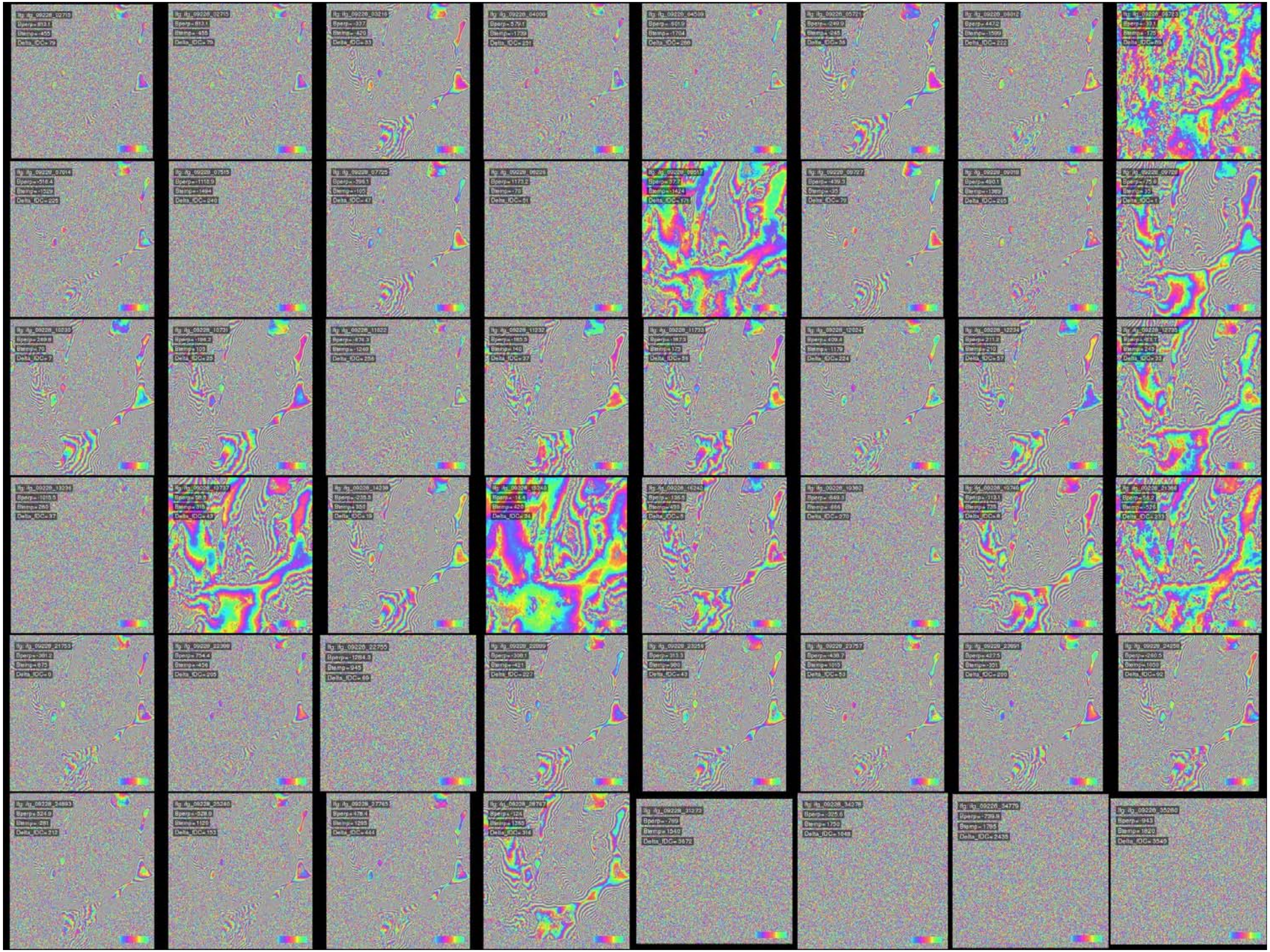

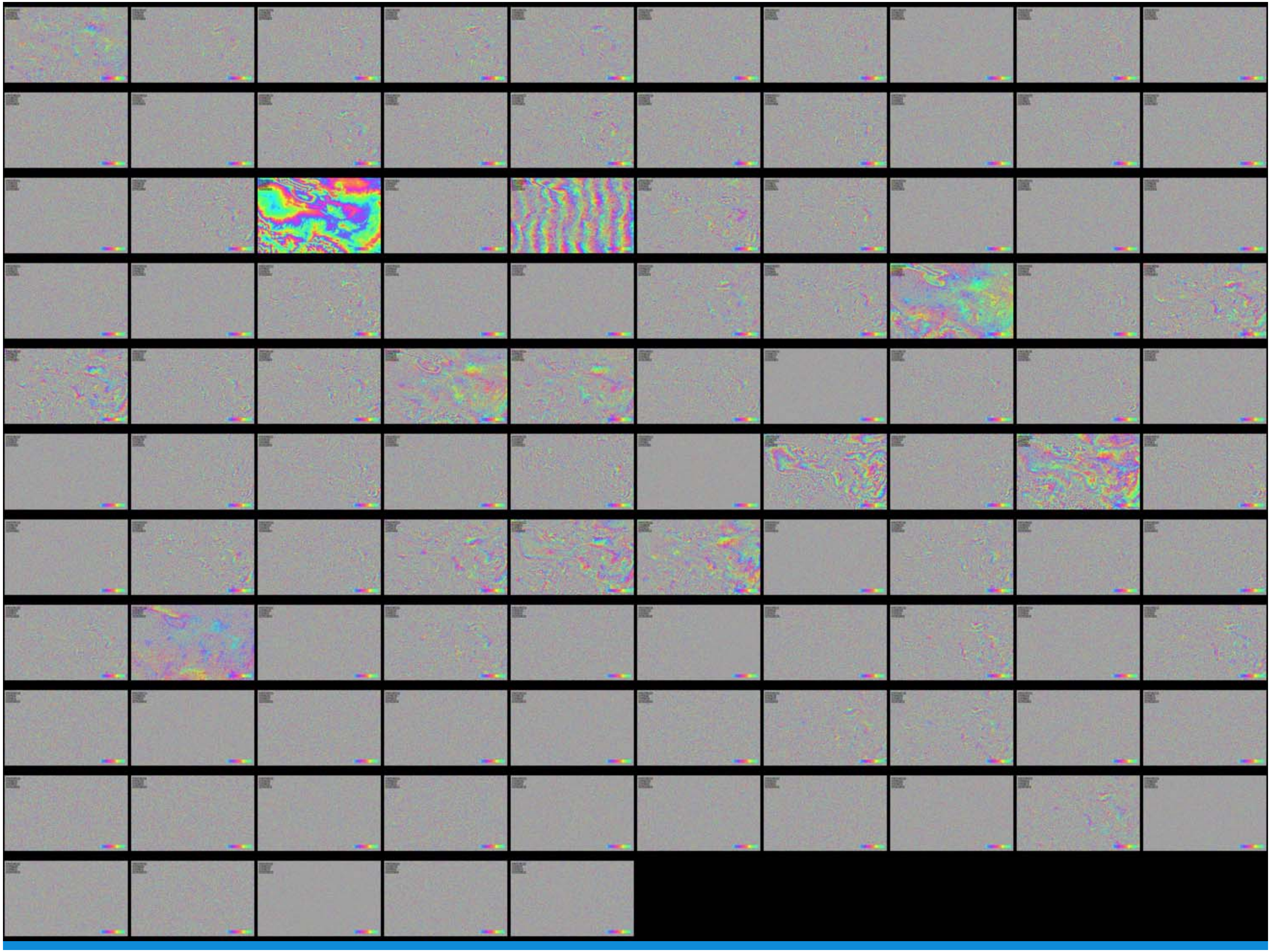

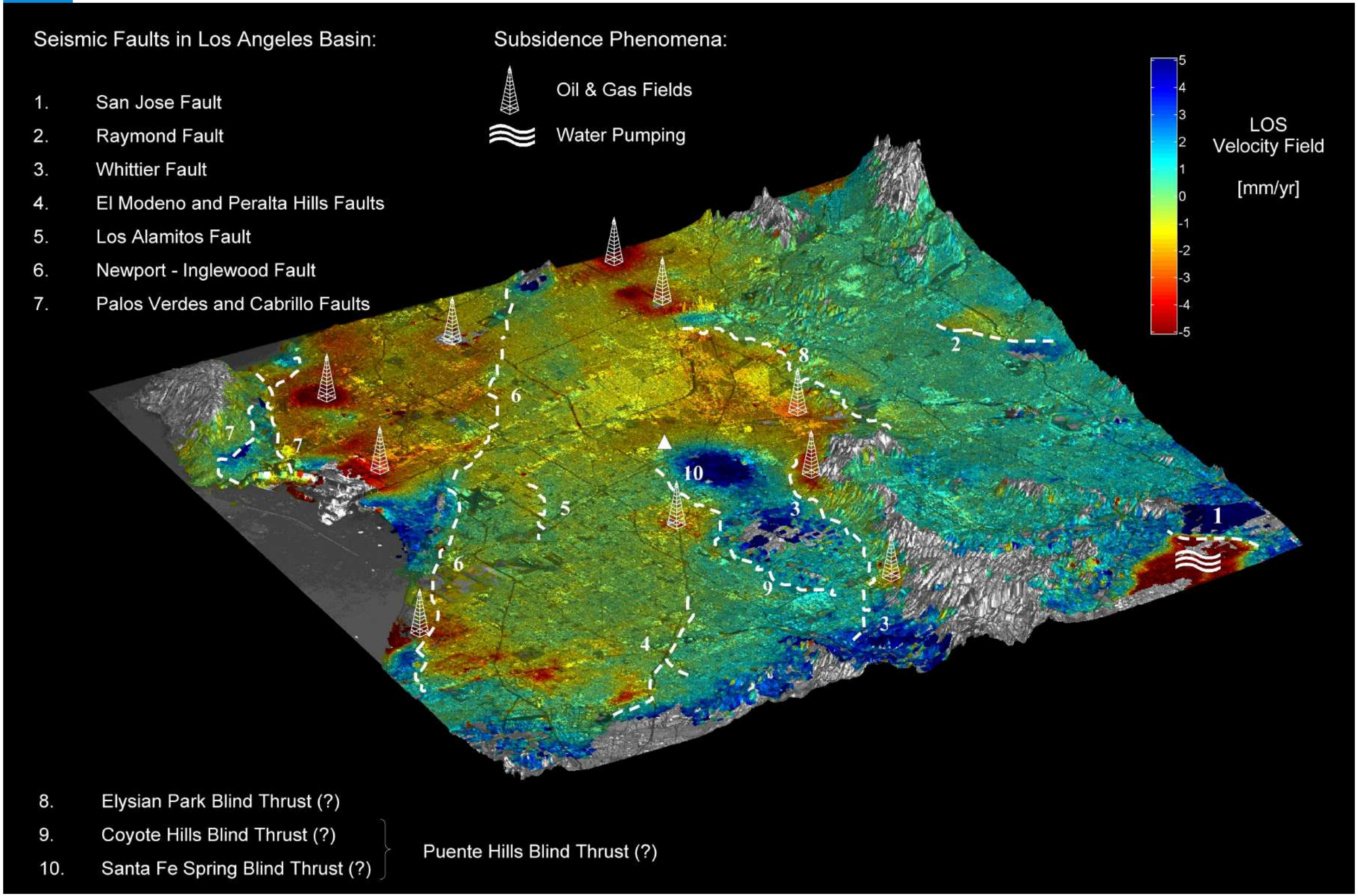
Seismic Faults in Los Angeles Basin:
1. San Jose Fault
2. Raymond Fault
3. Whittier Fault
4. El Modeno and Peralta Hills Faults
5. Los Alamitos Fault
6. Newport - Inglewood Fault
7. Palos Verdes and Cabrillo Faults
Subsidence Phenomena:
Oil & Gas Fields
Water Pumping
LOS Velocity Field
[mm/yr]
5
4
3
2
1
0
-1
-2
-3
-4
-5
8. Elysian Park Blind Thrust (?)
9. Coyote Hills Blind Thrust (?)
10. Santa Fe Spring Blind Thrust (?)
Puente Hills Blind Thrust (?)

Etna – Estimated Velocity Field (1995-2000)

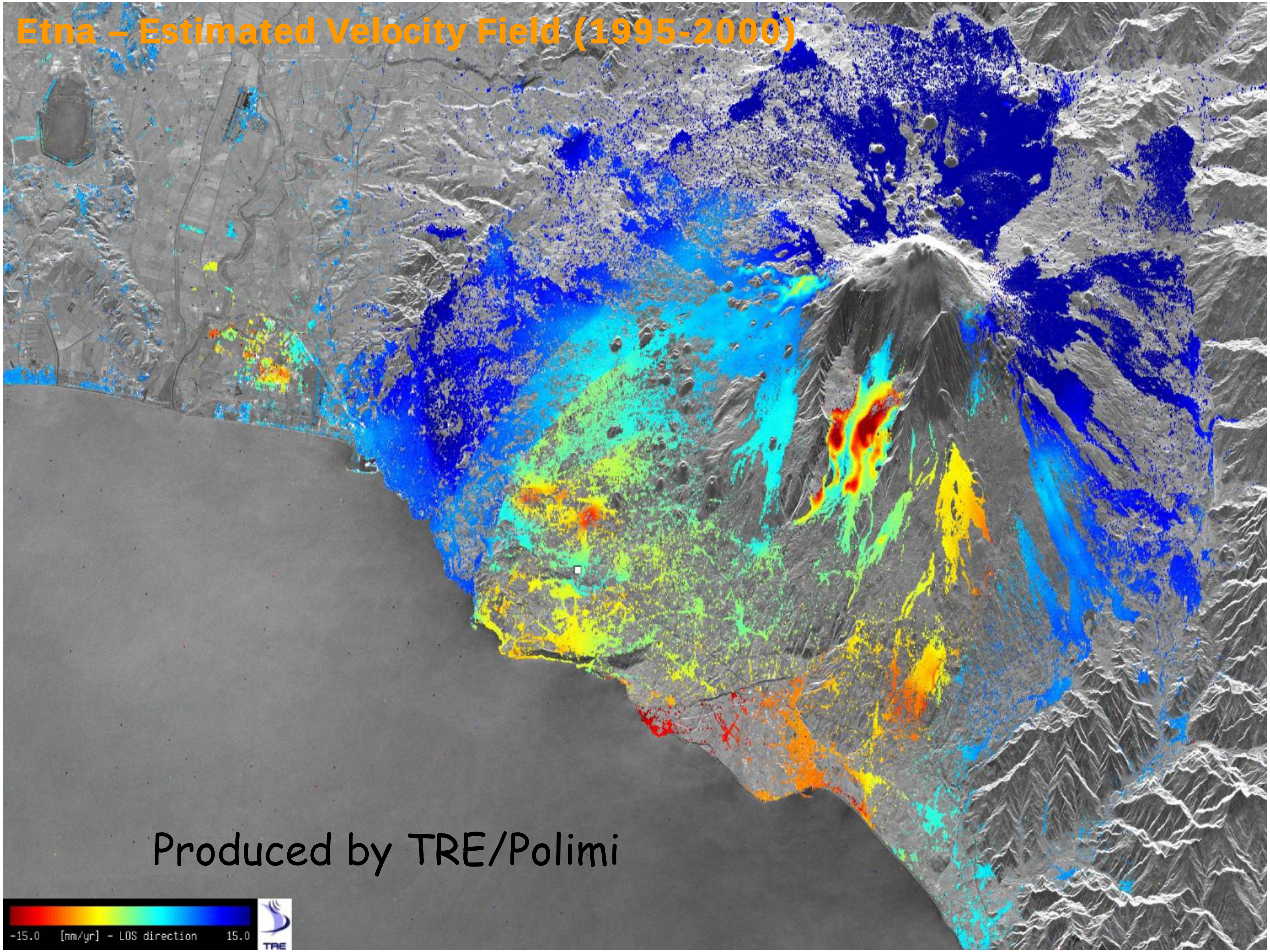

Examples: Nation-wide deformation model

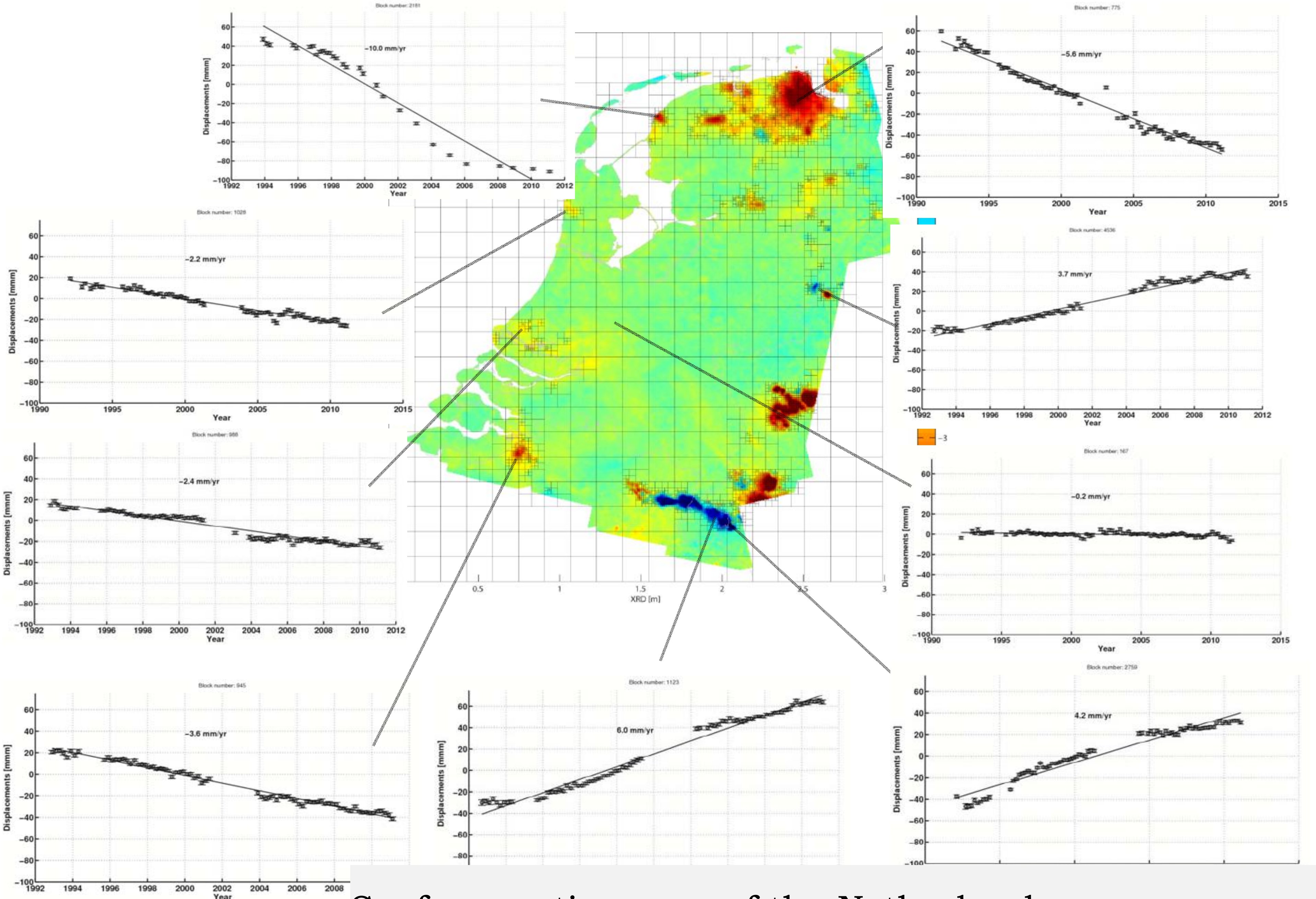

Surface motion map of the Netherlands

Infrastructure monitoring


1000 ft
200 m
©2006 Google - Imagery ©2006 Aerodata International Su
mm/y
a
−3.0
−2.0
−1.0
−0.0
1.0
2.0
3.0

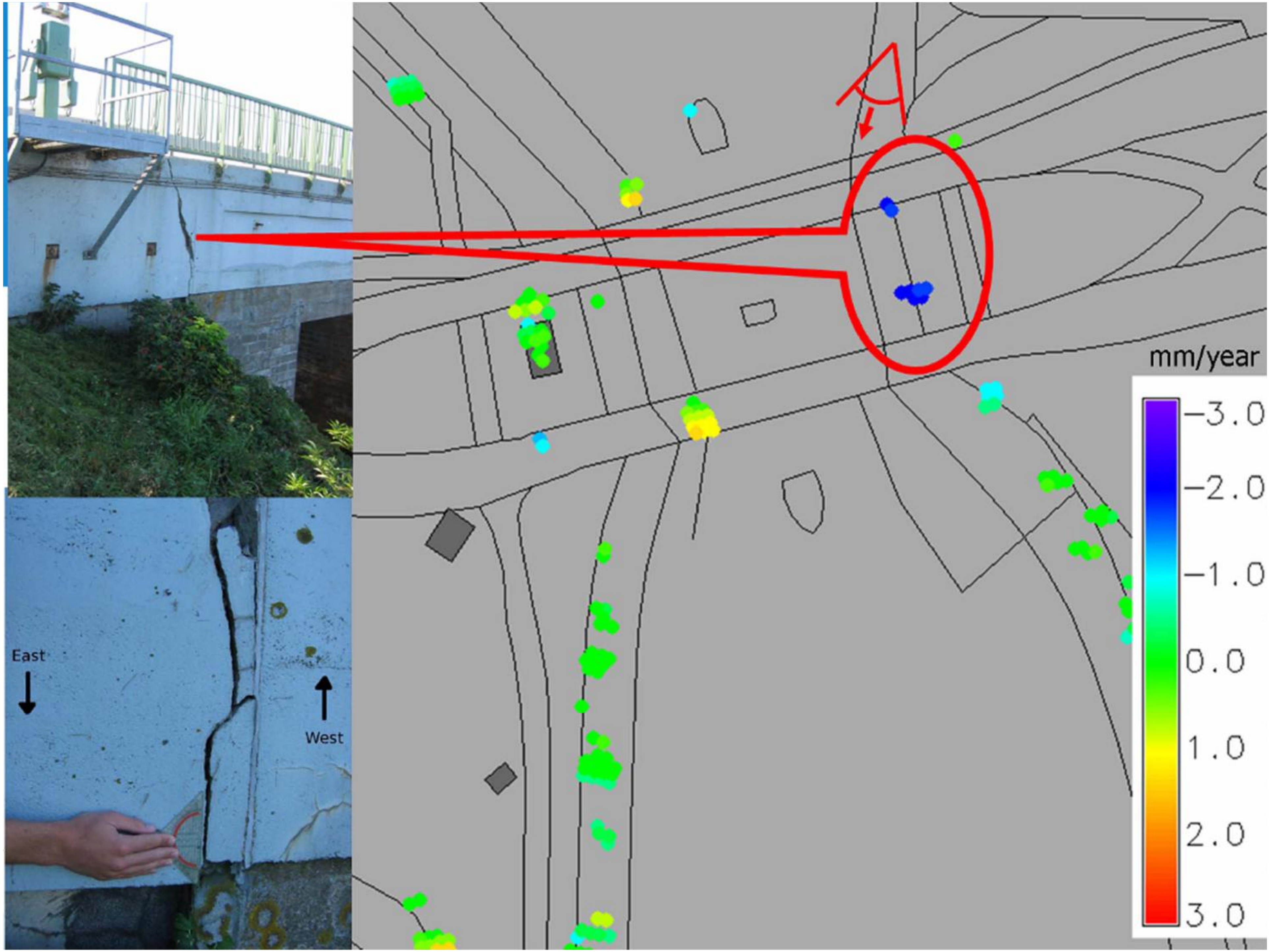

East
West
A
mm/year
−3.0
−2.0
−1.0
0.0
1.0
2.0
3.0

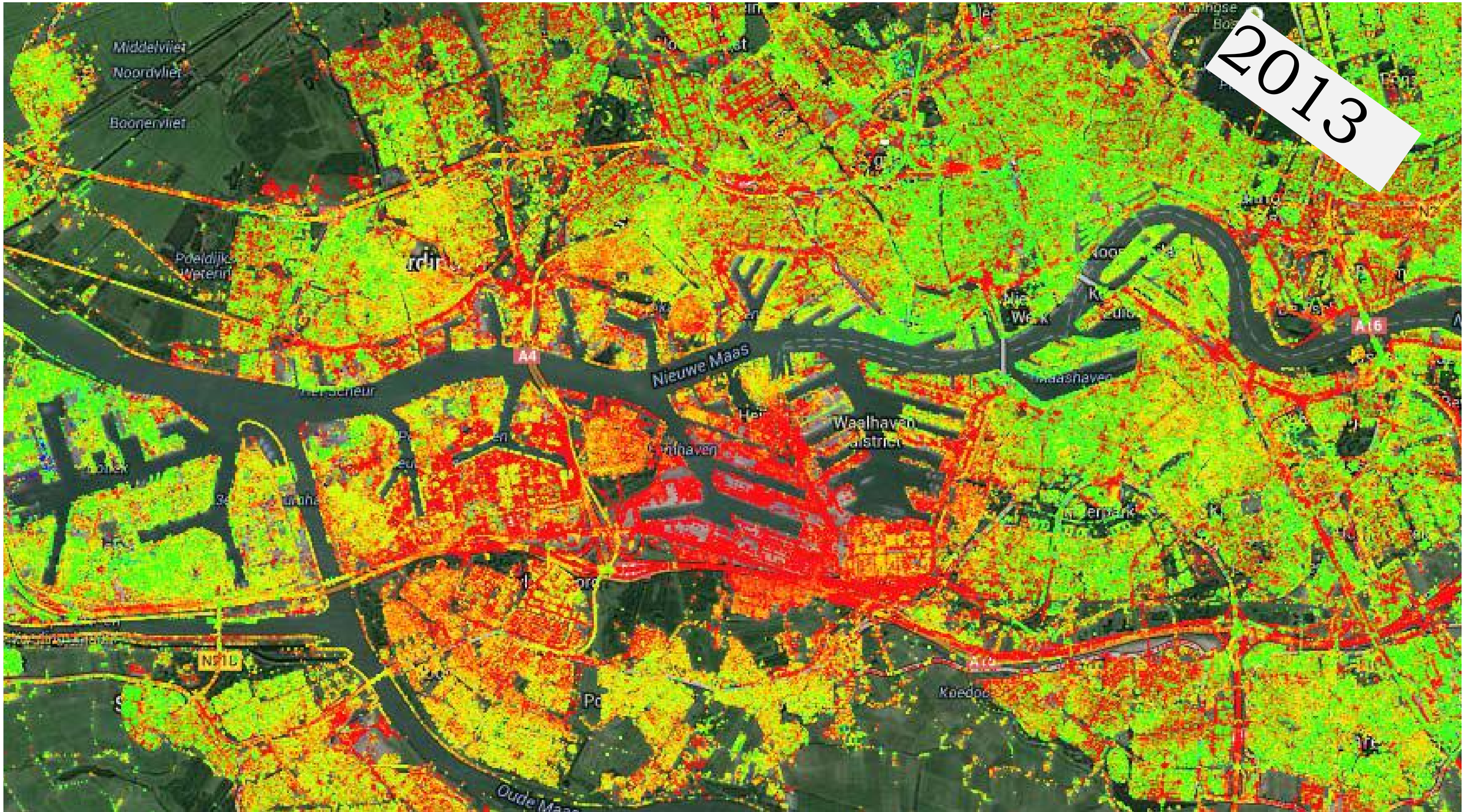

Rail monitoring

Ramon Hanssen, Ling Chang

TU Delft

The problem

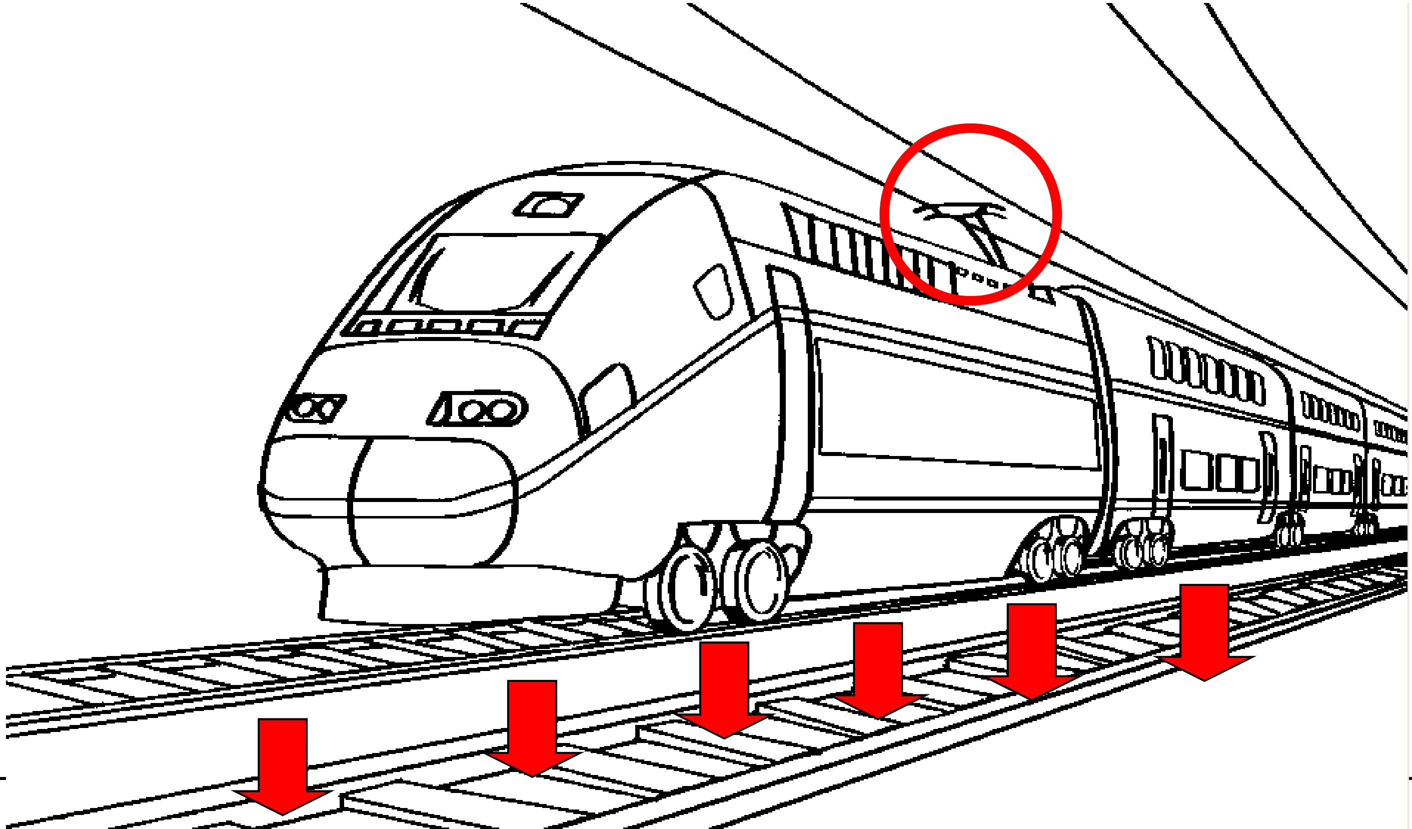

- Measuring rail stability from space

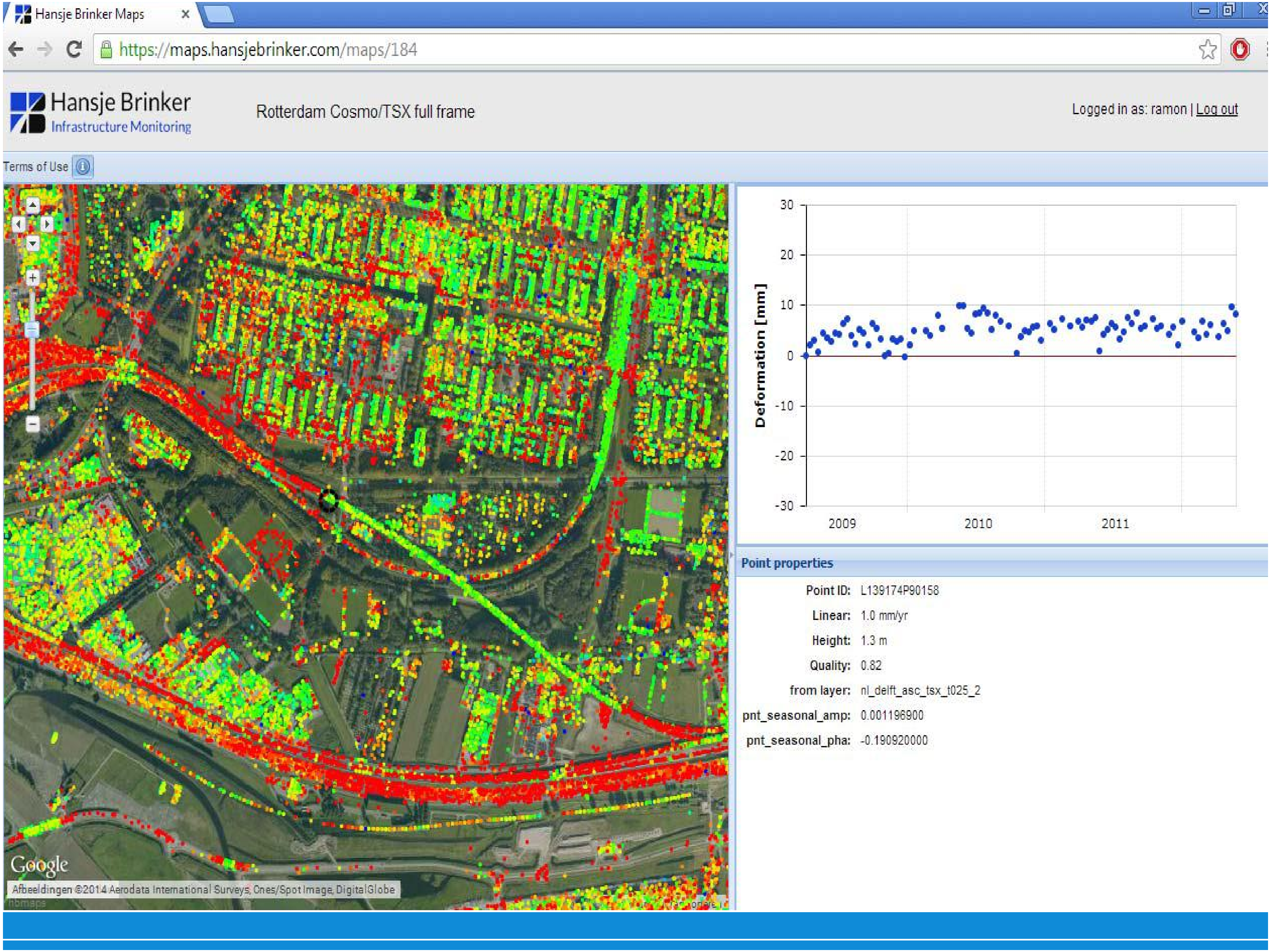
Hansje Brinker Maps
https://maps.hansjebrinker.com/maps/184
Hansje Brinker
Infrastructure Monitoring
Rotterdam Cosmo/TSX full frame
Logged in as: ramon | Log out
Terms of Use
Google
Afbeeldingen ©2014 Aerodata International Surveys, Cnes/Spot Image, DigitalGlobe
Deformation [mm]
30
20
10
0
-10
-20
-30
2009
2010
2011
Point properties
Point ID: L139174P90158
Linear: 1.0 mm/yr
Height: 1.3 m
Quality: 0.82
from layer: nl_delft_asc_tsx_t025_2
pnt_seasonal_amp: 0.001196900
pnt_seasonal_pha: -0.190920000

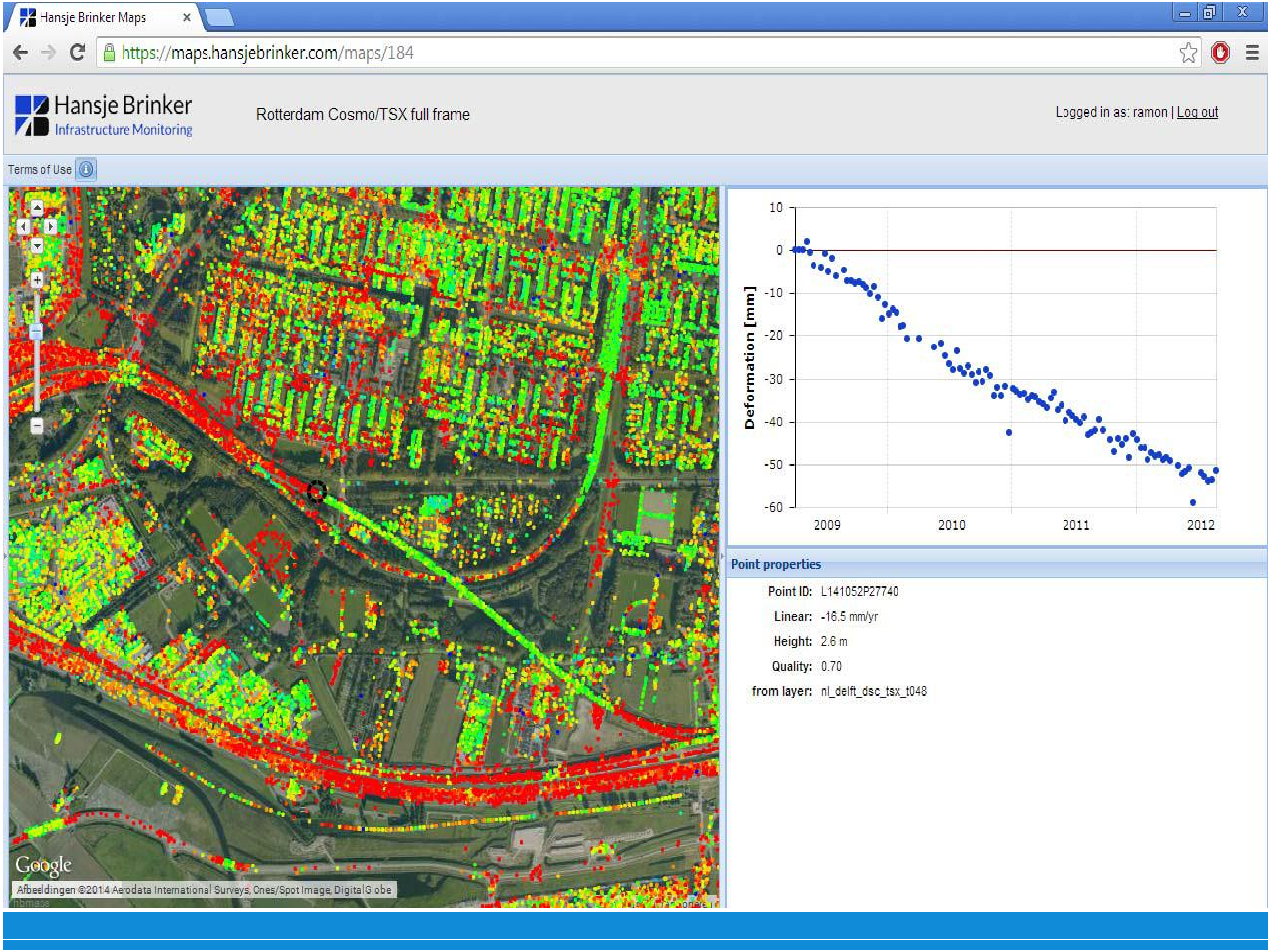
Hansje Brinker Maps
https://maps.hansjebrinker.com/maps/184
Hansje Brinker
Infrastructure Monitoring
Rotterdam Cosmo/TSX full frame
Logged in as: ramon | Log out
Terms of Use
Google
Afbeeldingen ©2014 Aerodata International Surveys, Cnes/Spot Image, DigitalGlobe
Deformation [mm]
10
0
-10
-20
-30
-40
-50
-60
2009
2010
2011
2012
Point properties
Point ID: L141052P27740
Linear: -16.5 mm/yr
Height: 2.6 m
Quality: 0.70
from layer: nl_delft_dsc_tsx_t048


Hansje Brinker Maps
https://maps.hansjebrinker.com/maps/184
Hansje Brinker
Infrastructure Monitoring
Rotterdam Cosmo/TSX full frame
Logged in as: ramon | Log out
Terms of Use
Google
Afbeeldingen ©2014 Aerodata International Surveys, DigitalGlobe
Een kaartfout rapporteren
Deformation [mm]
10
0
-10
-20
-30
-40
-50
-60
2009
2010
2011
2012
Point properties
Point ID: L143039P23524
Linear: -14.8 mm/yr
Height: -0.4 m
Quality: 0.65
from layer: nl_delft_dsc_tsx_t048

Horizontal and vertical deformation

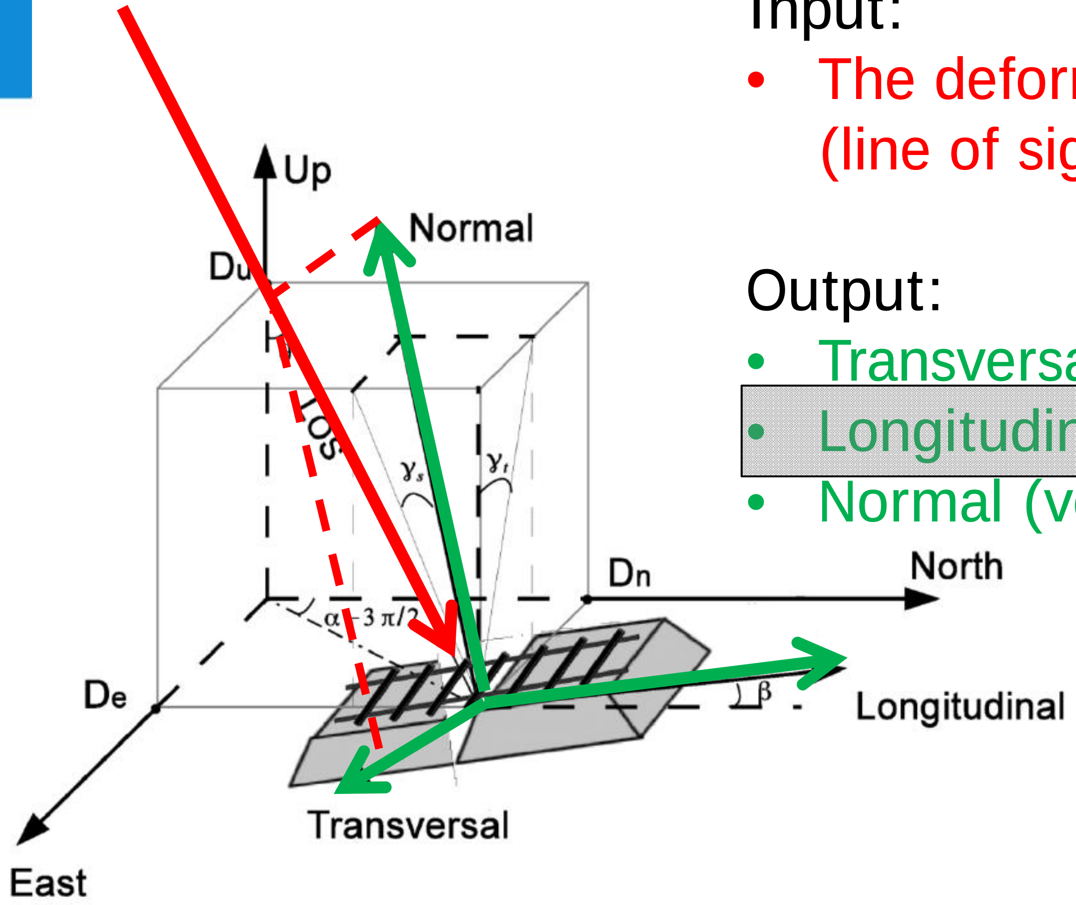

Input:

- The deformation (line of sight)

Output:

- Transversal,
- Longitudinal,
- Normal (vertical)

Track buckling

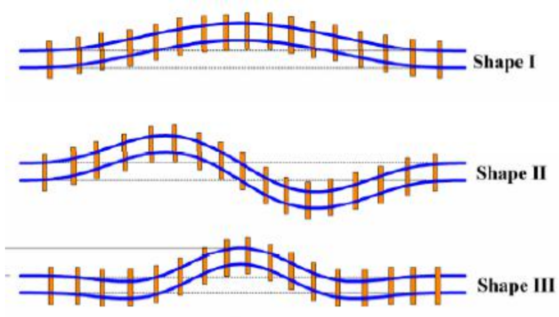

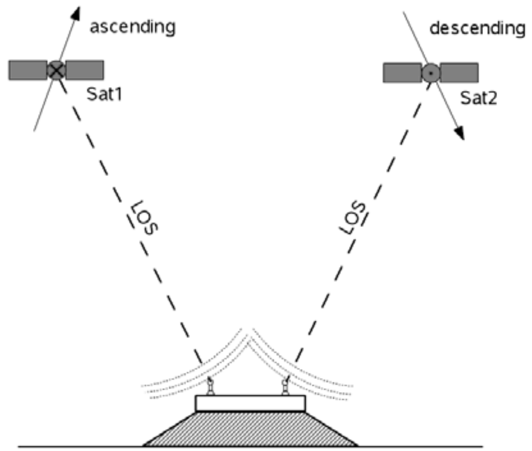

TU Delft

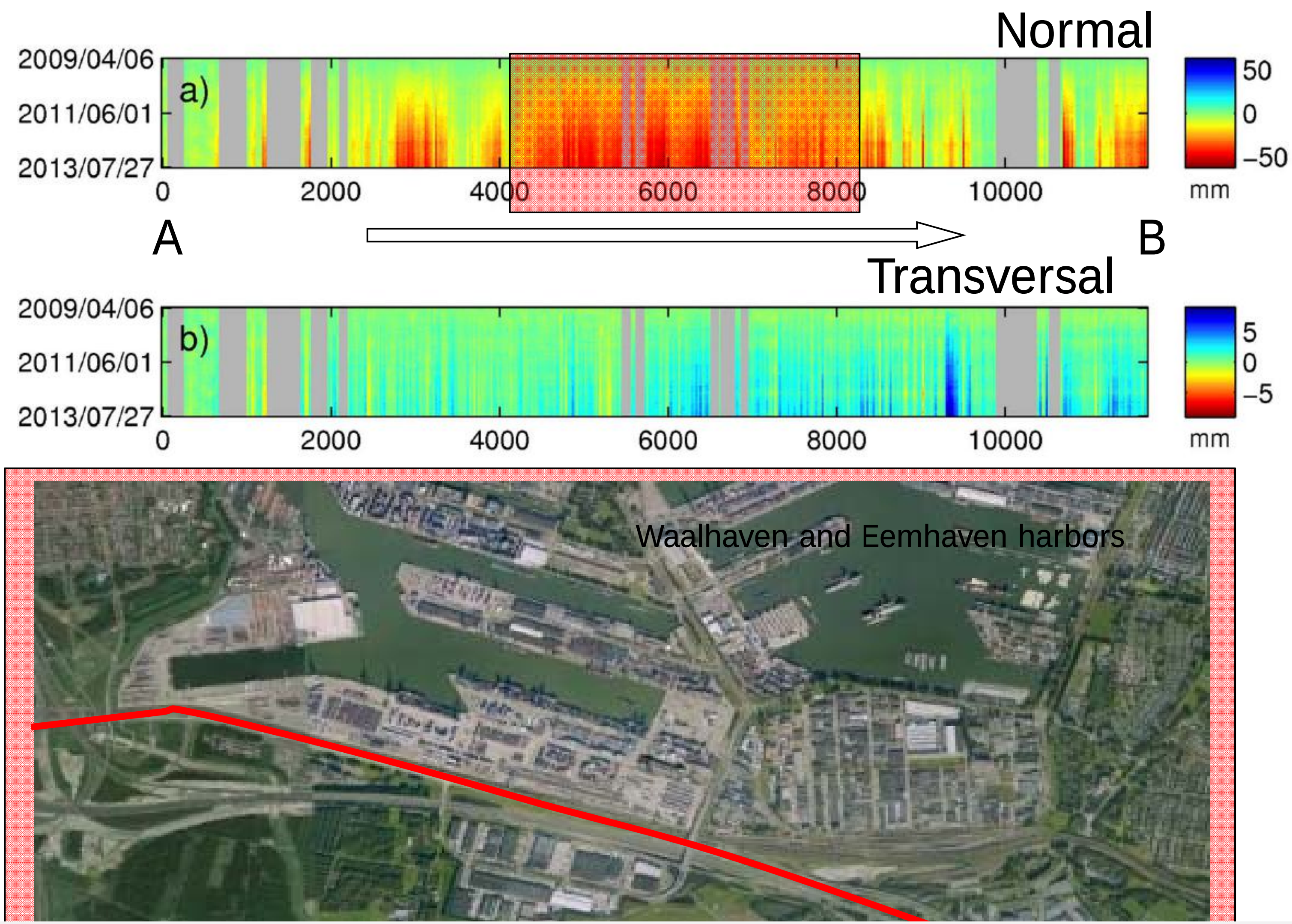

- Vertical ~1 mm precision
- Horizontal ~4 mm precision

Validation with measurement train

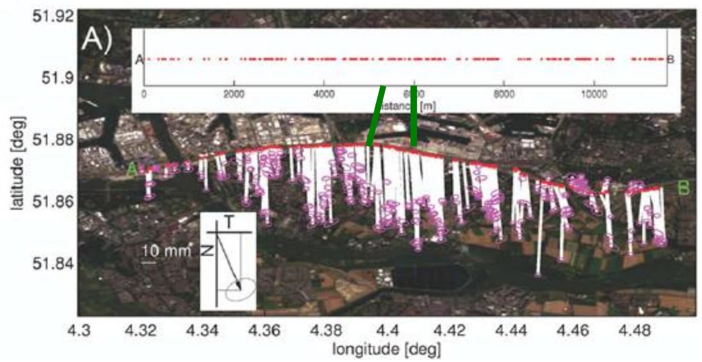

'Lifting' of the track, from surveying train

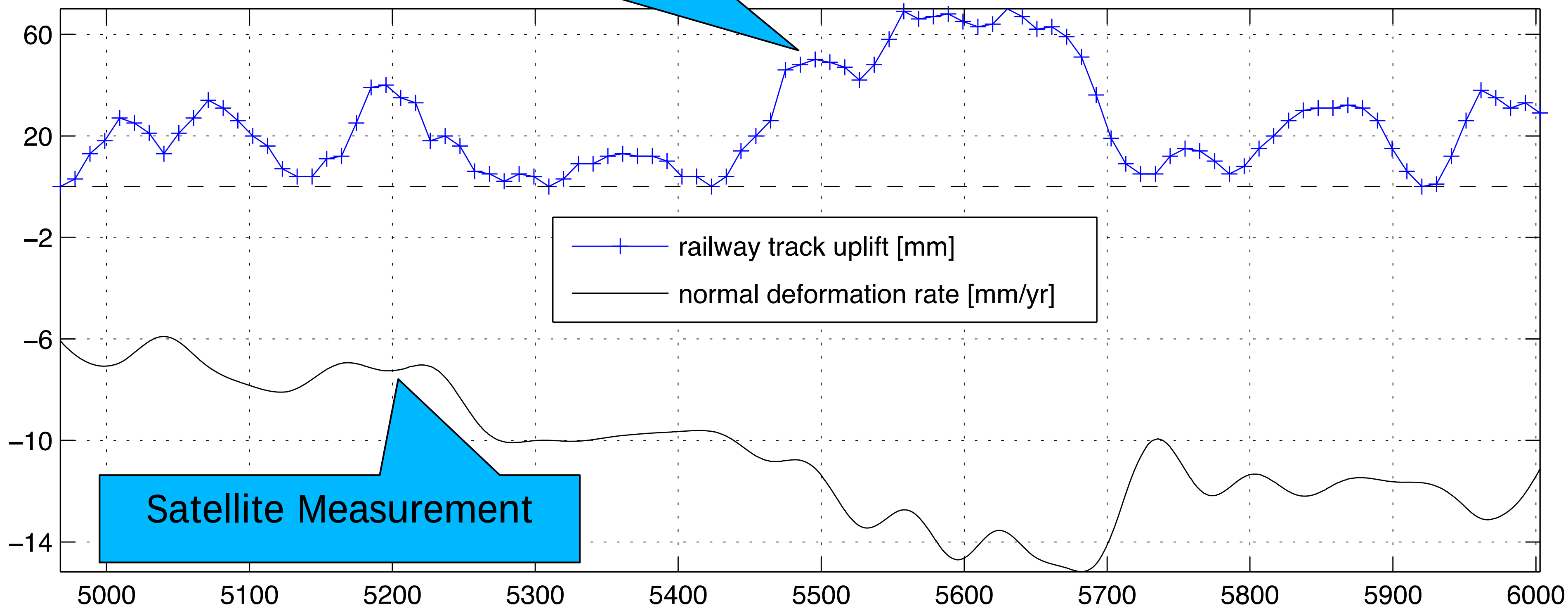

Satellite Measurement

TUDelft

Play with PSI data

- Data set made available by SkyGeo, the Netherlands
- Demo.skygeo.com
- Login:esa_course pw: esa_course7